Surveys in Geophysics
https://doi.org/10.1007/s10712-023-09811-x

Recent Reactivation of Variscan Tectonic Zones: A Case of Rodl-Kaplice-Blanice Fault System (Bohemian Massif, Austria/Czech Republic)

Pavel Roštínský[1] · Lubomil Pospíšil[2,3] · Otakar Švábenský[3] · Anastasiia Melnyk[4] · Eva Nováková[1]

Received: 10 March 2023 / Accepted: 30 September 2023

Abstract
The Rodl-Kaplice-Blanice fault system (RKB) of Variscan shear origin, repeatedly active since the Late Paleozoic to the Recent, is expressed by a number of lithological contacts, distinct geophysical gradients and many landforms. A general trend of the RKB as well as linear configuration of its internal architecture is fairly similar to those of topical near Rhine Graben and Alpine-Carpathian transition area as the two other consistent recently reactivated large-scale tectonic structures in the extended (thinned) crust of central Europe. In middle part of the RKB, the occurring linear topographic and geological features parallel to the main RKB sections point to the existence of a wide tectonic zone in the crust following the fault system. Our multidisciplinary study includes a summary of corresponding basic geological data, overview of seismic, regional geophysical and geomorphological conditions, primary model of recent kinematic activity in the RKB area derived from the space (Global Navigation Satellite System—GNSS) monitoring and terrestrial (repeated high precision levelling) geodetic data and comparison of these various information.
The obtained knowledge indicates that the RKB is active up to ~ 1.0 mm horizontally and > 0.5 mm vertically. The fault system area in the Bohemian Massif can be subdivided into the three parts of diverse tectonic structure and block kinematics. Sinistral horizontal movements are highest near the southern surface sections (Rodl-Kaplice, Rudolfov and Drahotěšice faults), whereas noticeable vertical differentiation is going on mainly along the Blanice and Kouřim faults in the north where the RKB activity is gradually decreasing towards the extensive Elbe shear zone with transverse movements. The middle part of the RKB is dislocated by a large active transverse tectonic structure of the South Bohemian Basins (SBB) with variable horizontal velocity vectors of surface GNSS stations. Most of the weak regional earthquakes have been recorded west of the RKB. Besides faults of the SBB, these were mainly associated with the RKB-subparallel Lhenice fault. Based on the earthquake distribution and foci depths, the latter fault can have similar structural position as the RKB related to lower part of the Variscan level in the ~ 10–12 km depth.

Keywords Rodl-Kaplice-Blanice active shear zone · Geophysics · Geomorphology · Global navigation satellite system · Recent kinematics · Foci

Extended author information available on the last page of the article

Article Highlights

- Integration of various geoscience data links surface movements to deeper crustal structures and seismicity
- Global Navigation Satellite System data can be used for compilation of geodynamic model of slowly deformed areas
- Major Variscan deep-seated faults in the Moldanubian unit of the Bohemian Massif manifest recent tectonic activity
- Movement along the study fault system can be considered a potential geodynamic risk for significant state infrastructure

1 Introduction

Many deep-seated fault systems in the Variscan crust of Europe, characterised by juxtaposed different structural levels, have been reactivated in various ways during the later Alpine orogeny and currently represent significant features of extension (thinning) or transtension. The repeated tectonic activity occurred in a consequence of spatial similarity of both the evolutionary phases largely forming outer Earth's layers of the continent, inherited crustal anisotropy and changing stress conditions exerted by moving lithospheric blocks including compressional, extensional or strike-slip regimes (e.g. Ziegler 1990; Scheck et al. 2002; Schumacher 2002; Michon et al. 2003; Uličný et al. 2009; Vauchez et al. 2012; Egli et al. 2017). A number of these important tectonic zones have been developing until the present time (Peterek et al. 2011; Coubal et al. 2015; Štěpančíková et al. 2019; Špaček et al. 2022) and some faults are even inducing the recent seismicity (Edel et al. 2007; Roštínský et al. 2013; Špaček et al. 2015; Babuška et al. 2016; Pospíšil et al. 2019). Hence, they can represent a hazard for humans including fundamental infrastructure and are significant objects of multidisciplinary research.

The same priority currently exists in the area of the Bohemian Massif (easternmost Variscides) fragmented by large tectonic zones into many crustal blocks (e.g. Röhlich and Šťovíčková 1968; Šťovíčková 1973; Blížkovský et al. 1975; Zeman 1978; Dvořák 1985; Matte et al. 1990; Brandmayr et al. 1995; Alexandrowski et al. 1997; Pitra et al. 1999; Cháb et al. 2010; Badura and Rauch 2014), where a number of geodynamic studies have focused on Quaternary activity of such fault systems. As outlined in Sect. 1, these works investigated diverse related phenomena or applied different methodological approaches. Hence, they represent well the extensive scope of research of recently reactivated tectonic zones worldwide. Both direct and indirect evidence of ongoing tectonic development were addressed. Several data pointing at strong influences of external (exogenous) processes on present-day geodynamic conditions in the central European crust (e.g. mass wasting or post-glacial isostatic rebound), frequently outweighing manifestations of movements along the fault systems coming from the Earth's interior, have been published as well.

The highest attention in the Bohemian Massif has been paid to research of the significant Western Bohemia / Vogtland seismic area (western part of the province; Fig. 1a) with frequent earthquake swarms (depths mostly 5–14 km; max. instrumentally recorded magnitude $M_L \sim 4.4$; Neunhöfer and Hemmann 2005; Fischer et al. 2014; Babuška et al. 2016; WEBNET 2022). The majority of earthquakes are related there to the N–S trending sinistral fault zones (Bankwitz et al. 2003), based on focal mechanisms conjugated with the WNW–ESE dextral faults (Havíř 2000; Vavryčuk et al. 2013). Holocene movements dated

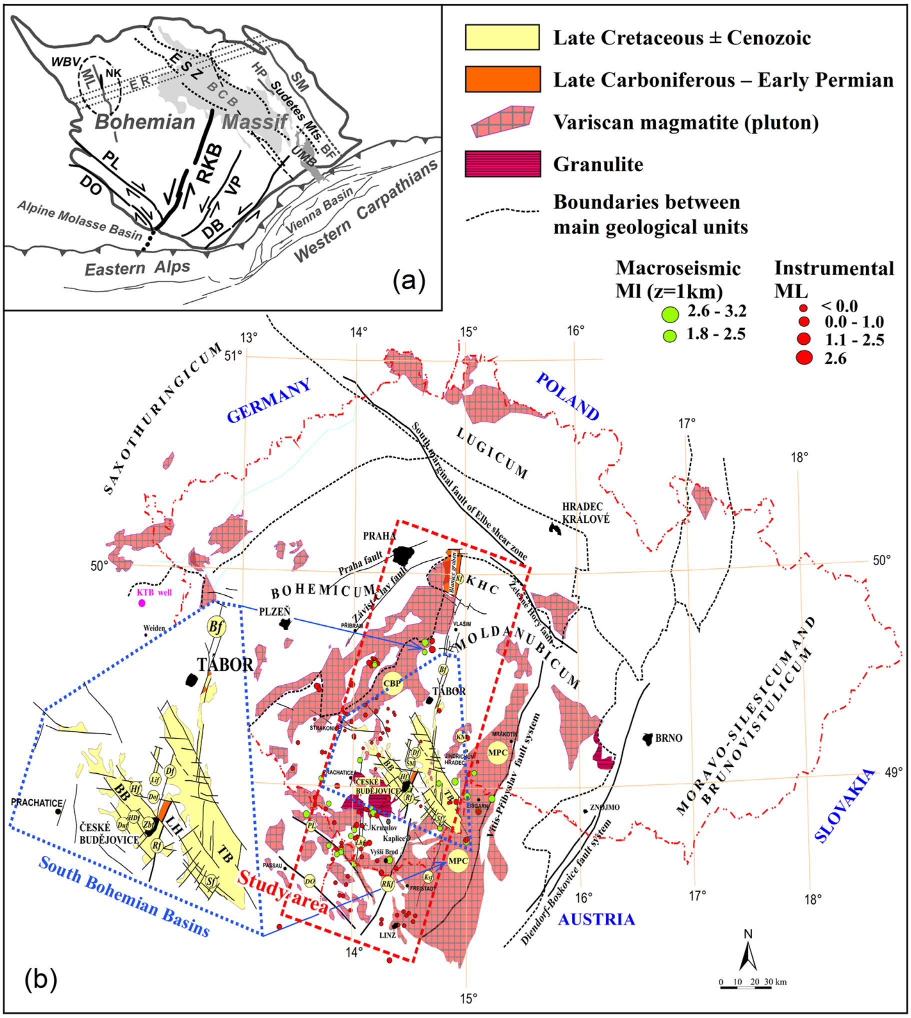

Fig. 1 **a** Location of the Rodl-Kaplice-Blanice fault system (RKB). BCB—Bohemian Cretaceous Basin; UMB—Upper Morava Basin. Other main recently active shear zones in the southern Bohemian Massif: DO—Donau fault system; PL—Pfahl Line fault system; VP—Vitis-Přibyslav fault system; DB—Diendorf-Boskovice fault system. Important fault-related phenomena in the northern Bohemian Massif: ER—Eger Rift; ML—Mariánské Lázně fault system; ESZ—Elbe Shear Zone; HP—Hronov-Poříčí fault system; SM—Sudetic Marginal fault system; BF—Bělá fault system. Main recent seismic regions in the Bohemian Massif: WBV—Western Bohemia / Vogtland (NK—most active Nový Kostel focal zone); Sudetes Mts. with adjacent areas. **b** Main tectonic elements in the study area along the RKB. The selected plutonic phenomena are visualised according to Klomínský et al. (2010): CBP—Central Bohemian Plutonic Complex; MPC—Moldanubian (South Bohemian) Plutonic Complex; KM—Klenov Massif; ŠM—Ševětín Massif. KHC—Kutná Hora Crystalline unit. Faults, basins and horsts: RKf—Rodl-Kaplice fault; Rf—Rudolfov fault; Df—Drahotěšice fault; Bf—Blanice fault; Kf—Kouřim fault (all as sections of the RKB); DO—Donau fault; PL—Pfahl Line fault; Lhf—Lhenice fault; Ksf—Karlstift fault; South Bohemian Basins: Duf—Dubné fault; HDf—Haklovy Dvory fault; Zbf—Zbudov fault; Hf—Hluboká fault; Dof—Dobřejovice fault; Lif—Líšnice fault; Sf—Stropnice fault; BB—Budějovice Basin; LH—Lišov Horst; TB—Třeboň Basin. Macroseismic and instrumental earthquake foci were added after Špaček et al. (2011). KTB—location of superdeep well (up to 9101 m) drilled within the German Continental Deep Drilling Programme

in paleoseismic trenches crossing the deep-seated Mariánské Lázně fault (Moldanubian / Teplá-Barrandian unit structural boundary) indicated there ongoing activity also of this NNW–SSE-oriented tectonic zone limiting the uplifting Erzgebirge Mts. (also referred to as Krušné hory Mts. in the Czech territory) against the Cheb Basin (Štěpančíková et al. 2019; max. estimated earthquake magnitude $M_w \sim 6.3–6.5$). The Quaternary activity of the latter zone was indirectly supported by anomalies in the regional fluvial network southwards: vertical (up to 20 m high) differences of analogous Ohře river terraces on the opposite Mariánské Lázně fault strands (Balatka et al. 2019) or places of young river piracy and increased stream incision into uplifting blocks along the middle fault section (Flašar and Štěpančíková 2022a). A dextral strike-slip regime along the fault in the Plio-Pleistocene period was mostly considered (e.g. Švancara et al. 2000; Schenk et al. 2012; Andreani et al. 2014; Štěpančíková et al. 2019). However, several authors supposed non-negligible sinistral movements instead (cf. Špičáková et al. 2000; Peterek et al. 2011).

Additionally, a large part of the Western Bohemia / Vogtland seismic area is located within the WSW–ENE striking Eger Rift as a component of the European Cenozoic Rift System expressed by extensive volcanism and many related phenomena (e.g. Ziegler and Dèzes 2007; Ulrych et al. 2013). The > 30-km-wide rift structure extends across the northern Bohemian Massif along the reactivated Teplá-Barrandian (Bohemicum) / Saxothuringian unit boundary. The youngest volcanic occurrences (middle Quaternary basalt hills and maar-diatreme volcanoes; Wagner et al. 2002; Mrlina et al. 2009; Rohrmüller et al. 2017) exist near the western margin of the Cheb Basin at the crossing of both mentioned deep-seated boundary structures. The persistent tectonic activity of the western Eger Rift is evidenced also by high heat flux associated with a number of thermal springs (max. temperature > 73 °C in Karlovy Vary) and places of CO_2 degassing, specifically with increased radon concentration (Hanzlík 1998; Geissler et al. 2005; Weinlich et al. 2006). The Eger Rift was active in the Quaternary also in its middle part, as supported by slickensides found there in middle Pleistocene loess and indirectly by a few fault deformations known in late Pliocene fluvial accumulations (Coubal and Adamovič 2000) or by a few existing thermal springs near the volcanic České středohoří Mts. As indicated by the results of morphotectonic analyses (Peterek et al. 2011; Andreani et al. 2014), several crustal blocks alongside the Eger Rift have been uplifted during the Quaternary against a morphological graben in axial part of the structure.

The second important recently active area in the Bohemian Massif involves the Sudetes Mts. (NE part of the province; Fig. 1a), oriented fairly consistently with a general trend of the Elbe-Oder fault system which extends across a large part of central Europe (e.g. Arthaud and Matte 1977; Scheck et al. 2002; Špaček et al. 2015). The corresponding boundaries between several structural units (crystalline Lugian, Teplá-Barrandian, Moldanubian and sedimentary Rhenohercynian) occur within this zone (Dvořák 1985; Cháb et al. 2010; Coubal et al. 2015). The prominent Upper Morava Basin system along the Haná fault, evolving in the regional dextral transtensional regime, also belongs to the active area (Grygar and Jelínek 2003; Špaček et al. 2015). A subsidence in middle parts of this graben structure has been associated with deposition of Plio-Pleistocene fluvial and lacustrine sediments, whose preserved thickness reaches up to 320 m (Špaček et al. 2015). The possible long-lasting landsliding detected in paleoseismic trench across the Kosíř fault in western part of the basin has obscured unequivocal young internal tectonic effects (Špaček et al. 2017). Close geodynamic relations of the Upper Morava Basin crossing the Bohemian Massif / Western Carpathians boundary to both the Bělá fault system (east) and the Nectava fault system (west) in adjacent segments of the Bohemian Massif were indicated by similar NW–SE trending belts of weak earthquakes (common depths 9–18 km; max. instrumentally recorded magnitude M_L ~ 3.8; Havíř 2002, 2004; Jelínek 2008; Špaček et al. 2015; Pospíšil et al. 2017, 2019) as well as by occurrences of numerous carbonated springs and a regionally increased CO_2 flux (Špaček et al. 2006). The youngest, presumably Bělá fault-related basaltic rocks in a small Pliocene to Early Pleistocene volcanic field near Bruntál (eastern Sudetes Mts.) were dated to 0.8–1.0 Ma (Šibrava and Havlíček 1980; Ulrych et al. 2013).

Another significant regional structure is the deep-seated Sudetic marginal fault, expressed on the surface as a prominent ~ 140-km-long NE front of the middle Sudetes Mts. with several generations of facets (Badura et al. 2007). It truncates middle and late Pleistocene terraces of the transverse Nysa Kłodzka river; 10–25 m high scarps have developed within them (Krzyszkowski et al. 2000). A number of reverse, normal or strike-slip deformations evolved along this fault in the Quaternary, as revealed by structural conditions in transverse and longitudinal paleoseismic trenches (Štěpančíková et al. 2010). Although dextral movements prevailed during the earlier fault history, sinistral strike-slips related to the Late Pleistocene post-glacial unloading appeared to be the last documented kinematic events (Štěpančíková et al. 2022). The ongoing regional tectonic activity is indicated by thermal springs in the adjacent Góry Złote Mts. (referred to as Rychlebské hory Mts. in the Czech territory) near the SE fault section (temperature up to 44 °C; Dowgiałło 2002).

The third main active part of the Sudetes Mts. includes the Hronov-Poříčí fault and adjacent structures (earthquake depths mostly 5–15 km; max. inferred historic magnitude M_w ~ 4.7; Schenk et al. 1989; Valenta et al. 2008; Špaček et al. 2015). The largest cluster of cold carbonated or thermal springs in the Polish Sudetes Mts. is located in the SE continuation of the Hronov-Poříčí fault (Duszniki area; Dowgiałło 2002). However, within a near > 1600-m deep boreholes in the northern Sudetes Mts. close to the eastern Eger Rift the water temperature reaches nearly 98 °C. A high heat flux was detected in the region as well. Both phenomena can be related to subsurface Quaternary volcanism (Dowgiałło 2002; Ulrych et al. 2013).

Additionally, deformations of speleothems were measured in several caves in the Sudetes Mts. area (Briestenský et al. 2014; Bábek et al. 2015; Szczygieł et al. 2021). The existing damages, several dated by various methods, were indirectly attributed to the Late Quaternary seismicity associated with an activity of the particular near main fault systems.

Much less features related to the active tectonics have been evidenced in the central and southern Bohemian Massif. The Quaternary movements accompanied by the locally increased seismicity (max. estimated magnitude M_w ~ 3.5; Špaček et al. 2022) were considered along deeper levels of the Diendorf-Boskovice fault (Roštínský et al. 2013). This fault separates at the surface the Bohemian Massif from the Western Carpathian foreland basin (Roštínský and Roetzel 2005), whereas in the footwall the Moravo-Silesian unit is limited against the Moldanubian and Brunovistulian units (Roštínský et al. 2013 and references therein). The recent subsidence in the Budějovice Basin was supported by Homolová et al. (2012; sedimentological study) and Popotnig et al. (2013; morphotectonic study). However, presumable transverse fault offsets or intact sedimentary bodies deposited at the end of the Pleistocene above the fault traces seemingly contradicts an ongoing activity of both mentioned tectonic structures (Špaček et al. 2017, 2022).

A distribution of the existing stress field in central Europe, induced by the continuing northward collision of Africa with the Eurasian plate, a transmission of the Mid-Atlantic Ridge push and locally by orogenic factors in the Alps or the Carpathians, drove there the recent dominant normal and strike-slip fault kinematics. While in the northern Bohemian Massif the NW–SE to NNW–SSE direction of S_H similar to that in the Western European stress domain largely occurs (Peška 1992, 1993; Havíř 2004; Ziegler and Dèzes 2007; Vavryčuk et al. 2013; Špaček et al. 2015; Stemberk et al. 2019; Jarosiński et al. 2021), in its southern part the N–S to NNE–SSW stress was inferred related to movements of frontal segments in the Eastern Alps and adjacent foreland basins (Reinecker et al. 2010; Levi et al. 2019). Various indicators have been used in the Bohemian Massif for the determination of stress direction, mostly focal mechanisms and borehole parameters. In several areas, a few different stress orientations were calculated (e.g. Havíř 2004; Jarosiński et al. 2021).

A highly reliable information about recent regional horizontal movement tendencies of crustal blocks provide data from the Global Navigation Satellite System (GNSS) monitoring. A construction of the GNSS networks on all continents began in late 1980s. Soon, the results allowing to identify hazardous active structures were obtained (e.g. Grenerczy et al. 2000; Grenerczy 2002; Hearn et al. 2010; Tong et al. 2013; Kierulf 2017; Tamay et al. 2021). After the regional permanent EPN network was built in Europe, epoch networks focused there on study of particular active fault systems (Hefty 2007; Ziegler and Dèzes 2007; Devoti et al. 2014; Lyros et al. 2021). The increasing number of GNSS monitoring stations enabled to unify the surface data for larger areas also in the Bohemian Massif (Kontny et al. 2004; Schenková et al. 2007; Švábenský et al. 2012; Roštínský et al. 2020), many along tectonically active faults (Wendt and Dietrich 2003; Schenk et al. 2009; Schenková et al. 2009; Roštínský et al. 2013; Kapłon et al 2014; Švábenský et al. 2014; Pospíšil et al. 2017). During the recent time, we processed and unified the data from permanent GNSS stations in southern part of the province focusing on geodynamics of the large-scale sinistral Rodl-Kaplice-Blanice fault system (RKB; Fig. 1b). Although only low seismicity occurs in the adjacent area ($M_L < 2.5$; Kárník et al. 1981; Lenhardt et al. 2007; WEBNET 2022), our results combined with the earlier estimation of regional Recent Vertical Movements (RVM; Vyskočil 1996) indicated non-negligible ongoing horizontal and vertical movements also along this tectonic zone.

The middle part of the RKB runs near (up to < 20 km) the Nuclear Power Plant Temelín (ETE) as a significant component of the Czech energy infrastructure. Hence, the research of recent regional geodynamics should follow the valid International Atomic Energy Agency Safety Standards for protecting people and the environment, primarily the 'Seismic Hazards in Site Evaluation for Nuclear Installations' (International Atomic Energy Agency Safety Standards Series 2022; Specific Safety Guide No. SSG-9) in order to relate its results to the knowledge from similar studies in the surrounding areas. In our paper, we additionally evaluated and compared selected data from the disciplines recommended in the mentioned Standard.

Our review study extends the current RKB-related knowledge by a:

1. summary of basic information about this fault system provided by geology, yet subdivided in a lot of previous studies;
2. overview of regional geophysical and geomorphological conditions based on newly processed and visualised existing data as a significant additional information about the RKB structure; and
3. compilation of regional kinematic model, primarily based on the GNSS monitoring data as a piece of information not yet considered in assessment of the recent RKB geodynamics; it took into account also selected repeated high precision levelling, seismological, topographic and geophysical data. The main kinematically different areas were distinguished.

2 RKB Setting, Evolutionary History and Internal Structure

2.1 General Setting

The RKB is located mostly in the Moldanubian unit of the Bohemian Massif. It extends on the surface > 200 km in the SSW–NNE direction between the Cenozoic Alpine Molasse Basin and the Bohemian Cretaceous Basin (Fig. 1a; Rajlich 1990; Wallbrecher et al. 1993; Brandmayr et al. 1995; Cháb et al. 2010; Špaček et al. 2022). We assessed a ~ 200 × 80 km large belt along the fault system (RKB study area; Fig. 1b). The southernmost section of the tectonic zone ~ 50-km-long is hidden beneath the foreland basin close to the present-day Alpine orogenic front (Wagner 1998; Pfleiderer et al. 2016; Hintersberger et al. 2017). To date, the RKB and transverse faults have been studied in detail only in selected subareas, mostly in the Temelín region (primarily for the Nuclear Plant safety assessment; e.g. research reports by Decker et al. 2010a, b; Špaček et al. 2011; Prachař 2014; Navrátilová and Nol 2018). The investigation of the fault system as a whole has focused mainly on its geological aspects. Works mutually evaluating outputs from more disciplines have been scarce there and devoted only to smaller structures or areas.

Besides the RKB, the following generally SSW–NNE trending sinistral fault systems (shear zones) developed in the southern Bohemian Massif during final stages of the Variscan orogeny in the Late Paleozoic (Fig. 1): Vitis-Přibyslav (Veselá 1976; Lenhardt et al. 2007; Špaček et al. 2022), Diendorf-Boskovice (Schermann 1966; Figdor and Scheidegger 1977; Roetzel 1996; Roštínský and Roetzel 2005; Roštínský et al. 2013; Pospíšil et al. 2017; Paoletti et al. 2022) and smaller Lhenice (Mísař et al. 1983; Rajlich et al. 1986; oriented approximately N–S), Karlstift (Brandmayr et al. 1999) or Freyenstein (Griesmeier et al. 2020). In the south, the RKB terminates the transverse WNW–ESE to NW–SE striking Pfahl Line and possibly also Donau dextral strike-slip fault systems (Thiele 1961; Führer 1978; Brandmayr et al. 1995; Wagner 1998; Pitra et al. 1999; Büttner 2007; Žák et al. 2014) as two significant components of a wide subparallel tectonic zone currently extending from the Rhine Graben in the Alpine foreland to the front of the Alpine orogen (e.g. Ziegler and Dèzes 2007; Pfleiderer et al. 2016), yet poorly constrained. Both the orthogonal sets of Late Palaeozoic fault systems, primarily arranged as kinematically conjugated, played a role during regional geodynamic evolution in the subsequent periods until the Recent (Malecha and Pícha 1963; Malkovský 1979, 1980; Schröder 1987; Brandmayr et al. 1995; Popotnig et al. 2013).

Brittle elements (strike-slip, normal and reverse faults) have developed within the RKB (Malecha 1964; Malkovský 1979; Vrána and Bártek 2005; Kadlec 2017) besides ductile deformations (Brandmayr et al. 1995; Büttner 2007; Iglseder 2013). During the ~ 303–280 Ma period (Late Paleozoic), deformations were related to the three main kinematic regimes: compressional, sinistral strike-slip (transtensional) and extensional (Zachariáš and Hübst 2012; Kadlec 2017; Bárta et al. 2021). At that time, sinistral horizontal displacement of the Bohemian Massif blocks along the RKB could reach up to 35 km (Hintersberger et al. 2017). However, lower displacement values are commonly considered based on the present-day distance of corresponding rock bodies on the opposite fault strands or other indicators (cf. Fuchs et al. 1968; Brandmayr et al. 1995; Vrána et al. 2005; Vrána and Bártek 2005; Büttner 2007; Iglseder 2013). An elongated depositional space filled with a thick sequence of Permo-Carboniferous deposits had evolved along the RKB in the main transtensional regime (Zachariáš and Hübst 2012). The formation of the SSW–NNE trending shear zones and corresponding elongated Permo-Carboniferous

Fig. 2 Significant SW–NE to SSW–NNE fault-related lithological contacts dominating the RKB structure ▶ with added important lithological boundaries in the SBB. Background: overview 1:500,000 scale Geological map after Kodym et al. (1967). Main RKB sections: 1—Rodl fault; 2—Kaplice fault; 3—Rudolfov fault; 4—Drahotěšice fault; 5—Blanice fault; 6—Kouřim fault; HG—Haselgraben structure (outcropping part). Blue dotted lines—geological sections across the RKB. AMB—Alpine Molasse Basin; BB—Budějovice Basin; LH—Lišov Horst; TB—Třeboň Basin; LG—Lhotice Graben; ČBG—Český Brod Graben; BCB—Bohemian Cretaceous Basin. ČB—České Budějovice; TA—Tábor; VL—Vlašim. ETE—Nuclear Power Plant Temelín. Brief lithology along the RKB-related boundaries: Basement rocks, Moldanubian unit: m—wide belt of mylonised crystalline rocks; 1—granite; 2—paragneiss; 3—granite; 4—paragneiss; 5—granodiorite; 6—paragneiss to migmatite; 7—granite; 8—orthogneiss, 9—paragneiss to migmatite; 10—granulite; 11—migmatite; 12—orthogneiss; 13—crystalline limestone; 14—amphibolite; 15—orthogneiss to metagranite; 16—migmatite; 17—granite to quartz diorite; 18—granite, Kutná Hora Crystalline unit (KHC): 19—mica-schist; 20—orthogneiss to migmatite. Cover rocks: 21—conglomerate, sandstone, siltstone, claystone, locally with limestone (Permian-Carboniferous); 22—conglomerate, sandstone, siltstone, claystone (Cretaceous of the Bohemian Cretaceous Basin); 23—conglomerate, sandstone, siltstone, claystone (Cretaceous of the South Bohemian Basins); 24—sand, silt, clay, diatomite (Neogene of the South Bohemian Basins)

basins, as well as an origin of many magmatic bodies in the Bohemian Massif surrounding the RKB (see Sect. 2.3 and Fig. 1b) are considered the main manifestations of gravitational collapse of the Variscan belt (e.g. Bárta et al. 2021).

Besides the corresponding longitudinal faults of N–S, SSW–NNE, SW–NE or WSW–ENE directions related to common RKB trends, a number of transverse (to oblique) sets of mostly NW–SE to NNW–SSE and less W–E to WNW–ESE faults have developed within the fault system area in the Late Paleozoic afterwards and during the following periods (Wallbrecher et al. 1993; Brandmayr et al. 1995; Wagner 1998; Zachariáš and Hübst 2012; Hintersberger et al. 2017). The largest transverse deformation system crossing the middle RKB is that of the South Bohemian Basins (SBB; Figs. 1, 2; Malecha et al. 1962, 1964; Malkovský 1980; Špaček et al. 2011; Popotnig et al. 2013) with preserved remnants of Late Cretaceous, Oligocene to Neogene and also Quaternary deposits. The SBB are composed of the NW–SE trending Budějovice Basin (BB) and the SSW–NNE elongated Třeboň Basin (TB), separated by the crystalline Lišov (or Rudolfov) Horst. The most significant discontinuities within the basins are the Hluboká fault along the NE rim and the Dubné fault along the SW rim of the BB and the Stropnice fault associated with a NW–SE graben along the SW margin of the TB. The combination of RKB and SBB structural trends has led in the basin system to development of a dense crustal fragmentation with numerous blocks arranged in a little regular 'parquet-like' system (Malkovský 1980).

The basement of the generally W–E elongated Alpine Molasse Basin near the RKB is cross-cut by numerous transverse faults as well, including the NW–SE to NNW–SSE-oriented ones at the southwestern margin of the Bohemian Massif and the SSW–NNE, SW–NE to WSW–ENE striking ones at its south-eastern margin; several of them reach surface in outcropping part of the Massif (Kröll et al. 2006; Pfleiderer et al. 2016). The southern RKB is located in an intersection space of both fault groups (Wagner 1998). The Bohemian Cretaceous Basin near the northern RKB is considered to be developed in a frame of the RKB-transverse WNW–ESE to NW–SE striking Elbe shear zone, a part of the reactivated Late Variscan Elbe-Oder fault system (Malkovský 1987; Uličný et al. 2009; Coubal et al. 2015). The basin was filled with up to > 1000 m (currently preserved thickness) Cenomanian to Santonian continental and marine clastic strata. The original basin size and thickness have been heavily reduced by erosion related to the subsequent tectonic movements (e.g. Malkovský 1980; Chlupáč et al. 2002; Danišík et al. 2012). At

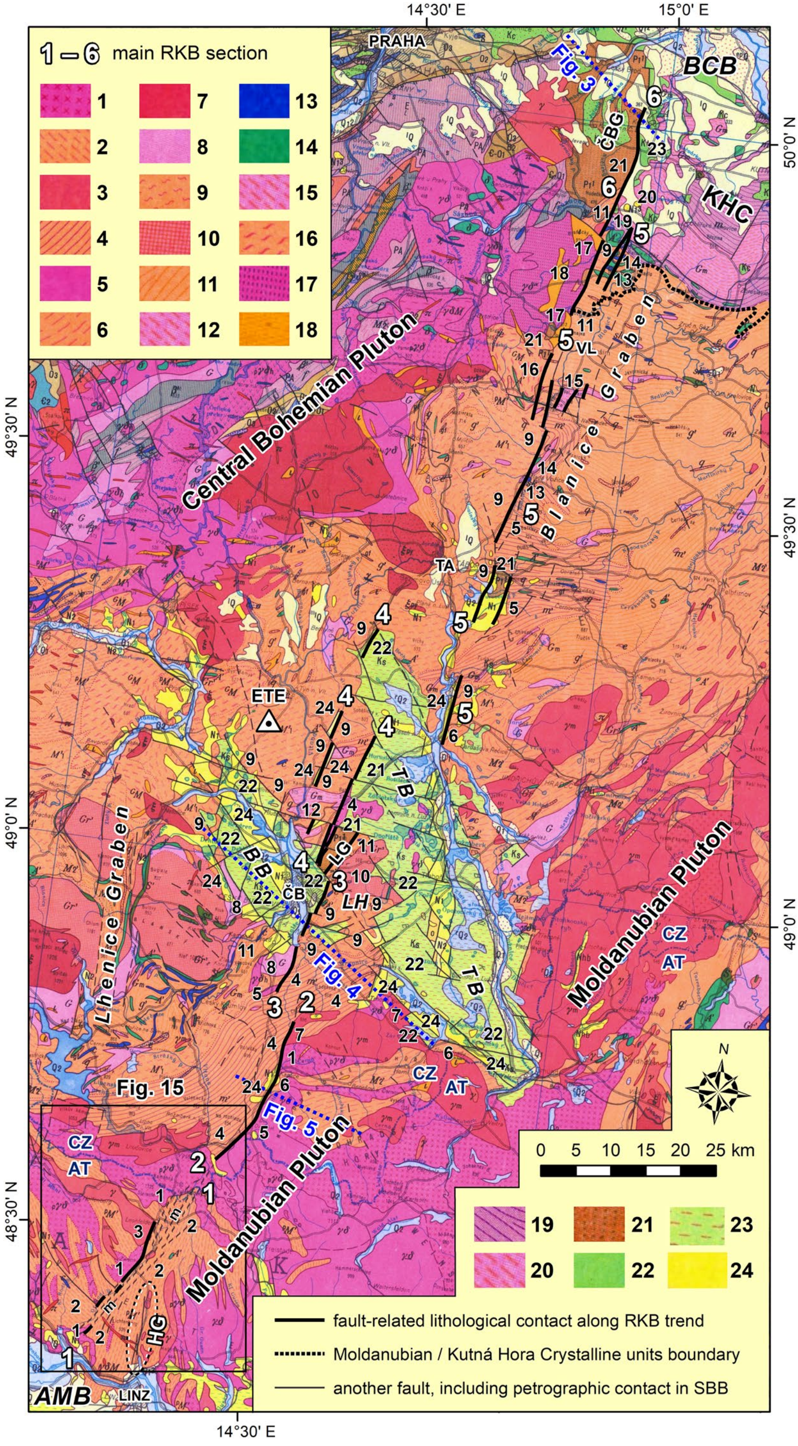
1 – 6 main RKB section
1
2
3
4
5
6
7
8
9
10
11
12
13
14
15
16
17
18
19
20
21
22
23
24
fault-related lithological contact along RKB trend
Moldanubian / Kutná Hora Crystalline units boundary
another fault, including petrographic contact in SBB
0 5 10 15 20 25 km
N
14°30' E
15°0' E
50°0' N
49°30' N
49°0' N
48°30' N
PRAHA
BCB
KHC
ČBG
Fig. 3
Fig. 4
Fig. 5
Fig. 15
Central Bohemian Pluton
Moldanubian Pluton
Blanice Graben
Lhenice Graben
VL
TA
ETE
TB
BB
LG
ČB
LH
CZ
AT
HG
AMB
LINZ

the present time, most of the Late Cretaceous deposits are preserved in the Labe Lowland area largely directed and constrained by the wide shear zone-related tectonic system with dextral features (e.g. Uličný et al. 2003). The RKB is limited by a fault zone at the southern margin of the Labe Lowland. Towards the SE, the zone includes the WNW–ESE to NW–SE striking Železné hory fault (Skácelová et al. 2008; Uličný et al. 2009; Švábenský et al. 2014; Coubal et al. 2019).

2.2 Lithological Contrasts and Other Fault-Related Features of the RKB and Near Structures

The geological maps (Čech 1962, 1989; Kodym 1963, 1989; Kodym et al. 1967; Fuchs et al. 1968; Krenmayr et al. 2006; CGS 2023) indicate fault-related boundaries between various rocks along the whole RKB (Fig. 2; see Sects. 2.3–2.5 for details of the basic lithology). The faults separate both basement crystalline and sedimentary cover (Permo-Carboniferous, Late Cretaceous, Cenozoic) units. The main spatially consistent phenomena accompanying the RKB are rock foliation or lineation, mylonite belts and dyke swarms (Malecha 1964; Wallbrecher et al. 1993; Vrána and Bártek 2005; Vrána et al. 2005; Vrána and Janoušek 2006; Zachariáš and Hübst 2012). Several oblique ruptures, primarily the > 20-km-long N–S running Haselgraben near Linz (Pfleiderer et al. 2016), are considered to be also the RKB components, although they had possibly developed under different stress conditions than the main SW–NE and SSW–NNE striking faults (e.g. Iglseder 2013, 2014a, b; Hintersberger et al. 2017). The Lhenice fault, located ~ 25 km to the west and associated with many subparallel lithological boundaries between rock bodies of different crustal levels as well (Rajlich et al. 1986; CGS 2023), is at the surface expressed by graben features (Mísař et al. 1983).

2.3 Moldanubian and Kutná Hora Crystalline Rocks

The Moldanubian unit (Moldanubicum) is the largest structural part of the Bohemian Massif composed of high-grade metamorphic rocks of presumably original Middle to Late Proterozoic age, strongly influenced by Cadomian and Variscan orogenic processes (Mísař et al. 1983; Matte et al. 1990; Dallmeyer et al. 1995; Cháb et al. 2010). During the Variscan evolution, a thrust and nappe system of crystalline complexes had formed within this unit (Fuchs and Matura 1976; Thiele 1984; Fuchs 1991). Later, magmatic rocks intruded into the metamorphic domain as numerous bodies of various depth, size and petrographic composition (Fig. 1b; Dudek et al. 1991; Finger et al. 2009; Cháb et al. 2010; Klomínský et al. 2010). The unit includes lower metamorphic complexes (Monotonous Group) mostly composed of biotite paragneiss and upper metamorphic complexes (Variegated Group), where paragneiss comprises numerous interbeds of crystalline limestone, amphibolite or quartzite. Granulite, eclogite, skarn and ultrabasic rocks are present as well. The largest Moldanubian (South Bohemian) pluton, occurring along southern and middle parts of the RKB, consists of acid (granitoid) rocks originated in a few phases at ~ 330–300 Ma (e.g. Gerdes et al. 2003). The second largest Central Bohemian pluton at the Teplá-Barrandian / Moldanubian unit boundary near the northern RKB is composed of acid to ultrabasic rocks, of which granodiorite is most common. Many isolated metamorphic occurrences affinitive to one of the surrounding crystalline complexes of Moldanubian, Teplá-Barrandian or Kutná Hora Crystalline units are preserved above (e.g. Klomínský et al. 2010). Several smaller bodies of different granitoids or durbachites exist near the middle RKB (CGS 2023).

The Kutná Hora Crystalline unit at the northern rim of the Moldanubicum has a different crustal history. It consists of Late Proterozoic rocks metamorphosed during the Variscan orogeny to a lower grade than the latter unit, mainly orthogneiss, mica-gneiss and mica-schist; Variscan plutonites were not been incorporated into its structure. Hence, it has been frequently included in a different structural level (Kachlík 1999; Verner et al. 2009; Cháb et al. 2010).

2.4 Permo-Carboniferous Sediments Along the Blanice Graben

The Permo-Carboniferous terrestrial clastic sediments with local coal seams (Late Carboniferous—Gzhelian, Stephanian C up to Early Permian—Autunian) were deposited along the RKB in a SSW–NNE trending structural depression originated at ~ 303–290 Ma (Zachariáš and Hübst 2012; Pešek and Sivek 2016; Kadlec 2017; Bárta et al. 2021). At ~ 288–280 Ma, several horsts and graben-like subbasins had developed along its strike in association with growth of a number of longitudinal faults (Bárta et al. 2021). A geometry of the depositional spaces was influenced also by transverse NW–SE-, WNW–ESE- or W–E-oriented faults dated to ~ 290–270 Ma (Kadlec 2017).

The strata in the depression commonly dip 10–40°. Their dominant eastward dip direction and transverse Permo-Carboniferous infill asymmetry were related to a higher tectonic activity of the eastern marginal Blanice and Kouřim faults combining horizontal movements with vertical movements up to a few kilometres (Kadlec 2017). The accumulation in the eastern parts was coarser (frequent conglomerates or breccia of alluvial fans) compared to the central and western parts (prevailing deltaic or lacustrine sediments; Fig. 3; Chlupáč et al. 2002).

At the present time, only fault-limited fragments of the original sedimentary infill are preserved in a belt ~ 120 km long and ~ 15 km wide because of later tectonic events and strong denudation of the upper crust reaching a few kilometres (Chlupáč et al. 2002). The area of the sedimentary belt used to be commonly termed as the Blanice Graben (BG). This name has been sometimes applied also to the whole RKB (e.g. Hintersberger et al. 2017; Kadlec 2017). However, in our paper we attribute the term BG only to northern part of the RKB including the Blanice and Kouřim faults. The maximum preserved thickness of Permo-Carboniferous clastics differs between the individual small grabens along the BG (Pešek and Sivek 2016; Kadlec 2017): in Lhotice Graben in the SBB area nearly 800 m, in the Tábor area up to > 800 m, in the Vlašim area only 50–100 m and in northernmost Český Brod Graben near the Bohemian Cretaceous Basin > 800 m.

2.5 Cretaceous and Cenozoic Sediments of the SBB

In the Turonian to Campanian (Late Cretaceous) and several Cenozoic periods (Oligocene, Miocene, Pliocene, Quaternary), the SBB area acted as a depocentre of fresh- or brackish-water formations (clastics, sometimes with local coal seams or diatomite horizons) and in the latter era also of marine sediments from several ingressions coming through the Stropnice Graben from the Molasse basin related to thrusting of the Alpine and Carpathian nappes over the European foreland (e.g. Peresson and Decker 1997; Wessely et al. 2006; Froitzheim et al. 2008). Several stages of basins inversion related to the Alpine orogeny caused a development of hiatuses and high erosional reduction in most

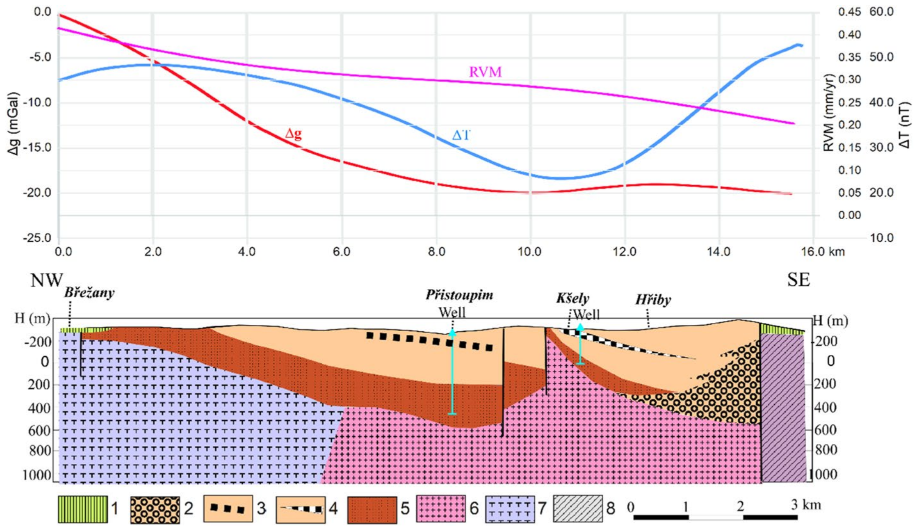

Fig. 3 Geological section across Permo-Carboniferous strata in the Blanice Graben (Český Brod Graben, northern RKB). Modified after Kadlec (2017) with a support of interpreted gravity (Δg) and magnetic (ΔT) data. See the location in Figs. 2, 7, 8, 9, 11 and 18. 1—Upper Cretaceous sediments; Permo-Carboniferous sediments (2–5): 2—breccia to conglomerate; 3—limestone horizon; 4—upper formation with coal; 5—lower formation with coal; 6—intrusive rocks (Central Bohemian Pluton); 7—metamorphic rocks (Teplá-Barrandian unit); 8—metamorphic rocks (Kutná Hora Crystalline unit). RVM—Recent Vertical Movements after Vyskočil (1996)

deposited formations (Malkovský 1980). A number of small remnants of Cenozoic cover are currently located up to tens of kilometres far from the preserved larger continuous Late Cretaceous sedimentary occurrences in the BB and TB centres. The thickness of Late Cretaceous deposits (Klikov Fm.) reaches today in both basins up to > 300 m and of Cenozoic strata with the most important Mydlovary Fm. (Early / Middle Miocene) up to ~ 100 m in the Stropnice Graben (Fig. 4; Malecha et al. 1964; Krásný 1980; Chlupáč et al. 2002). A cumulative thickness of the whole sedimentary cover in the SBB is up to ~ 375 m (Špaček et al. 2011).

2.6 RKB Segmentation

Based on geological and geomorphological characteristics, the following main fault sections have been commonly distinguished within the RKB (Figs. 1, 2):

1. Rodl fault (SW–NE trend; length of > 30 km or > 80 km including its subsurface part in the south) is associated with an up to > 3-km-wide rupture zone comprising a few hundred metres wide belts of mylonite. The fault is followed by contacts between different types of paragneisses and granitoids, locally strongly migmatised, or occurrences of schistose gneiss (Proterozoic or Paleozoic rocks).
2. Kaplice fault (length of ~ 30 km) is considered to form a zone curved from the SW–NE to the SSW–NNE; all fault sections in its northern continuation (3–6) trend in the latter direction. The Kaplice fault is associated with a boundaries between paragneiss

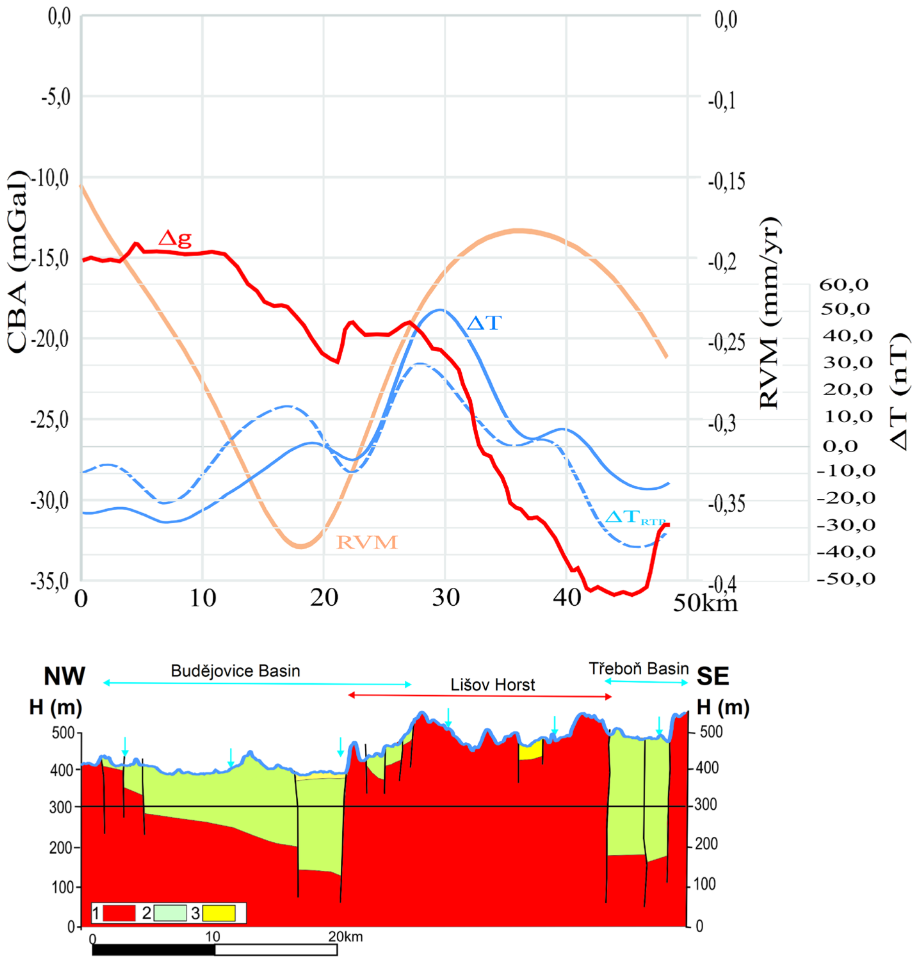

Fig. 4 Geological section across the South Bohemian Basins (middle RKB). Modified after Krásný (1980) with a support of interpreted gravity (Δg) and magnetic (ΔT, $ΔT_{RTP}$—Reduced To Pole version) data. See the location in Figs. 2, 7, 8, 9, 11 and 18. 1—crystalline complexes (Moldanubian unit); 2—Cretaceous sediments; 3—Cenozoic sediments. RVM—Recent Vertical Movements after Vyskočil (1996)

to migmatite rocks in the NW and various granitoid bodies in the SE (Fig. 5). Locally, small tectonic fragments of quartzite or amphibolite and parallel narrow gneissic belts occur. Near Kaplice, a small half-graben structure filled with the Mydlovary Fm. has developed along the fault after the sediment deposition (CGS 2023).

3. Rudolfov fault (length of > 20 km) separates crystalline rocks of the Lišov Horst (paragneiss or migmatite of original Proterozoic or Early Paleozoic age) from Late Cretaceous sedimentary infill of the BB.
4. Drahotěšice fault (length of ~ 20 km) is the main rupture of ~ 30-km-long and ~ 10-km-wide horst-and-graben structure between northern parts of the BB and the TB. A number of faults separate there rocks of various types and age (Proterozoic, Late Paleozoic, Cretaceous, Miocene). Dykes of Late Paleozoic granodiorite were locally emplaced between older crystalline and Permo-Carboniferous sedimentary rocks along

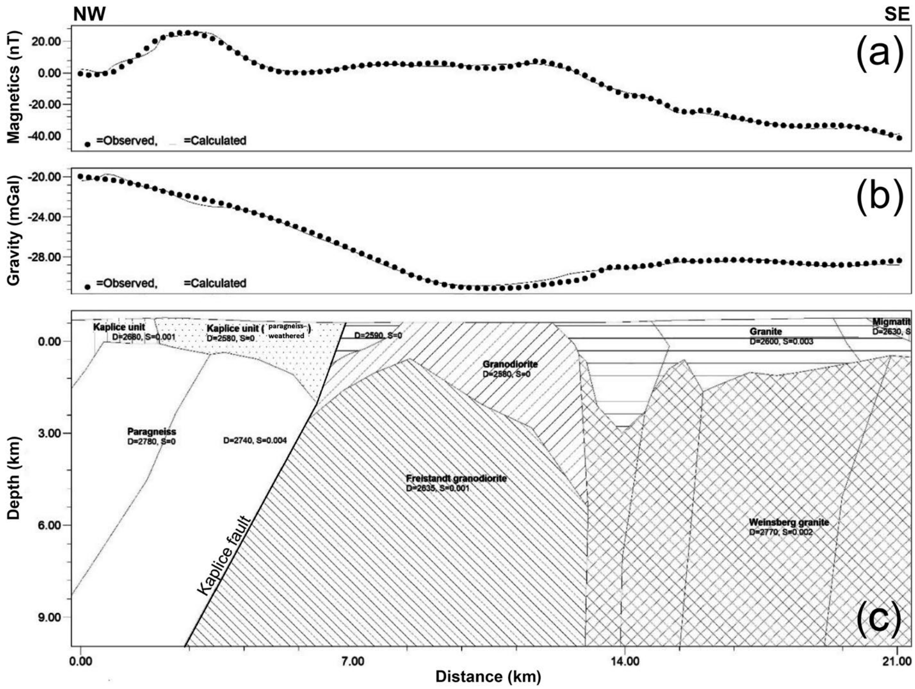

Fig. 5 Structure of the upper crust near the Kaplice fault (southern RKB), modelled based on geological, **a** magnetic and **b** gravity data. **c** Resulting cross section. Modified after Melnyk (2017) and Melnyk et al. (2022). See the location in Figs. 2, 7, 8, 9, 11 and 18

the fault at the end of the Variscan orogeny (Vrána and Janoušek 2006). To the west, the Drahotěšice fault is accompanied by narrow grabens filled with the Mydlovary Fm. or younger Neogene deposits.

5. Blanice fault (length of > 60 km) is geometrically consistent with many other ruptures reported in its vicinity. They separate different Proterozoic rocks, Late Paleozoic rocks or Lower Badenian deposits and create also a part of the Moldanubian / Kutná Hora Crystalline unit boundary.
6. Kouřim fault (length of > 50 km) runs in the south along the Moldanubian / Kutná Hora Crystalline unit boundary (west / east). Towards the north, only fault contacts between different cover rocks (Permo-Carboniferous deposits of the Český Brod Graben—west / Cretaceous clastics of the Bohemian Cretaceous Basin—east) occur on the surface, but in the basement the Moldanubian unit or Central Bohemian Pluton / Kutná Hora Crystalline unit boundary is supposed. The western limit of the Český Brod Graben is also considered to be Kouřim fault-related (e.g. Hintersberger et al. 2017).

Hintersberger et al. (2017) grouped the RKB sections into the two main fault sets: Rodl–Kaplice (1–2) and Rudolfov–Kouřim (3–6). Any clear boundary structural features between the sections 1 and 2 are unknown. Hence, they are commonly termed together as the Rodl-Kaplice fault. The tectonically predisposed residual occurrences of Permo-Carboniferous deposits are considered to be the main common features of the sections 3, 4, 5 and 6.

2.7 Main Faults, Structural Pattern and Middle to Late Cenozoic Development of the SBB

The structural location of the SBB was predisposed by faults of primarily NW–SE to NNW–SSE and SSW–NNE directions. The SBB as a whole or their individual faults separate different crustal segments of the Moldanubian crystalline (Šťovíčková 1973; Mísař et al. 1983). The faults form boundaries also between Cretaceous sequences and Proterozoic / Early Paleozoic rocks at the margins of the BB. In the TB area, Proterozoic rocks of the Lišov Horst and Miocene infill of the Stropnice Graben are fault-limited against different Proterozoic / Paleozoic complexes or Cretaceous deposits (Fig. 2). The linear SW limits of the BB and the TB are additionally fragmented by transverse SW–NE or WSW–ENE faults (Malecha et al. 1964; Špaček et al. 2011).

The SBB are characterised by a prominent horst-and-graben structure, largely completed in the Plio-Pleistocene period (cf. Flašar and Štěpančíková 2022b). On the basin floors, basement rocks only rarely protrude from beneath the sedimentary cover. In the BB, a central NW–SE graben filled with the Mydlovary Fm. is paralleled along both strands by belts of Cretaceous deposits. In the TB, much more complex and denser fault pattern has developed in its N–S trending central depression comprising numerous subsided blocks overlain with Neogene sediments (Mydlovary and the younger formations) limited by NNW–SSE and SSW–NNE faults. On the surface, this N–S depression separates the upper (west) from lower (east) sequence of the Cretaceous Klikov Fm. Both basins of the SBB differ also in dip direction of their crystalline basement (NE in the BB / SW in the TB). The separation of basins by the Lišov Horst uplift is considered to be of Late Pliocene or Early Quaternary age; the vertical differentiation in their boundary area has presumably continued also in younger parts of the Quaternary (cf. Homolová et al. 2012; Popotnig et al. 2013; Flašar and Štěpančíková 2022b). An uplift of the marginal SBB blocks and altitudinal differentiation between both basin floors could be simultaneous events. The young tectonic processes mentioned above have occurred within the frame of horst-and-graben segmentation of the whole Bohemian Massif (e.g. Malkovský 1980; Czudek 2005).

Since the start of the main tectonic activity at the Early / Middle Miocene transition, the overall vertical basement differences have reached in the BB up to 350 m along the Hluboká fault and ~ 250 m along the Rudolfov fault, and in the TB within the Stropnice Graben up to 300 m. Along the zones of the Dubné and Stropnice faults, total uplift values of 400–500 m can possibly be considered (Krásný 1980; Krásný et al. 2012).

A lot of geological, mostly sedimentological evidence from the SBB and the surrounding areas point to significant changes in a direction of the regional drainage during the middle to late Cenozoic. Since the Oligocene until the middle Miocene, streams ran to the east, southeast or south (Malkovský 1975; Tyráček and Havlíček 2009—Early / Middle Miocene deposits; Nehyba and Roetzel 2010—Oligocene to Early Miocene deposits). The present-day drainage to the north by a single stream of the Vltava river (Elbe river tributary) was presumably set up during the Pliocene (Balatka and Sládek 1962; Chlupáč et al. 2002). The reasons of this important change have not yet been satisfactorily explained; they were possibly related to a young general uplift of the Bohemian Massif accompanied by the differential movements of its individual blocks with a formation of new drainage courses in between (Czudek 2005; Flašar and Štěpančíková 2022b). The modifications of regional

Fig. 6 Map of Vertical Gravity Gradient (mGal/m) in the RKB area with added possibly active faults ▶ (Špaček et al. 2011; Navrátilová and Nol 2018), earthquake foci (Špaček et al. 2011) and horizontal velocity vectors of GNSS stations. BG—Blanice Graben. Faults in the SBB area: Tes.f—Těšínov fault; Vlf—Vlhavy fault. Explanation of other fault abbreviations see in Fig. 1

paleohydrography are indicated by a number of fluvial or lacustrine sedimentary remnants at the present-day Vltava / Donau rivers watershed (North Sea / Black Sea drainage divide), either at summit locations or as a few paleo-valley infills stratigraphically attributed to various parts of the Oligocene—Miocene period (Přibyl 1999; Chábera and Huber 2000; Krenmayr et al. 2006; Nehyba and Roetzel 2010).

3 Data Sources and Methods

3.1 Regional Geophysics

The gravity data, allowing to study density structure of the crust, are available in a high detail for the whole Czech Republic (e.g. Blížkovský and Novotný 1981; Lenhardt et al. 2007). The fault-related density boundaries could be traced in the basic Complete Bouguer Anomaly map, derivative maps or visualisations of vertical density contrasts (Linsser 1967; Lenhardt et al. 2007). Additionally, the interpreted gravity profiles allowed to quantify density boundary parameters. The density contacts in the profiles were confronted with the Stripped Gravity map of the Bohemian Massif (Blížkovský and Novotný 1981), providing a structural image of its crystalline basement also beneath sedimentary basins. In this paper, we used the Complete Bouguer Anomaly map for 2.67 g.cm^{-3} reduction density (100 m grid; Geofyzika Brno / Czech Geological Survey—Geofond) and visualised the derivative maps of Vertical Gravity Gradient for Radii (R) of 500 m and 4 km (Fig. 6), Horizontal Gravity Gradient for R of 500 m and 3 km (Fig. 7) and Linsser indications (added in several figures). We created them in the Oasis Montaj Software (Version 162; Geosoft Ltd. 2015), same as the presented overview magnetic and radiometric maps. Most of the resulting regional figures visualising geophysical, geomorphological or geodetic data were made in the ArcGIS software (Esri Inc.).

The magnetic data are suitable to detect faults mostly in volcanic or strongly metamorphosed structural units in those places, where high magnetic susceptibility contrasts occur between adjacent rock complexes. They covered the whole RKB area (Geofyzika Brno / Czech Geological Survey—Geofond; Šalanský 1995; Aric et al. 1997). In this paper, we present the basic Magnetic map of ΔT (Fig. 8), providing an image of distribution of magnetic structures (sources) and their boundaries in the crust. We also considered information in the derivative maps of Vertical Magnetic Gradient, Horizontal Magnetic Gradient, Structural Lines and Euler Deconvolution.

The radiometric data, coming from the Radiometric map of the Czech Republic (Mannová and Matolín 1995), reflect natural radioactivity of rocks. The parameters characterising this radioactivity are gamma-ray dose rate (Da [nGy.h^{-1}]) and mass concentration of potassium (% K), uranium (ppm eU) and thorium (ppm eTh). The radioactive field is expressed in Da 1 m above the land surface. However, the radionuclide concentration in near-surface autochthonous covers well characterises properties of basement rocks in the depth. Hence, the isoline map constructed with 10 nGy.h^{-1} basic interval highlights large geological objects, whereas the radioactive image of local objects

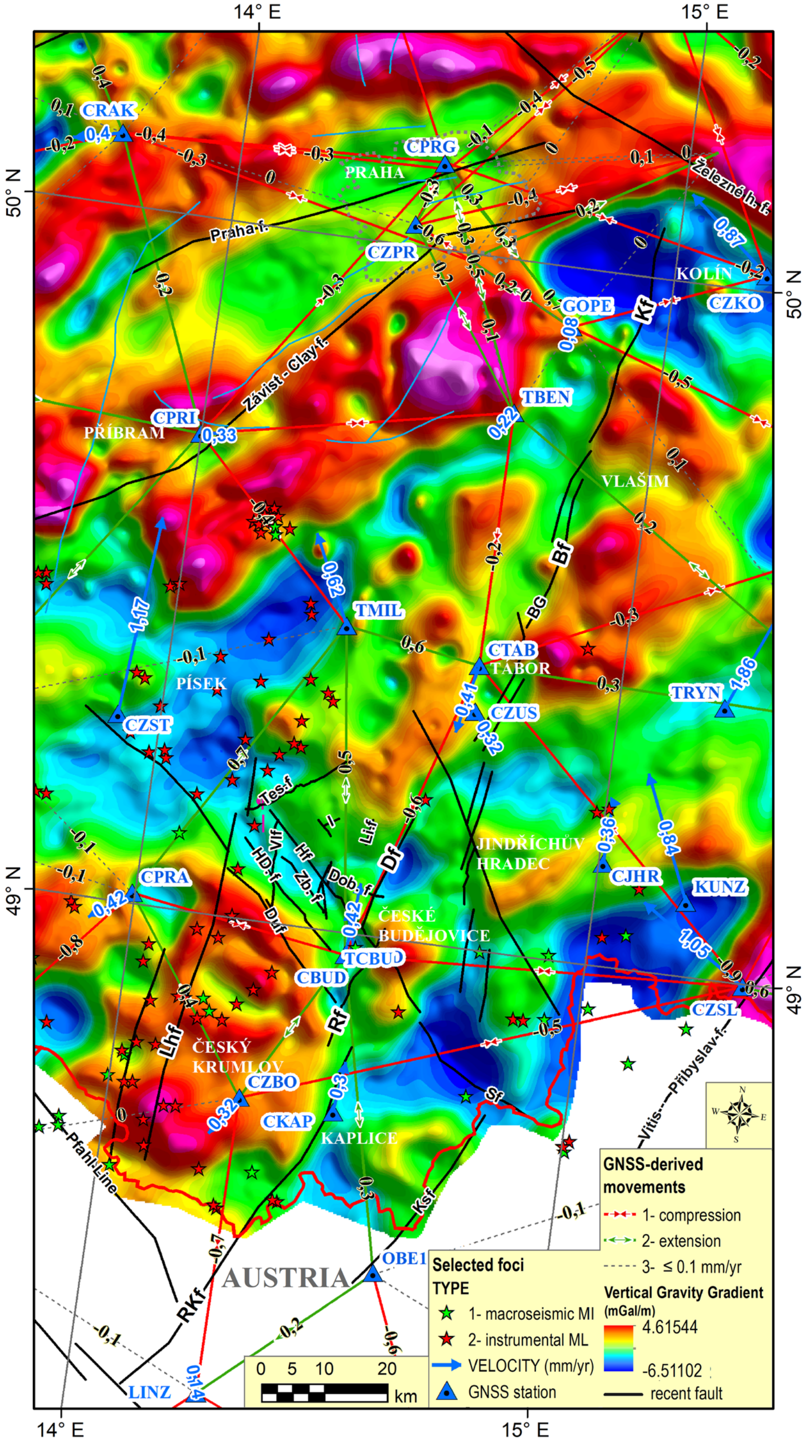

14° E
15° E
50° N
49° N
PRAHA
KOLÍN
PŘÍBRAM
VLAŠIM
PÍSEK
TÁBOR
JINDŘICHŮV HRADEC
ČESKÉ BUDĚJOVICE
ČESKÝ KRUMLOV
KAPLICE
AUSTRIA
CRAK
CPRG
CZPR
GOPE
CZKO
TBEN
CPRI
TMIL
CTAB
CZUS
TRYN
CZST
CPRA
TCBUD
CBUD
CJHR
KUNZ
CZSL
CZBO
CKAP
OBE1
LINZ
Praha f.
Závist - Clay f.
Železné h. f.
Kf
Bf
BG
Df
Rf
Lhf
RKf
Sf
Ksf
Pfahl-Line
Vitis---Přibyslav-f.
Tes.f
Vlf
Hf
HD. f
Zb. f
Dob. f
Duf
Llf
Selected foci
TYPE
1- macroseismic MI
2- instrumental ML
VELOCITY (mm/yr)
GNSS station
GNSS-derived movements
1- compression
2- extension
3- ≤ 0.1 mm/yr
Vertical Gravity Gradient (mGal/m)
4.61544
-6.51102
recent fault
0 5 10 20 km

Fig. 7 Map of Horizontal Gravity Gradient (mGal/m) in the RKB area with added possibly active faults, ▶ location of geological sections across the RKB, earthquake foci (Špaček et al. 2011; IG CAS—Institute of Geophysics of the Czech Academy of Sciences: WEBNET 2022) and horizontal velocity vectors of GNSS stations. Explanation of the fault abbreviations see in Figs. 1, 6

is suppressed. In this paper, we visualise a part of the Radiometric map for the RKB area (Fig. 9).

Finally, we reviewed archive vertical electric sounding data, reflection seismic data and complex geophysical studies obtained in the SBB and the Bohemian Cretaceous Basin (research reports by Kadlec et al. 1975; and those in Vacek ed. 1983) to improve the knowledge of location and dip direction of fault planes and support the transverse geological section in the SBB by geophysical curves. Noteworthy, seismic data (distribution of crustal velocities) from the significant regional refraction profiles (CEL09, S04; Hrubcová et al. 2005, 2010) do not offer a useful information for detailed research of the RKB structure.

3.2 Geomorphology

The new schematic overview map (Fig. 10) illustrates surface expressions of the RKB, SBB and Lhenice fault structures and indicates a linear plan of their surroundings; such a geomorphological view of the study area has not yet been presented. For the figure creation, we used a merged digital elevation model based on airborne scanning (light detection and ranging method) with 10-m grid in the Austrian territory (Land Oberösterreich 2021) and with 5-m grid in the Czech territory (CUZK 2022). The elevation model was partly compared to the satellite Landsat 7 ETM + (colour syntheses 321, 531 or 753) and SRTM (1 arc-second resolution) images, both provided by the NASA/USGS (2023). In the map, we drew over the regional topography manually extracted representatives (elements) of selected significant geomorphological phenomena. Hence, the approach involved a generalisation of all landforms included. We applied various visualisation modes of the data used (contours, digital elevation model, hillshade) during delineation of the elements. The following steps led to indication and assessment of the phenomena spatially concordant or discordant to the main regional faults, primarily of (straight-)linear character.

1. Basic geographical directions were categorised as longitudinal (N–S, SSW–NNE, SW–NE and WSW–ENE) and transverse (W–E, WNW–ESE, NW–SE and NNW–SSE) with regard to the general strike of the RKB.
2. Slope sections (outside valleys), elongated ridges and valley sections as the three basic types of distinct linear landforms at the local scale were searched for in the whole RKB area and drawn in the map according to their prevailing trend within one of the two direction categories mentioned in the step (1). The slopes were delineated as lines at their feet, where the highest changes in gradient commonly occur. We distinguished the two types of slope landforms (length > 500 m): scarps (steep surfaces of a high lateral continuity; max. height > 20 m, max. gradient > 20°) and significant topographic gradients (more complex higher slopes separating gently inclined lower surfaces from higher surfaces at boundaries of adjacent topographic segments; max. height mostly > 50 m). The distinct elongated ridges are represented in the map by their longitudinal axes (length > 500 m, max. relative height > 30 m). The (straight-)linear

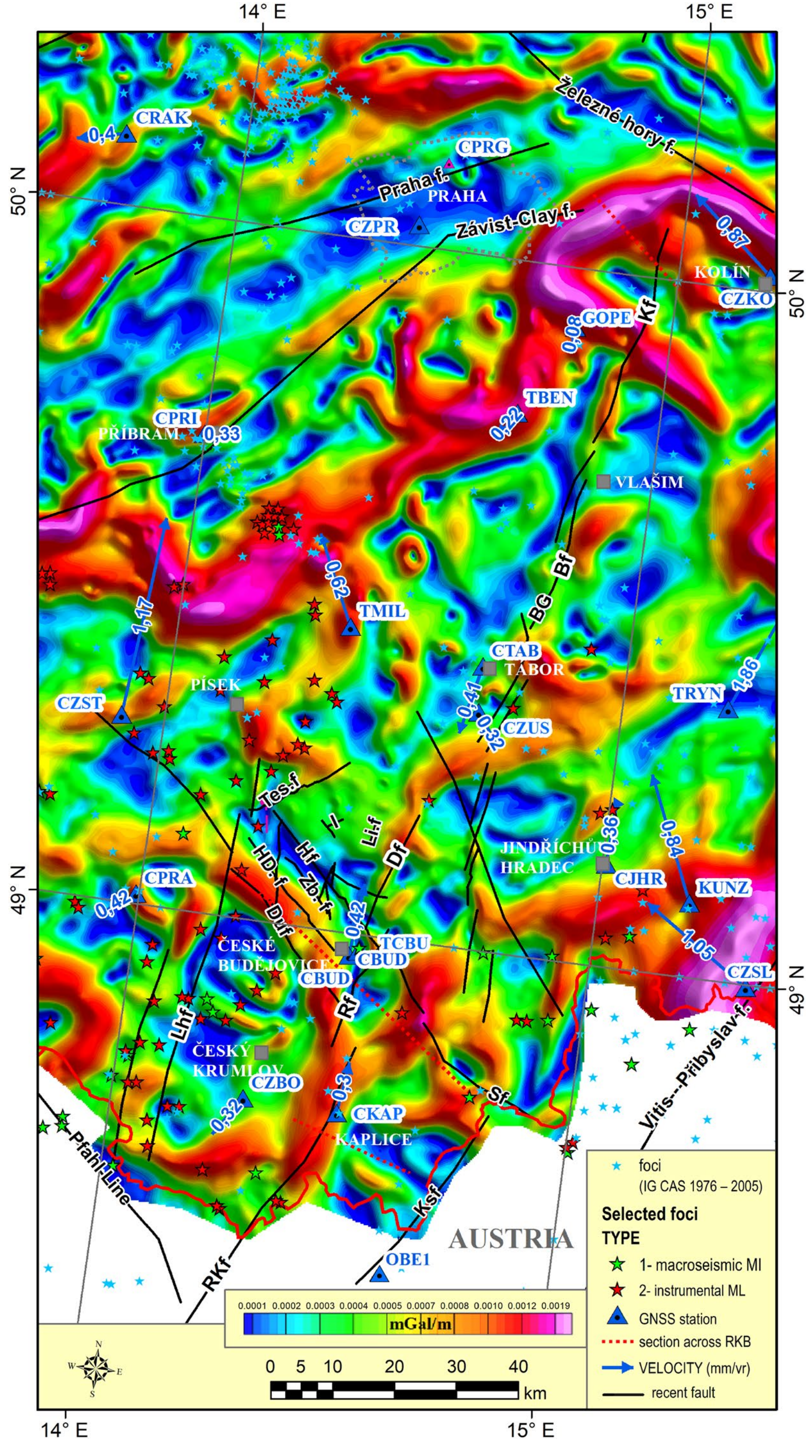
14° E
15° E
50° N
49° N
CRAK
0,4
CPRG
Praha f.
PRAHA
CZPR
Závist-Clay f.
Železné hory f.
0,87
KOLÍN
CZKO
GOPE
0,08
Kf
TBEN
0,22
CPRI
PŘÍBRAM
0,33
VLAŠIM
0,69
1,17
TMIL
BG
Bf
CTAB
TÁBOR
PÍSEK
CZST
0,41
0,32
CZUS
TRYN
1,86
Tes.f
Li.f
Hf
HD.f
Zb.f
Df
JINDŘICHŮV HRADEC
0,36
0,84
CJHR
KUNZ
CPRA
0,42
TCBU
CBUD
ČESKÉ BUDĚJOVICE
Rf
1,05
CZSL
Lhf
ČESKÝ KRUMLOV
CZBO
0,32
0,3
CKAP
KAPLICE
Sf
Pfahl-Line
Vitis--Přibyslav-f.
Ksf
AUSTRIA
OBE1
RKf
0.0001 0.0002 0.0003 0.0004 0.0005 0.0007 0.0008 0.0010 0.0012 0.0019
mGal/m
0 5 10 20 30 40
km
foci
(IG CAS 1976 – 2005)
Selected foci
TYPE
1- macroseismic MI
2- instrumental ML
GNSS station
section across RKB
VELOCITY (mm/yr)
recent fault

Fig. 8 Magnetic map of ΔT (nT) in the RKB area. Possibly active faults, location of geological sections ▶ across the RKB, earthquake foci (Špaček et al. 2011; IG CAS: WEBNET 2022) and horizontal velocity vectors of GNSS stations are added in the image. Explanation of the fault abbreviations see in Figs. 1, 6

valley sections, including both simple landforms and elongated belts of meanders, were drawn as valley floor axes (length > 500 m, max. depth > 30 m).

3. The three other related phenomena of point character at the given scale were added in the map: distinct saddles, (commonly associated with two counter-directed linear valley heads together forming larger elongated landforms of linear nature; relative depth > 25 m), abrupt changes (bends) in valley (or stream) direction into trend of a significant fault (RKB section or the Lhenice fault; change in orientation > 30°) and facets (roughly planar triangular or trapezoidal surfaces in a sense by Fairbridge 1968; Keller and Pinter 2002; or Burbank and Anderson 2011). The first type of phenomena was marked only in a vicinity of the significant fault structures (RKB, SBB, Lhenice), the second type only at large rivers near these structures and the third type in the whole area. The features of all three types could be also distinguished as RKB-longitudinal or transverse ones based on their geometric properties, either own (strike of facet surface, trend of valley section subparallel to the fault down the distinct bend) or of supplementary landforms (the case of saddles).
4. Selected similarly oriented linear landforms were spatially grouped in the two ways, based on their relation to the RKB trend and different style of their spatial arrangement: (i) oriented in longitudinal directions and frequently fairly concentrated in narrow linear zones of common 5–15 km width; and (ii) oriented in transverse directions and mostly distributed only in wider subareas with one prevailing surface trend. Hence, both the types of groups were marked and termed differently in the map (Fig. 10) as (i) longitudinal linear landform zones and (ii) transverse linear landform sets. Additionally, the former groups (longitudinal landform zones) were classified based on a strike similarity to the significant fault structures into the sub-categories I (SW–NE; strike of the Rodl fault); II (SSW–NNE; strike of the Rudolfov, Drahotěšice, Blanice and Kouřim faults); III (approximately N–S; strike of the Lhenice fault); IV (purely N–S; strike of the Haselgraben); and V (WSW–ENE; strike of the Závist-Clay fault system in its NE section).
5. Finally, spatial relations between longitudinal and/or transverse elements were assessed. We schematically highlighted (i) in the whole RKB area abrupt terminations of the longitudinal landform zones against another linear zones or transverse landform sets in those places where the particular linear surface trends do not continue on the opposite strands of the crossing landform groups, and (ii) in the marginal areas of the SBB the main topographic segments (blocks) of a low crustal disruption and relative high surface related to their lower surroundings commonly associated with an increased density of linear landforms.

As to the recent tectonic activity, facets and distinct scarps can be the results of the related processes (cf. Keller and Pinter 2002; Burbank and Anderson 2011). However, the geometry of these landforms does not directly indicates the date or the way of their origin. In the slowly deformed areas, strong landform modifications by syn- and post-genetic surface erosion or significant influences of different rock resistance on the opposite fault strands used to be involved in their development.

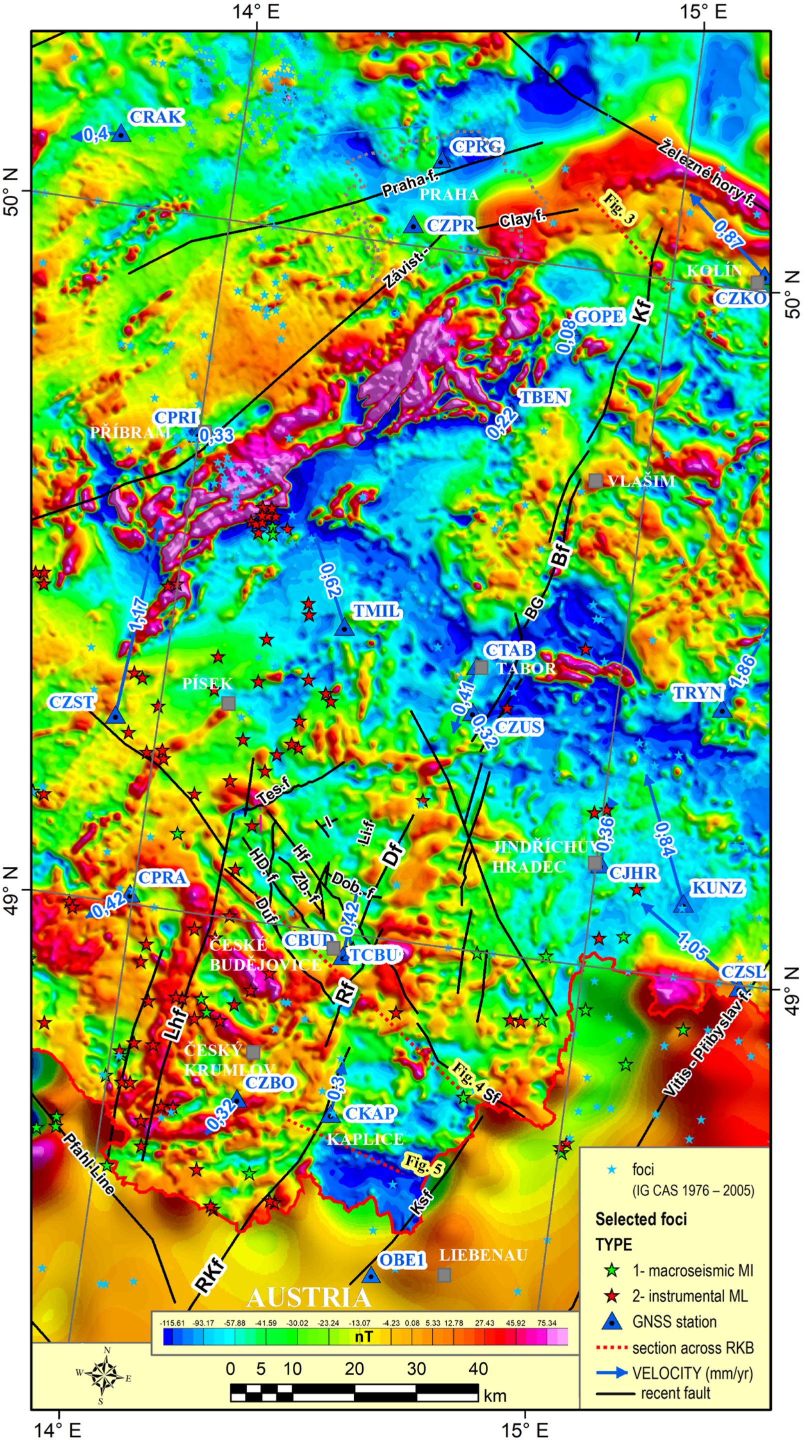
14° E
15° E
50° N
49° N
CRAK
0,4
CPRG
PRAHA
Praha f.
CZPR
Clay f.
Závist
Železné hory f.
Fig. 3
0,87
KOLÍN
CZKO
GOPE
0,08
Kf
TBEN
0,22
CPRI
PŘÍBRAM
0,33
VLAŠIM
Bf
BG
0,92
TMIL
1,17
CTAB
TÁBOR
PÍSEK
CZST
0,41
0,32
CZUS
TRYN
1,86
Tes.f
Li.f
Df
Hf
HD.f
Zb.f
Dob. f
Duf
0,36
0,84
JINDŘICHŮV HRADEC
CJHR
KUNZ
CPRA
0,42
1,05
CBUD
TCBU
ČESKÉ BUDĚJOVICE
CZSL
Rf
Lhf
ČESKÝ KRUMLOV
Fig. 4
Sf
Vitis - Přibyslav f.
CZBO
0,3
0,32
CKAP
KAPLICE
Fig. 5
Pfahl Line
Ksf
RKf
OBE1
LIEBENAU
AUSTRIA
-115.61 -93.17 -57.88 -41.59 -30.02 -23.24 -13.07 -4.23 0.08 5.33 12.78 27.43 45.92 75.34
nT
0 5 10 20 30 40
km
N
W
E
S
foci
(IG CAS 1976 – 2005)
Selected foci
TYPE
1- macroseismic MI
2- instrumental ML
GNSS station
section across RKB
VELOCITY (mm/yr)
recent fault

Fig. 9 Part of the Radiometric map of the Czech Republic (Mannová and Matolín 1995; Da values in nGy/h), with added possibly active faults, location of geological sections across the RKB, earthquake foci (Špaček et al. 2011; IG CAS: WEBNET 2022) and horizontal velocity vectors of GNSS stations. Explanation of the fault abbreviations see in Figs. 1, 6 ▸

3.3 Seismology

The regional seismicity was taken into account based on the data in the catalogues of instrumentally recorded earthquakes covering large areas of the Czech Republic (Kárník et al. 1981; Sýkorová et al. 2019; WEBNET 2022). We visualised the earthquake foci in the maps of regional geophysical fields as phenomena related to deeper parts of the crust. Data presented in the significant regional studies or reports (Lenhardt et al. 2007; Špaček et al. 2011; Prachař 2014) were considered as well, including interpretations of earthquake properties. Additionally, we compiled three cross-section models transverse to the RKB with orthogonally projected earthquake foci categorised according to the magnitudes to illustrate a different seismic activity west and east of the RKB, and north and south of the SBB.

3.4 Geodesy

3.4.1 Repeated High Precision Levelling

The Czech Republic is covered by the State Levelling Network. Based on the results of remeasurement of the levelling lines of orders I and II in a 30-years interval, Vyskočil (1996) compiled a Recent Vertical Movements map, later reambulated (estimated vertical accuracy L $\times$ 0.04 mm yr^{-1}, where L is a distance in km between the particular points). We used a part of the map for assessment of vertical movement tendencies in the RKB area (Fig. 11).

3.4.2 GNSS Monitoring

The procedures used for the processing of the GNSS geodetic data to assess kinematic behaviour of individual crustal blocks were described in our earlier works (Pospíšil et al. 2017; Roštínský et al. 2020). In this paper, we present the analysis of recent horizontal movement tendencies of 20 suitably spaced active permanent stations of the EPN, CZEPOS, GEONAS, TOPNET, VESOG and VRS-NOW networks in an area of southern Bohemia surrounding the RKB. However, the GNSS data from a larger region were considered. The processed data volume involved for each year two consecutive days (2×24 h) in the spring as well as in autumn period for available parts of the considered time span (2005–2021; totally 6.1–13.0 years for the individual stations). The evaluation parameters included elevation mask angle 10º, CODE precise satellite orbits and Earth's rotation parameters, CODE absolute offsets and variations of antenna phase centres, QIF ambiguity solution strategies and tropospheric parameters estimated in 1-h intervals. The resulting solution was obtained using an iono-free combination of the phase data on both carrier frequencies (L1, L2). The assessment of the data was done by individual days. The coordinate solution of each day in IGS14 reference frame we obtained by a connecting to the reference (fiducial) GNSS points WTZR, GOPE (IGS network) and CLIB, CPAR, CTAB, LINZ and POUS (EPN network) by minimally constrained adjustment. We used the Bernese Software 5.2 (Dach et al. 2015) and reprocessing support products (CODE REPRO 2015).

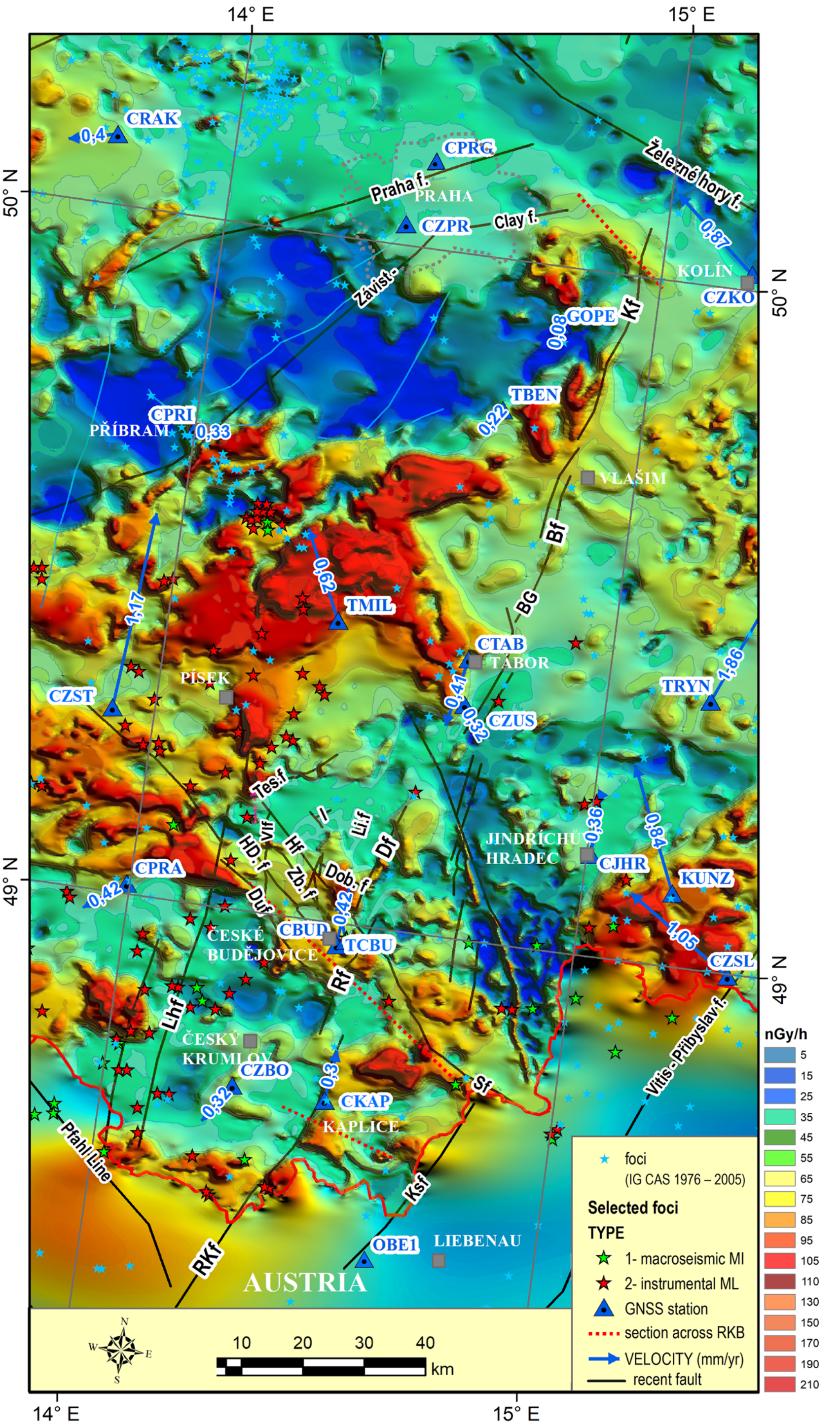
14° E
15° E
50° N
49° N
CRAK
0,4
CPRG
PRAHA
Praha f.
CZPR
Clay f.
Železné hory f.
0,87
KOLÍN
CZKO
Závist.
GOPE
0,08
Kf
TBEN
0,22
CPRI
PŘÍBRAM
0,33
VLAŠIM
Bf
0,62
TMIL
BG
1,17
CTAB
TÁBOR
PÍSEK
CZST
0,41
0,32
CZUS
TRYN
1,86
Tes.f
Vlf
HD.f
Hf
Zb.f
Li.f
Df
Dob.f
JINDŘICHŮV HRADEC
0,36
CJHR
0,84
KUNZ
CPRA
0,42
Duf
0,42
CBUD
TCBU
ČESKÉ BUDĚJOVICE
1,05
CZSL
Rf
Lhf
ČESKÝ KRUMLOV
CZBO
0,32
0,3
CKAP
KAPLICE
Sf
Vitis - Přibyslav f.
Pfahl Line
Ksf
RKf
OBE1
LIEBENAU
AUSTRIA
foci
(IG CAS 1976 – 2005)
Selected foci
TYPE
1- macroseismic MI
2- instrumental ML
GNSS station
section across RKB
VELOCITY (mm/yr)
recent fault
10 20 30 40
km
nGy/h
5
15
25
35
45
55
65
75
85
95
105
110
130
150
170
190
210

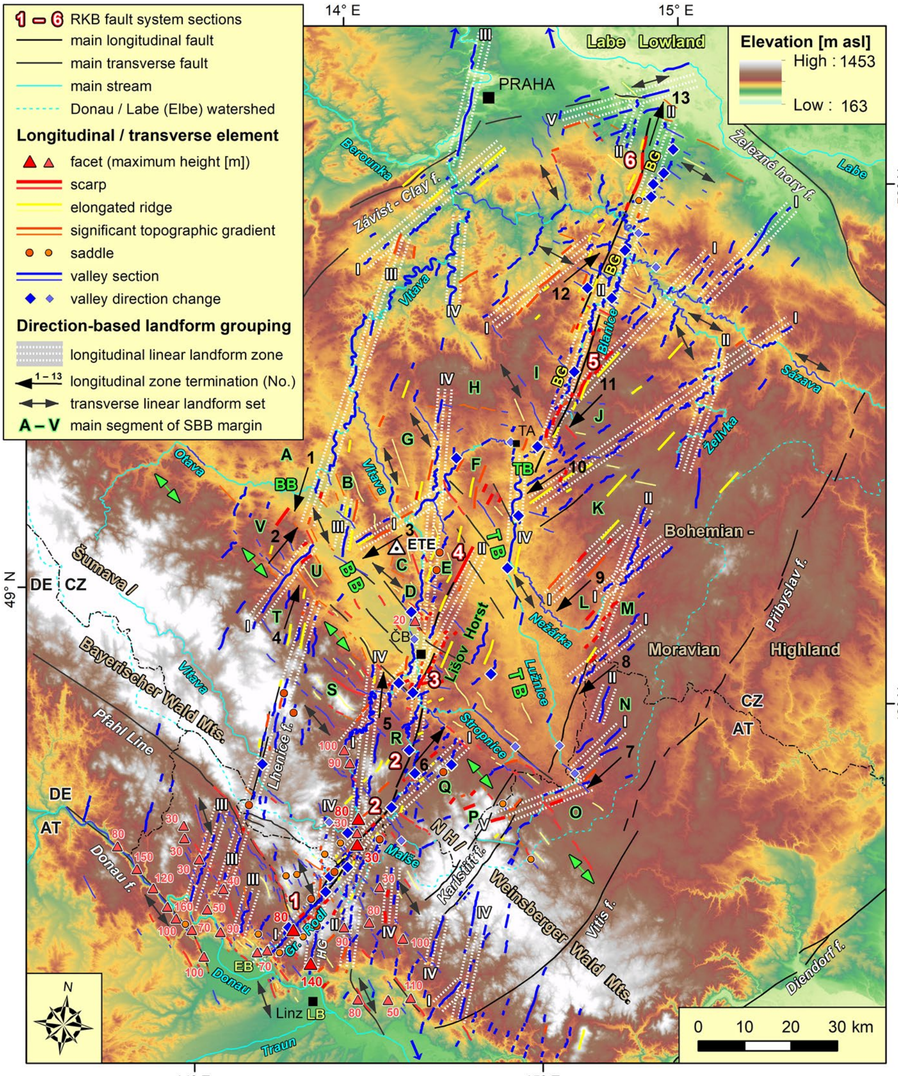

Fig. 10 Significant geomorphological features in the RKB area. The main linear landforms are categorised as longitudinal (N–S, SSW–NNE, SW–NE and WSW–ENE) or transverse (W–E, WNW–ESE, NW–SE and NNW–SSE) with regard to the general trend of the complex RKB fault system. The uppermost river reaches are missing in the figure because of spatial ambiguity of several major streams. The main RKB sections are the same as in Fig. 2. Main general trends (sub-categories) of the longitudinal linear landform zones: I—SW–NE; II—SSW–NNE; III—approximately N–S; IV—purely N–S; V—WSW–ENE. Alpine Molasse Basin: EB—Eferding Basin; LB—Linz Basin. NH—Nové Hrady Mts. SBB—South Bohemian Basins (phenomena indicated by light green map elements, descriptions or masks): BB—České Budějovice Basin; TB—Třeboň Basin, both separated by the Lišov Horst; smaller abbreviations indicate basin segments without Cretaceous sedimentary infill but with preserved larger bodies of Cenozoic deposits; green double side arrows—fairly continuous trend of the southwestern SBB marginal zone against the Bayerischer Wald–Weinsberger Wald Mts. BG—Blanice Graben. ČB—České Budějovice; TA—Tábor. ETE—Nuclear Power Plant Temelín

4 Results

4.1 Geophysical Fields

4.1.1 Gravity

The regional gravity field mostly reflects granitoid bodies of the Central Bohemian and Moldanubian plutons inducing large negative anomalies (e.g. Figs. 3, 5). Many anomalies are related to higher depths of rock bodies reaching 5–8 km. A large gravity minimum extends from the middle RKB area towards the south, where it is amplified by Mesozoic and Cenozoic sedimentary cover in front of and within the northern Alps (Wessely et al. 2006; Lenhardt et al. 2007; Pfleiderer et al. 2016). The RKB is reasonably traceable in both presented images of Vertical Gravity Gradient (Fig. 6) and Horizontal Gravity Gradient (Fig. 7). A sharp gradient between paragneiss and granitoids has developed along the Kaplice fault (Fig. 5). A zone of distinct gradients occurs also along the southern and middle BG. In the SBB, the gravity field is influenced by transverse horsts and grabens. However, two individual blocks along the Rudolfov and Drahotěšice faults are associated with the SSW–NNE elongated positive anomalies consistent with the dominant RKB trend. In the north, the WNW–ESE to NW–SE-oriented gravity anomalies correspond to the Elbe shear zone geometry.

4.1.2 Magnetics

In the magnetic field, a number of consistent anomalies have developed along large parts of the RKB (Fig. 8). The highly fragmented SBB and several surrounding areas are characterised by mostly negative ΔT values. Local positive anomalies reflect metamorphic rocks in the basement, sometimes of ultrabasic character (e.g. the western margin of the TB near the Rudolfov and Drahotěšice faults). The northern Rodl-Kaplice fault sharply separates a positive area in the NW from a smaller negative area in the SE, the latter also limited against another positive anomaly along the SW–NE striking Karlstift fault. The Lhenice fault is followed by a subparallel positive anomaly belt. A trend of the transverse Železné hory fault within the Elbe shear zone corresponds well to the WNW–ESE orientation of another positive anomaly belt north of the Kouřim fault.

4.1.3 Radiometry

The variable radioactivity in the RKB area (Fig. 9) reflects changing rock lithology and different evolution of the individual crustal units (e.g. Mannová and Matolín 1995). In the Monotonous Group of the Moldanubian unit, biotite and sillimanite paragneiss to migmatite (Da 55–75) and mica-schist (Da 60–90) are characteristic rocks, frequently with a fairly uniform field of radioactivity values. The metamorphosed rocks of the Moldanubian Variegated Group, represented by quartzite, quartz gneiss, crystalline limestone and amphibolite, form local radioactivity minima (Da 35–75). The granulite bodies are associated with a low radioactivity (Da 35–60), mainly caused by a low abundance of uranium and thorium (K: 2–4%, U: 1 ppm, Th: 1–8 ppm). Orthogneiss occurs in smaller bodies of various radioactivity; to the most active ones belong Choustník orthogneisses at the southern BG (Da 70–110). The Kutná Hora Crystalline unit, mostly comprising orthogneiss and mica-schist, provides intermediate radioactivity values

Fig. 11 Recent vertical movements (RVM; mm/yr) in the RKB area (after Vyskočil 1996; arranged by the ▶ authors). Possibly active faults, location of geological sections across the RKB and horizontal velocity vectors of GNSS stations are added in the map. Note the most distinct NNW–SSE trending subsidence zone between the town of Příbram and the Czech-Austrian border. Explanation of the fault abbreviations see in Figs. 1, 6

(Da 60–90). The Moldanubian and Central Bohemian plutons (Da 50–200) are composed of numerous rock types, several of a high radioactivity. On the contrary, sediments of the Permo-Carboniferous basins are characterised by a uniform low radioactivity (commonly Da < 50). Cretaceous and Tertiary sediments of the SBB have the radioactivity values of Da 60–110, reflecting deposition in a closed basin space and influence of rocks coming from the surrounding crystalline units. The increased radioactivity of Quaternary sediments deposited by the Lužnice river in the TB is induced by a high content of thorium (K: 2.6%, U: 6.3 ppm, Th: 32.3 ppm).

Although the Radiometric map primarily expresses a character of the surface crust layer, it displays also many sharp gradients correlatable to the known faults in a deeper structure as visible along the Rodl-Kaplice fault and several parts of the BG. The fault-consistent radiometric elements occur also in the SBB, remarkable of which are a large NNW–SSE trending negative anomaly in the TB and sharp gradients along faults in the BB subparallel to the Drahotěšice fault. The Železné hory fault is manifested by low radioactivity values.

4.2 Geomorphological Features

4.2.1 General Topography

The RKB is accompanied by a diverse mountain (southern part), highland or hilly (middle and northern parts) topography within ~ 10–20-km-wide belt. On the surface, the fault system runs from the northern margin of the Alpine foreland basin (small Eferding Basin) through the contact area between the Bayerischer Wald (referred to as Šumava in the Czech territory) and the Weinsberger Wald (referred to as Nové Hrady in the Czech territory) as the two highest segments of a NW–SE trending middle-mountain range, across the SBB, longwise an elongated depression related to the BG structure crossing the NW Bohemian-Moravian Highland, up to the southern Labe Lowland (Fig. 10). The differences in local relief along the RKB reaches from ~ 100 m (SBB) up to ~ 600 m (Bayerischer Wald–Weinsberger Wald Mts.). The fault system commonly separates dissimilar geomorphological units; distinct subparallel horsts, grabens or significant (up to > 300 m high) sharp vertical surface differences between its opposite strands commonly occur. The floor of the BB, geomorphologically well-constraint against the basin rims, is located > 50 m lower as compared to the less prominent floor of the TB, partly because of lower base level of the major Vltava river.

4.2.2 Topographic Features Related to the Main Faults

Among the extracted linear geomorphological features in Fig. 10, valley sections are most common, followed by slope sections and less visualised elongated ridges. The faults of the RKB are accompanied also by significant saddles and sharp valley (stream) bends.

The Rodl fault separates surface levels of unequally elevated crustal segments at the SE termination of the Bayerischer Wald Mts. (difference up to ~ 200 m) with marginal topographic gradients, scarps and several facets up to 100 m high in between. The fault trace is best expressed by the linear direction of several slightly meandering Grosse Rodl

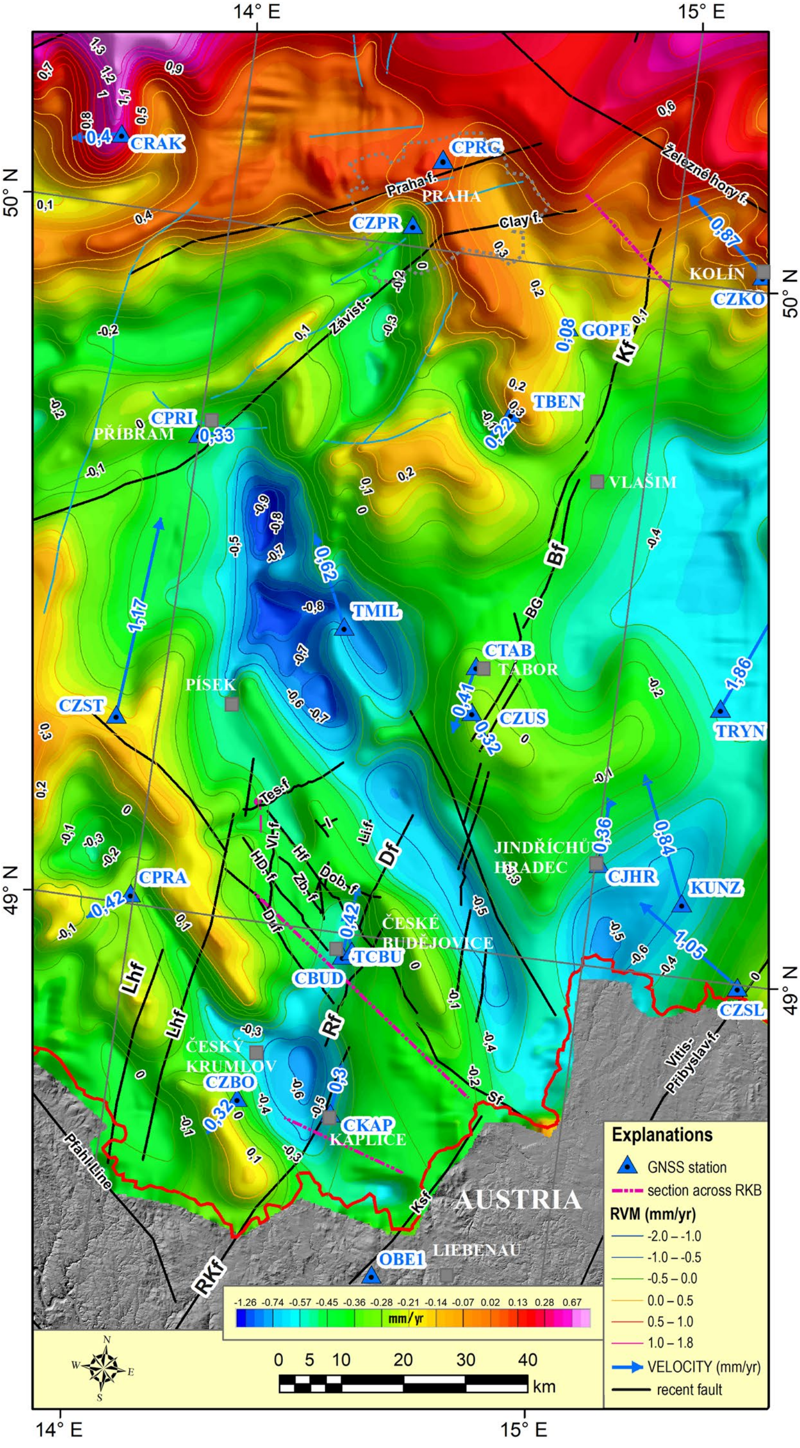

14° E
15° E
50° N
49° N
CRAK
0,4
CPRG
PRAHA
Praha f.
CZPR
Clay f.
Železné hory f.
0,87
KOLÍN
CZKO
Závist.-
GOPE
0,08
Kf
TBEN
0,22
CPRI
PŘÍBRAM
0,33
VLAŠIM
0,92
Bf
BG
TMIL
1,17
CTAB
TÁBOR
PÍSEK
CZST
0,41
CZUS
0,32
1,86
TRYN
Tes.f
Vl.f
Hf
Li.f
Df
HD.f
Zb.f
Dob.f
Du.f
JINDŘICHŮV HRADEC
0,36
CJHR
0,84
KUNZ
CPRA
0,42
ČESKÉ BUDĚJOVICE
TCBU
CBUD
1,05
CZSL
Lhf
Rf
ČESKÝ KRUMLOV
CZBO
0,32
0,3
CKAP
KAPLICE
Sf
Vitis-Pribyslav.f.
Pfahl Line
Ksf
AUSTRIA
RKf
OBE1
LIEBENAU
Explanations
GNSS station
section across RKB
RVM (mm/yr)
-2.0 – -1.0
-1.0 – -0.5
-0.5 – 0.0
0.0 – 0.5
0.5 – 1.0
1.0 – 1.8
VELOCITY (mm/yr)
recent fault
-1.26 -0.74 -0.57 -0.45 -0.36 -0.28 -0.21 -0.14 -0.07 0.02 0.13 0.28 0.67
mm/yr
0 5 10 20 30 40
km
N
E
S
W

river valley sections. In a close vicinity of the Kaplice fault, a significant change in trend of the large Vltava river valley from the NW–SE (upper reach) into the S–N (middle reach) occurs. Another consistent abrupt valley bend has developed along the Malše river running from the opposite SE direction. The distinct low scarp along the Rudolfov fault is a part of the sharp BB / Lišov Horst boundary. The Drahotěšice fault runs along the eastern margin of another horst between the BB and the TB elongated SSW–NNE, with summit surfaces 100–150 m above both basin floors similarly to those of the near Lišov Horst. The former horst is accompanied by a few subparallel elongated scarps, ridges, valley sections and chains of small grabens filled with Miocene deposits, separated by saddles. The Blanice fault and associated ruptures correspond to up to 15-km wide and 150-m deep asymmetric depression in the southern BG. A number of scarps, topographic gradients, valley sections and elongated ridges occur mostly along the eastern margin of this structure. The floor of the depression is followed by several reaches of the meandering Blanice river and in its northern part by a distinct offset-like section of the larger Sázava river, generally running in the transverse ESE–WNW direction consistent with the general trend of the Elbe shear zone. The Kouřim fault is accompanied by several slightly curved scarps between higher surfaces in the west and lower surfaces in the east (difference up to 150 m) in a total length of > 15 km, most distinct of which are related to the structural boundary between Permo-Carboniferous and Cretaceous sedimentary covers.

Besides the RKB, the following other regional fault structures have significant topographic manifestations. The Lhenice fault is accompanied by an elongated depression with distinct saddles crossing a higher terrain. Near its possible northern continuation, the middle Otava river direction abruptly changes from the W–E into the S–N consistently with the Lhenice fault strike. In the TB, several valley bends into trends of significant faults have developed along the Stropnice and Lužnice rivers. The SE part of the Pfahl Line is expressed by a ~ 40-km-long chain of distinct slope sections within the Bayerischer Wald Mts. (heights up to 400 m, mean gradients ~ 15°).

4.2.3 Spatial Groups of Similarly Oriented Linear Surface Phenomena

In the RKB area, we distinguished > 35 narrow longitudinal landform zones indicated by their approximate axes (white polylines) and > 12 transverse landform sets marked differently by double side dark grey arrows (Fig. 10). Based on their general trends, the linear landform zones accompany large parts of the significant fault structures mentioned in Sect. 3.2, item 4. Additionally, their sub-category I occurs along SW part of the Kaplice fault, at the eastern margins of the BB and TB, and obliquely to the BG. The zones of the sub-category II have developed at the eastern margin of the TB and parallel to the BG. The sub-category III exists in the westernmost RKB area, whereas the sub-category IV in its middle and southern parts including zones along the middle Vltava river valley down the sharp bend of the stream and one along the middle Lužnice river valley. The zones of the sub-category V occur only south of the TB and north of the BG. In total, we marked in the study area > 10 (I), > 5 (II), 5 (III), > 5 (IV) and 2 (V) linear zones, respectively. The landform zones commonly mutually intersect. However, at least 13 of their abrupt terminations exist (marked by one side black arrows in Fig. 10). Most of these terminations (~ 10) are developed in the SBB and their marginal areas, the remaining ones along the BG.

The latter groups (transverse landform sets) seem to occur most densely in the Bayerischer Wald–Weinsberger Wald Mts. and in the SBB as the two geomorphological units characterised by dominant NW–SE to NNW–SSE-oriented landforms (8 and 4 indicative symbols in the same map, respectively); fairly continuous boundary between both these large units (highlighted by double side light green arrows) runs consistently, as well as the Donau fault and Pfahl Line fault structures. The transverse landform sets are more continuous phenomena than the landform zones, as they run across large parts of the investigated area and only rarely sharply diminish within landform groups of different directions.

4.2.4 SBB Segmentation

The SBB represent a structure densely fragmented by linear landforms, including its marginal areas or even floors of the main basins (BB, TB). The groups of linear phenomena, both longitudinal and transverse ones, limit there a number of smaller topographic blocks. We marked schematically 22 such larger individual segments (Fig. 10; A–V). The longitudinal zones have influenced the fragmentation more significantly (~15 segment boundaries) than the concentrated transverse elements (~5 segment limits). The block contacts are frequently related to changes in prevailing linear landform trends between the opposite strands (at least 8 such cases).

4.2.5 Possible Young Morphotectonic Features

The facets along the main RKB sections, sometimes with more discernible generations of surfaces, are scarce phenomena; they occur only in southern part of the fault system (Fig. 10; sections 1, 2 and possibly 3). However, well-shaped facets up to 100 m high have evolved along several oblique N–S rupture zones (Haselgraben, middle Vltava river valley south of the SBB). Steep scarps, presumably genetically related to the faceted slopes, are most distinct and continuous along the BB / Lišov Horst boundary in the SBB. The morphotectonic features related to the RKB mentioned above complete more numerous sets of similar phenomena along the transverse NW–SE to NNW–SSE faults in the southernmost Bohemian Massif. These are most abundant at the Donau fault (incised Donau river valley, northern Eferding Basin), where the facets reach heights of even > 100 m and are only little modified by erosion.

4.3 Recent Movement Tendencies

4.3.1 Vertical Movements

A newly visualised segment of the RVM map (Vyskočil 1996) in Czech part of the study area is presented in Fig. 11. The velocity gradients fairly parallel the southern and northern RKB, whereas in the intervening SBB area significant NW–SE to NNW–SSE transverse trends dominate (velocity differences up to ~ 1 mm yr^{-1}). The NW–SE velocity gradients detected near the Lhenice fault system support recent block architecture also in this region. In the BG area, vertical movements between the uplifting western blocks and the subsiding eastern blocks differ by up to ~ 0.7 mm yr^{-1}. At the northernmost RKB, the trend of velocity gradients changes into the general NW–SE direction existing in the southern Labe Lowland.

4.3.2 Horizontal Movements

We performed a regression analysis of multi-annual coordinate time series of the denser regional network of the GNSS stations with the aim to obtain a preliminary information about their recent horizontal movement trends (vectors). Subsequently, linear tendencies of changes in vector lengths between the stations were determined, based on time series of results from individual days. The vector components of horizontal displacement rates of particular stations were related to the total average movement of the Eurasian tectonic plate (Altamimi et al. 2017). The estimated horizontal movement parameters (velocity components and vectors) of GNSS stations used in the analysis are given in Table 1. The time series of lengths of inter-station vectors (baselines) presented in Fig. 12 illustrate quality (frequency, accuracy) and trend of the GNSS-derived information from the middle and northern RKB area. The first three graphs (a–c) used the one-day results and other three graphs (d–f) used the two-day results. Several near pairs of GNSS stations, each one located on the opposite RKB strand or within block separated by an important transverse fault, indicate counter movements and thus possible occurrence of strike-slip movement in the crust in between.

Table 1 Horizontal movement parameters of permanent GNSS stations in Czech part of the RKB area used for assessment of regional horizontal crustal block kinematics

Station	Velocity components		Velocity vector		RMS
	v_N (mm/yr)	v_E (mm/yr)	A (deg)	v (mm/yr)	σ_v (mm/yr)
CBUD	0.42	0.04	4.967	0.42	0.2
CJHR	0.36	0.03	4.028	0.36	0.3
CKAP	0.07	0.29	14.291	0.30	0.4
CPRI	0.02	0.33	86.900	0.33	0.2
CPRA	−0.19	−0.38	243.54	0.42	0.2
CPRG	0.21	0.19	42.883	0.28	0.1
CZBO	−0.24	−0.21	221.489	0.32	0.3
CZKO	0.43	−0.76	−60.942	0.87	0.2
CZPR	0.05	0.35	82.168	0.35	0.2
CZSL	0.43	−0.96	−65.942	1.05	0.2
CZST	1.16	0.17	8.308	1.17	0.3
CZUS	−0.17	0.27	123.261	0.32	0.2
PLZN	0.45	−0.11	−13.475	0.46	0.3
POUS	−0.23	−0.61	−110.525	0.65	0.2
TBEN	−0.16	−0.15	222.561	0.22	0.3
TCBU	0.22	−0.09	−22.718	0.24	0.2
TMIL	0.5	−0.36	−35.528	0.62	0.2
TRYN	1.55	1.02	33.473	1.86	0.4
TSUS	0.36	−0.11	−17.652	0.38	0.2
VACO	0.39	−0.29	−36.444	0.49	0.2

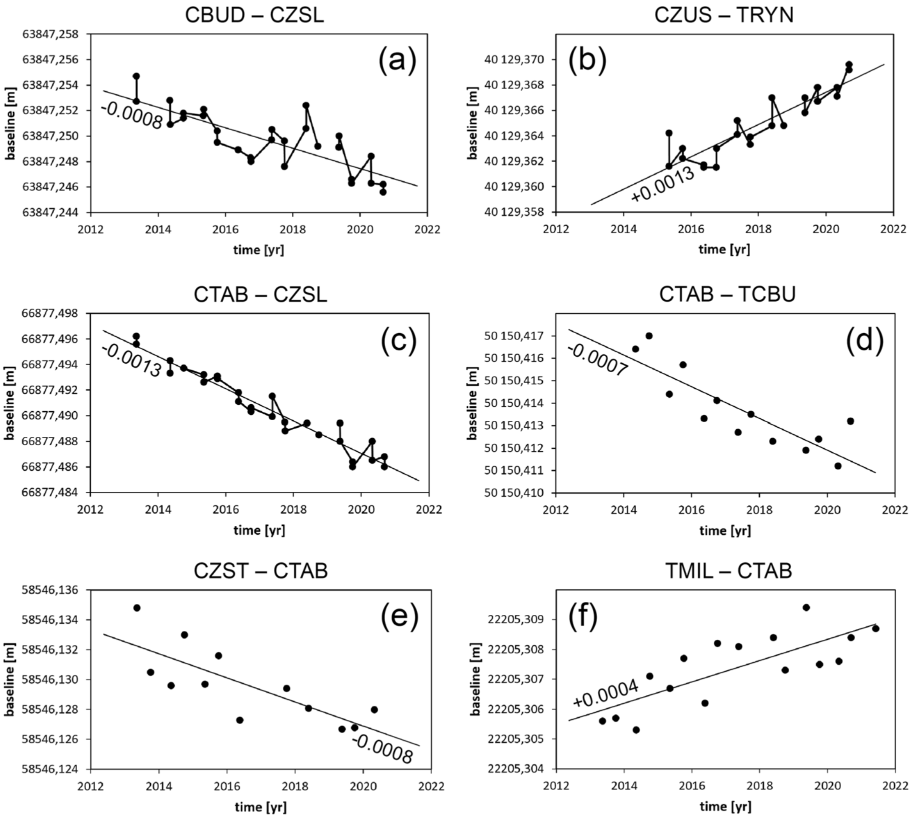

Fig. 12 Time series of lengths of inter-station vectors (baselines) crossing the middle and northern RKB

Based on the derived horizontal velocity vectors of GNSS stations, we compiled a map of annual horizontal changes in distances between pairs of near GNSS stations (Fig. 13). The inter-station lines are distinguished by a sense of relative kinematics, which is used for assessment of the movement between particular crustal blocks (compressional / extensional regime).

5 Discussion

5.1 Structural Conditions

Movements of large blocks are induced in deeper parts of the crust. Hence, the recent geodynamics of the Bohemian Massif is hardly possible to resolve without geophysical and partly also geomorphological data serving as an important instrument for verification of kinematic conditions in those subsurface levels. The geophysical results show a fair correlation of particular gradients to faults recorded on the surface and the large tectonic zones can be traced in them in a more continuous way. The anomalies in the maps (Figs. 6, 7, 8 and 9) allow to follow changes in a crust density, magnetic susceptibility or radioactivity in fault surroundings and thus to estimate the existing geological conditions

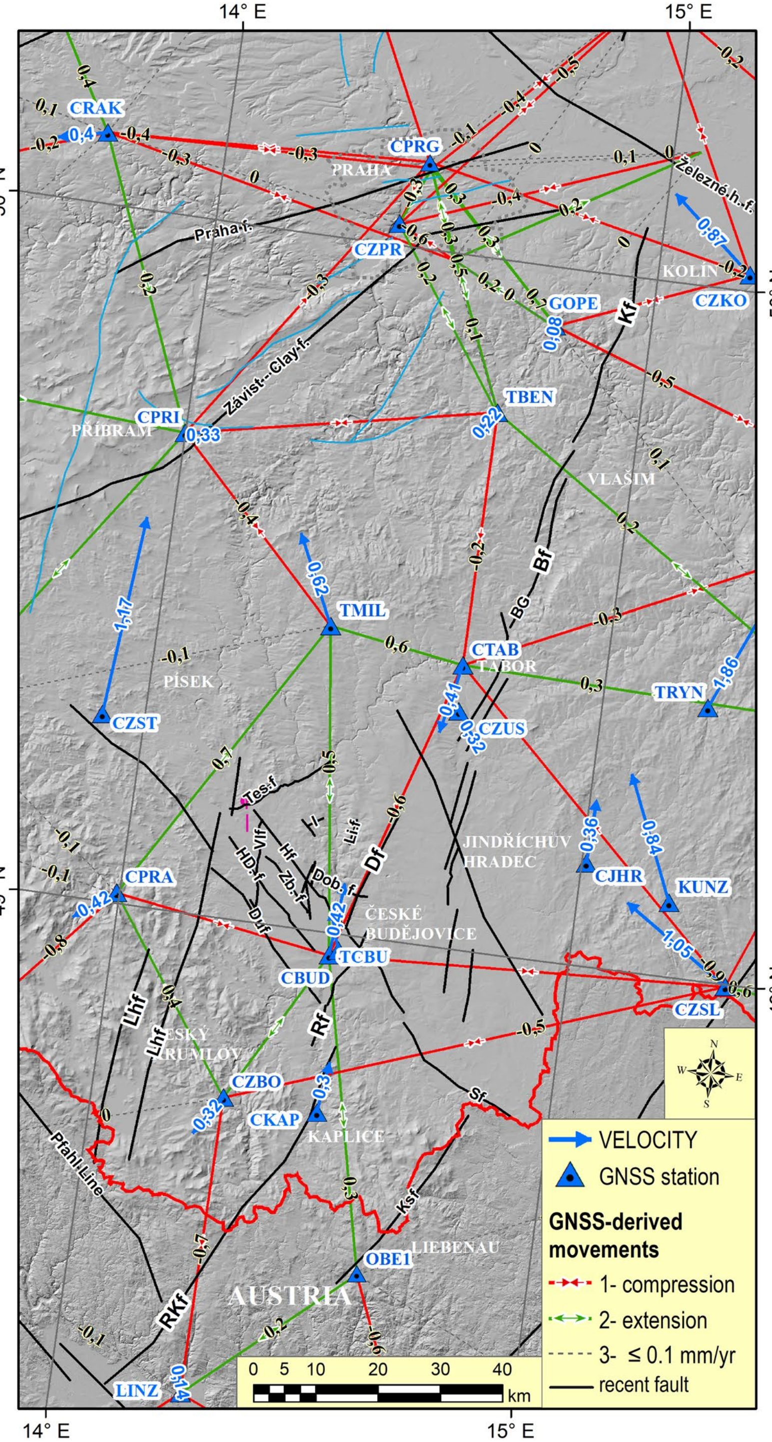

Fig. 13 Evaluated annual baseline change rates (mm/yr) and directions (horizontal velocity vectors) of permanent GNSS stations in the RKB area. Explanation of the fault abbreviations see in Figs. 1, 6

in the depth. The last presented geophysical image of residual gravity anomalies (Fig. 14) supresses the effects of large deep-seated plutonic bodies (gravity minima) and highlights the influences of near-surface gravity sources. Hence, it is suitable for a comparison to surface phenomena primarily considered during the compilation of the regional kinematic model (Sects. 5.2, 5.3).

Although the geomorphological knowledge was based only on the schematic map output, it seems to complete the information about near-surface crustal levels. The indicated dislocation zones are not proposed solely along the main known faults but also in the surrounding RKB area, sometimes in those places where ruptures have not yet been considered in its geological structure. The prevailing SW–NE trend characteristic of the Rodl-Kaplice fault occurs frequently also in case of longitudinal landform zones east of the TB, where it combines with the SSW–NNE striking longitudinal zone elements characteristic of the RKB sections in the SBB and the BG (Fig. 10). Hence, the distribution of features of both directions points to a different structural geometry in the wider southern RKB area compared to its middle and northern parts. The significant changes in an arrangement of drainage network just near the Kaplice fault, where a transition between both orientation styles is located, Flašar and Štěpančíková (2022b) attributed to the Pliocene–Quaternary tectonic activity. Additionally, the density of the proposed longitudinal landform zones and facets (as indicators of significant late Cenozoic vertical tectonic activity) is the highest in the Bayerischer Wald Mts. / Weinsberger Wald Mts. boundary area in the Rodl-Kaplice fault vicinity (southern RKB). On the contrary, the most apparent change in trends of the transverse landforms sets occurs in the northern RKB area, where the general NW–SE directions characteristic of the SW part of the Bohemian Massif (Bayerischer Wald–Weinsberger Wald Mts., SBB area) are replaced with the WNW–ESE directions prevailing in the Elbe shear zone (Uličný et al. 2009).

The SSW–NNE trending middle RKB is followed in a ~ 30 km distance by another belt of subparallel longitudinal zones extending from the eastern TB towards the Sázava river valley in the north, consistently with trends of near gravity or magnetic gradients (Figs. 6, 7 and 8). It indicates there existence of a structural zone > 100-km long and > 30-km wide, whose flanks sharply limits Cretaceous deposits preserved in central part of the TB (cf. geological conditions in Fig. 2). These spatial parameters approximate a little to those of other large deep-seated tectonic zones within the Bohemian Massif: Elbe shear zone (length > 350 km, width > 50 km; Uličný et al. 2009; Špaček et al. 2015), Eger Rift (length > 300 km, width > 30 km; Mlčoch and Konopásek 2010; Ulrych et al. 2013; Andreani et al. 2014), West Bohemian shear zone including the Mariánské Lázně fault (length > 150 km, width > 20 km; Pitra et al. 1999; Zulauf et al. 2002; Peterek et al. 2011) or the Sudetic Marginal fault–Bělá fault system (length > 200 km, width > 30 km; Buday et al. 1995; Badura et al. 2007; Pospíšil et. al. 2019).

The existing terminations of longitudinal landform zones just at the BB, TB or BG margins indicate a block character of all three graben-like structures; the corresponding boundaries possibly run along the recorded faults or their continuations (Hluboká—termination No. 3, Dubné—terminations No. 4–6, Stropnice—termination No. 7, Blanice—terminations No. 11, 12). Several terminations correspond to geophysical gradients, mainly at the SW limits of the BB and TB (Figs. 6, 7, 8 and 9), which points at the deeper character of these boundaries. Both geological (tectonic, sedimentological) and frequently spatially corresponding geomorphological indicators (dense block segmentation) evidence that the SBB areas is much larger (min. 100 km × 100 km) than that covered with the existing basins with fairly continuously preserved Cretaceous, Tertiary and locally Quaternary sediments (BB and TB s.s.).

Fig. 14 Residual Gravity Anomaly map (R = 500 m; values in mGal) in the RKB area. Structural ▶ lineaments derived from the gravity data are added in the image, as well as possibly active faults, location of geological cross sections, earthquake foci (Špaček et al. 2011; IG CAS: WEBNET 2022) and horizontal velocity vectors of GNSS stations. Explanation of the fault abbreviations see in Figs. 1, 6

As to the general RKB trend and high linear complexity of the region surrounding this fault system, the two topical similar large-scale structures with the locally increased seismicity partly related to the ongoing sinistral strike-slip activity occur in near central Europe, mostly in front of the Alpine-Carpathian orogen: Rhine Graben (~400 km towards the west) and Alpine-Carpathian transition area (~200 km towards the east), loosely limited by the Diendorf-Boskovice shear zone and the western Danube Basin (Schumacher 2002; Cloetingh et al. 2006; Decker et al. 2005; Edel et al. 2007; Ziegler and Dèzes 2007; Roštínský et al. 2013; Pospíšil et al. 2017). Although developed in different geological settings, both structures are also characteristic of increased concentration of SW–NE, SSW–NNE and even N–S linear features predisposed by extensive (continental-scale) fields of consistent linear ruptures and geometric configurations analogous to those of the RKB have been frequently formed within them. Similar geological and geomorphological linear elements are abundant also within the SSW–NNE zone running from the Cheb Basin area towards frontal parts of the Alps (~200 km to the west; cf. Špičáková et al. 2000; or Štěpančíková et al. 2019). Such a regular structural geometry created by large tectonic zones may exist in other regions of extended crust worldwide.

5.2 Recent Kinematic Conditions

The data used for compilation of the presented kinematic model indicated that the RKB is not evolving uniformly and allowed to loosely divide the fault system area into the following three main parts of different structural character and style of recent tectonic activity.

5.2.1 Rodl-Kaplice Fault Area

The complex Rodl-Kaplice fault is composed of a number of subparallel deformations, forming sinistral shear zone (Brandmayr et al. 1995; Dallmeyer et al. 1995). It is manifested by lithological boundaries, mylonite belts, several elongated grabens, geophysical gradients (most distinct in the radiometric field), a number of consistent landforms nearly along the whole fault trace in a belt up to > 5-km wide including several facets and scarps or boundaries of RVM anomalies (Figs. 2, 6, 7, 8, 9, 10, 11 and 15). Based on the foliation parameters of mylonite, the Rodl fault is steeply inclined towards the NW (~80°; Wallbrecher et al. 1993). The fault plain of the Kaplice fault is similarly inclined (dip 70–80° towards the WNW; Melnyk 2017; Melnyk et al. 2022). Figure 5 well illustrates the relation between paragneisses of the Kaplice unit (west) and the Moldanubian granitoid complex (east).

The Pliocene to Pleistocene tectonic activity of the Kaplice fault is indicated by young changes in river network of the surrounding area, deduced from the morphostratigraphic correlation of moldavite-bearing and related fluvial deposits (Flašar and Štěpančíková 2022b). As an important evidence for its recent sinistral strike-slip fault activity, we consider the detected consistent counter movement of the near GNSS stations located on

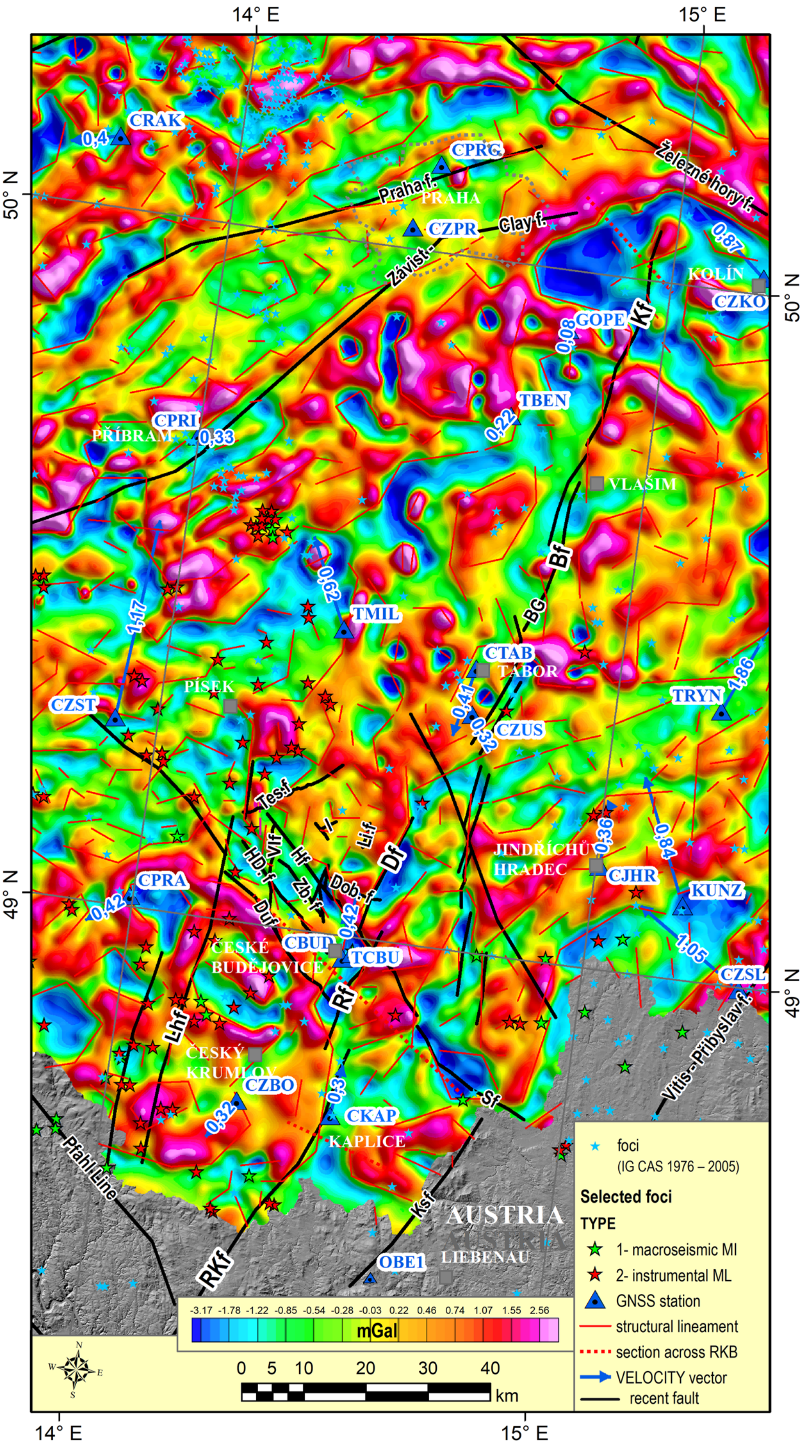
14° E
15° E
50° N
49° N
CRAK
0,4
CPRG
PRAHA
Praha f.
CZPR
Clay f.
Závist-
Železné hory f.
0,87
KOLÍN
CZKO
GOPE
0,08
Kf
TBEN
0,22
CPRI
PŘÍBRAM
0,33
VLAŠIM
Bf
BG
0,92
TMIL
1,17
CTAB
TÁBOR
PÍSEK
CZST
0,41
0,32
CZUS
TRYN
1,86
Tesf
Li.f
Vlf
Hf
HD.f
Df
Zb.f
Dob.f
0,36
0,84
JINDŘICHŮV HRADEC
CJHR
KUNZ
CPRA
0,42
Duf
0,42
1,05
CBUD
TCBU
ČESKÉ BUDĚJOVICE
CZSL
Rf
Lhf
ČESKÝ KRUMLOV
CZBO
0,32
0,3
CKAP
KAPLICE
Sf
Vitis - Přibyslav f.
Pfahl Line
Ksf
AUSTRIA
RKf
OBE1
LIEBENAU
-3.17 -1.78 -1.22 -0.85 -0.54 -0.28 -0.03 0.22 0.46 0.74 1.07 1.55 2.56
mGal
0 5 10 20 30 40
km
foci
(IG CAS 1976 – 2005)
Selected foci
TYPE
1- macroseismic MI
2- instrumental ML
GNSS station
structural lineament
section across RKB
VELOCITY vector
recent fault

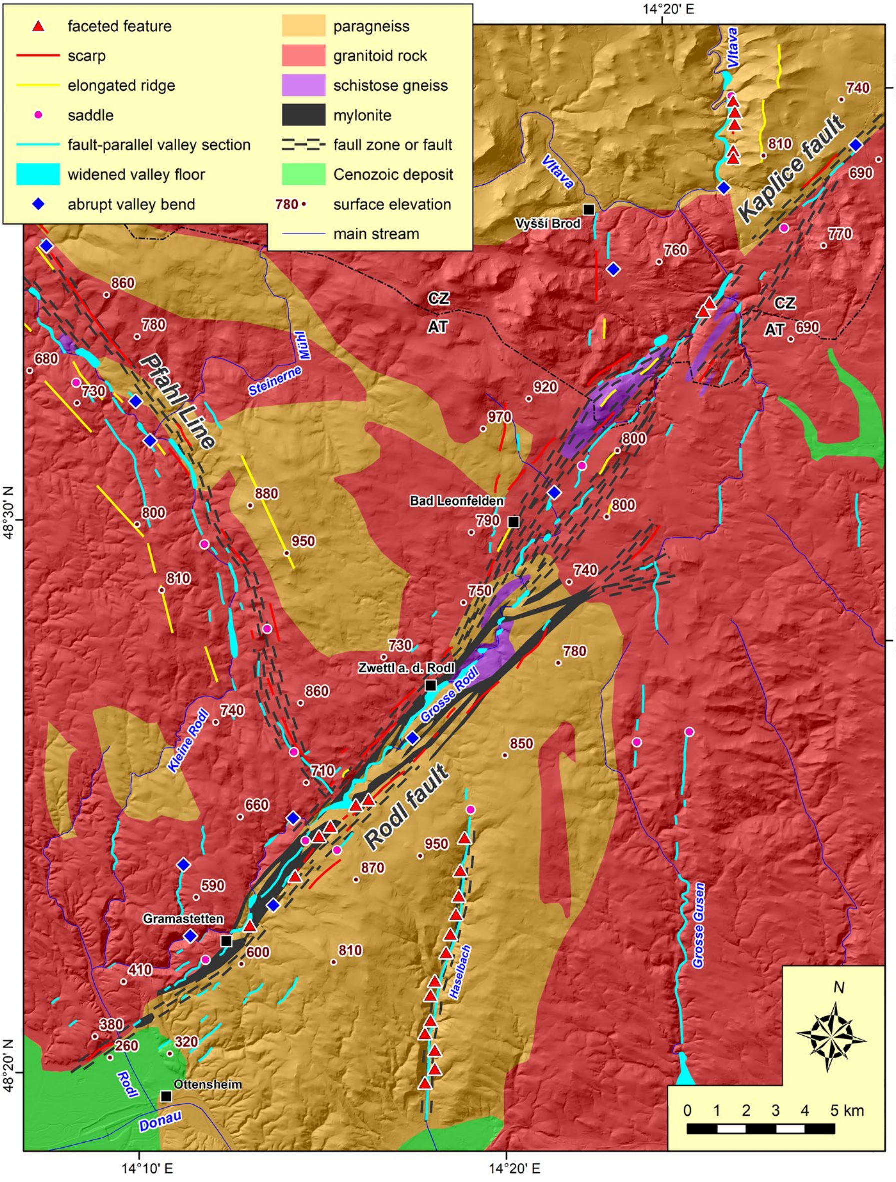

Fig. 15 Significant geological and geomorphological features along middle part of the Rodl-Kaplice fault and SE part of the Pfahl Line. The areal geological scheme was created primarily based on the map by Krenmayr et al. (2006). All listed crystalline rocks belong to the Moldanubian unit of the Bohemian Massif. Note a number of differences in surface elevation (m a.s.l.) along nearly the whole length of visualised part of the RKB

its opposite strands, reaching > 0.6 mm yr^{-1} (Fig. 13; CZBO / CKAP and LINZ). Based on processed GNSS data not included in this paper, movements of the GNSS stations in the adjacent Alpine Molasse Basin (hidden RKB section area) are decreased and their directions more variable.

Numerous subparallel N–S structures in the Rodl-Kaplice fault surroundings, on the surface mostly expressed by streams creating incised valleys and by a few slopes systems with facets (Haselgraben, middle Vltava river valley), can represent rejuvenated Paleozoic phenomena (Iglseder 2013, 2014a, b; Pfleiderer et al. 2016) as Riedel shears related to this section of the RKB. Taking into account the absence of GNSS-derived counter movements in the SE block of the Rodl-Kaplice fault, the subparallel N–S valley structures have likely developed in a W–E extensional regime associated with late Cenozoic evolution of the broader Bayerischer Wald–Weinsberger Wald Mts. region where a complex horst-and-graben structure occurs (Fischer 1965; Flašar and Štěpančíková 2022b). Foci of significant earthquakes do not occur close to the Rodl-Kaplice fault. However, the existence of young morphotectonic features also along ruptures transverse to the trend of this fault (most distinct within the Donau fault system; Fig. 10) indicates a recent tectonic activity of the wider area surrounding the southern RKB with diminishing strike-slip movements of the RKB towards the SW.

5.2.2 South Bohemian Basins Area

The RKB-related zone crossing the SBB is up to > 20-km wide, as shown by the geological data (Figs. 2, 4). Scarps, elongated ridges and several small valleys belong to the corresponding geomorphological features. The Rudolfov and Drahotěšice faults are also expressed as a consistent trend of gradients in all evaluated regional geophysical fields (Figs. 6, 7, 8 and 9).

Based on the GNSS monitoring data (CBUD and TCBU stations), the eastern BB between the Hluboká and Dubné faults moves (up to 0.4 mm yr^{-1}) towards the north fairly consistently with the dominant trend detected further east to the RKB (~ 1.0 mm yr^{-1}; surroundings of the CJHR station; Fig. 13). It indicates in the SBB a local suppression of the dominant RKB sinistral geodynamic regime. The spatial continuity of the RKB has been in the upper crust of the basin area strongly disturbed by an activity of the transverse NW–SE to NNW–SSE faults. Hence, the verification of recent kinematics in the middle RKB, where the fault system root is located in a higher depth beneath them, is complicated. The earlier movements along the SBB faults induced a development of smaller grabens limiting Middle Miocene, Late Miocene and Pliocene deposits; the activity of marginal ruptures lasted at least until the end of Neogene (Špaček et al. 2011; Prachař 2014). The morphometric comparison of the Hluboká and Rudolfov faults (Popotnig et al. 2013) pointed even to a higher recent activity of the former and a continuing moderate Lišov Horst uplift along the latter fault, although movements were not directly proved in the crossing trenches (Špaček et al. 2017). The young fault activity could be associated with the Late Quaternary aggradational regime in the eastern BB; the oldest fluvial sediments were there dated to MIS 5 or even a later period. Either recent BB floor surface subsidence or stability related to the near NE basin margin uplifted along both the marginal faults was thus considered for evolution of their depositional setting (Homolová et al. 2012). A subsidence of this part of the basin is supported also by the RVM data (Fig. 11).

The GNSS-derived movements, RVM and properties of the regional seismicity generally indicate a variable character of the recent geodynamic activity in the SBB, as well as the differences between eastern and western parts of this transverse tectonic structure. The prevailing NW–SE to NNW–SSE-oriented gradients and anomalies occur there in the RVM map (Fig. 11). A newly highlighted narrow NNW–SSE striking extensional zone with a relative subsidence up to 1 mm yr^{-1}, extending from the Závist-Clay fault system along the

TB axis up to the SE margin of this basin, appears to be the most significant such feature. It spatially fits to the largest discontinuity in the RKB trace between the Drahotěšice and Blanice faults, mutually located ~ 10 km apart (Fig. 2; CGS 2023). The extensional zone is associated also with consistent geophysical indications (Figs. 6, 7, 8 and 9) and many landforms (topographic gradients, elongated flat-top ridges, valley sections; Fig. 10). At the northern zone end, a significant earthquake cluster has been recorded (Figs. 6, 7, 8 and 9; Špaček et al. 2011). The NE margin of the extensional zone corresponds to the most important change in GNSS-derived horizontal movement tendencies in the RKB area. The velocity vectors of the stations west of the Blanice fault (GOPE, TBEN and CTAB) point to an increase in the surface velocity from the north towards the SBB in the south (Fig. 13), but in the opposite direction as compared to the velocity vectors in the eastern BB (CBUD and TCBU stations). The transverse NNW–SSE extensional zone can serve just as a compensation structure of both counter-directed trends. The two stations located at its northern rim move approximately in opposite ways, TMIL significantly towards the NNW and CZUS towards the SE (> 0.9 mm yr^{-1} relative difference), which indicates there an additional dextral kinematic component. Hence, the extensional zone appears to separate a more uniform crust segment in the north from the much more fragmented SBB structure composed of blocks moving in variable, from the RKB trend frequently different directions.

In the western BB, GNSS stations are absent. However, both the main transverse marginal faults (Hluboká, Dubné) are limited or dislocated there by the N–S Lhenice fault or accompanying subparallel ruptures (Špaček et al. 2011; CGS 2023; geophysical maps in Figs. 6, 7 and 8). West of the Lhenice fault, the two GNSS stations detected significantly counter-directed movements (CPRA towards the SW / CZST much faster towards the N; the difference > 1.3 mm yr^{-1}). Supported by an existence of spatially corresponding Linsser indications, a belt of preserved small Miocene to Pliocene sedimentary remnants (Fig. 2) or many geomorphological features (Fig. 10), the NW–SE Dubné fault could continue also to this area. Additionally, this region is characterised by the increased seismicity (Fig. 16a; Špaček et al. 2011), mostly in the Strakonice-Písek-Orlík surroundings and near the Lhenice fault where the earthquake foci are mostly located in the < 10 km depths. As proposed already by Melnyk et al. (2022), the latter tectonic zone can thus be at floor level of the Variscan crust interconnected with the subparallel RKB; normal and listric (to the depth) geometry was considered for the possible uniting deep structure.

While west of the RKB a fairly high earthquake density with the foci located mostly in < 10 km depths has occurred, east of the fault system the seismic events have been only scarce and generally induced in higher depths (Fig. 16b). This finding can be related to different thickness of the particular Moldanubian blocks in the complex Variscan structure (e.g. Stackebrand and Franzke 1989; Dudek et al. 1991; Vrána and Štědrá 1997) with a common floor of the Variscan level in the 10–12 km depth (Hrubcová et. al. 2008). A difference in the foci distribution exists also between the northern and southern RKB area (Fig. 16c, d). In the former part, the foci located < 10 km have not been recorded near the RKB, whereas in the latter part, a few such phenomena have appeared near the fault system (M_L ~ 1–2).

5.2.3 Blanice Graben Area

The RKB width in the BG area reaches 15–20 km (Figs. 2, 10). This part of the fault system is characterised by the highest concentration of remnant grabens with Permo-Carboniferous

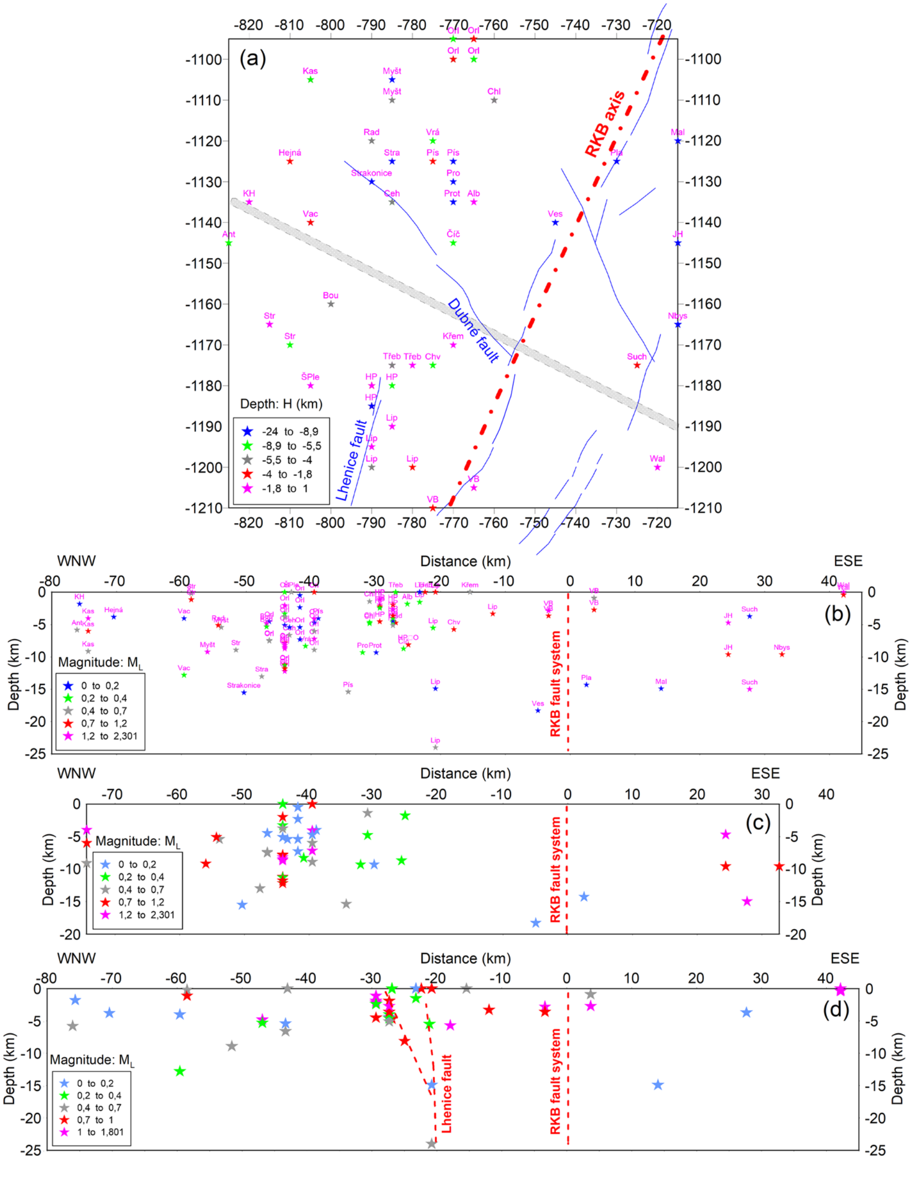

Fig. 16 Foci of instrumentally recorded regional earthquakes (Špaček et al. 2011) orthogonally projected into selected WNW–ESE striking vertical cross section perpendicular to the RKB axis (view from the south). **a** Spatial distribution of all foci included (national S-JTSK kilometric coordinate system used in the map) along with the considered RKB axis and the selected cross section (bold light grey line) approximately separating northern and southern part of the fault system area. Selected faults are added in the image for its location. Points of the places mentioned in the text: Stra—Strakonice; Pis—Písek; Orl—Orlík. **b** Modelled projection of all foci in the delimited area. **c** Selected foci in northern part of the area, including the South Bohemian Basins and Blanice Graben structures. **d** Selected foci in southern part of the area, including the Rodl-Kaplice fault structure. A depth indication of the main faults added in the b–d images is schematic

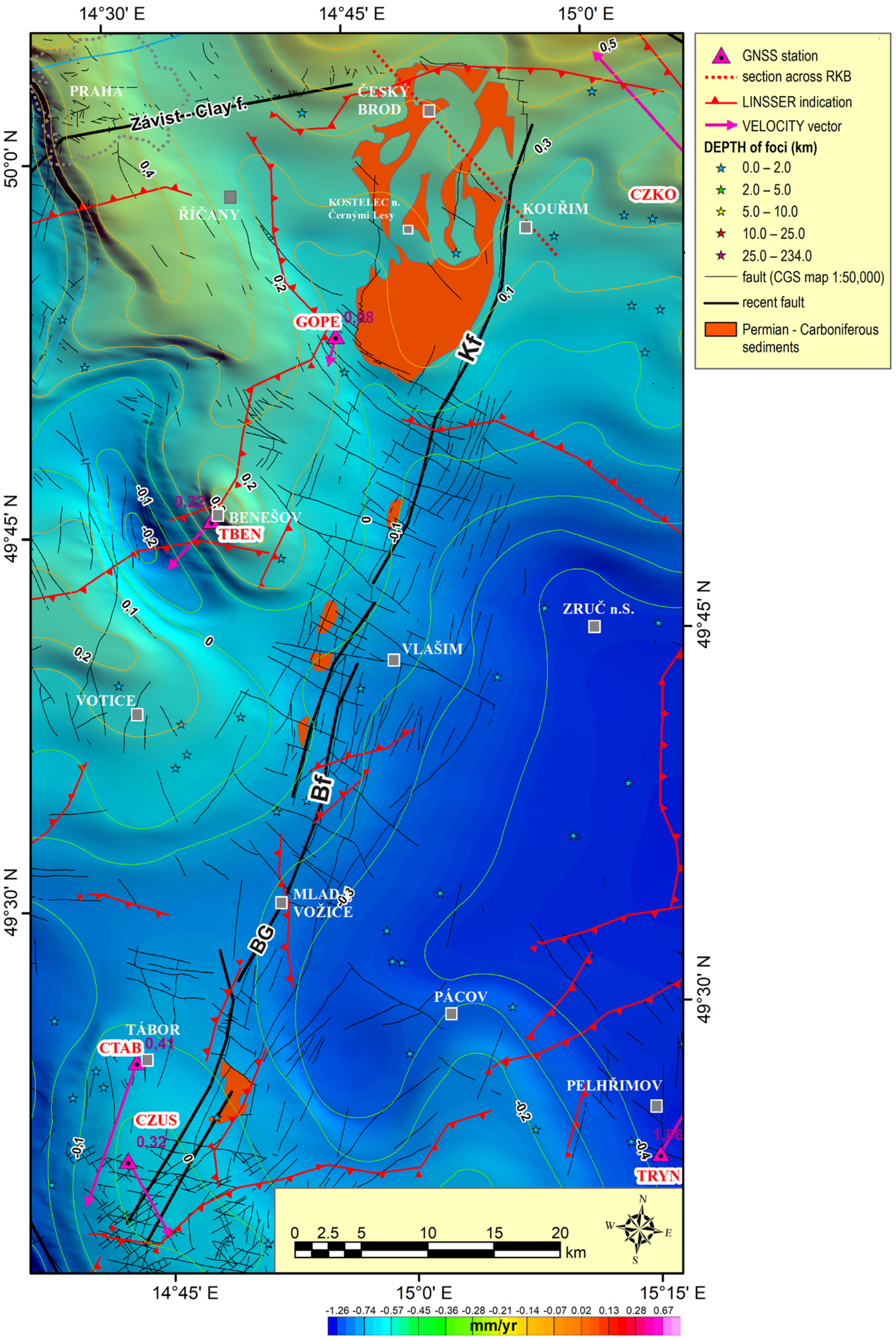

Fig. 17 Selected geological features in the Blanice Graben area (CGS 2023) drawn over the RVM image (after Vyskočil 1996; arranged by the authors; values in mm/yr), with added vertical density boundaries (Linsser indications compiled for 4-km depth level), earthquake foci (WEBNET 2022) and horizontal velocity vectors (mm/yr) of GNSS stations. BG—Blanice Graben; Bf—Blanice fault; Kf—Kouřim fault. CGS—Czech Geological Survey

sediments (Fig. 17). Besides the surface topography (subparallel elongated graben structure with distinct marginal slopes and consistent valley network on its floor, a few distinct scarps), the BG is well-visible also in the gravity and partly in magnetic images (Figs. 6, 7 and 8).

A significant change in geodynamic regime occurs along the BG. Based on the GNSS velocity vectors, a uniform trend of horizontal movements exists in middle and southern parts of the graben structure (Fig. 13). Although the GNSS stations on the eastern BG strand are located further from the RKB, it is possible to assume a sinistral recent movement along the driving Blanice fault and related ruptures. On the contrary, along the northern BG non-negligible vertical movements were primarily recorded (Fig. 11). At the northern termination of the RKB, this extensional regime is replaced with the NW–SE-oriented dextral movement activity within the Elbe shear zone (e.g. Uličný et al. 2003; see also the corresponding significant velocity vector of the CZKO station). Hence, the change in kinematic regime is there similar to the southern RKB termination.

5.3 Regional Kinematic Model

The resulting preliminary kinematic model of the RKB area is visualised in Fig. 18. The non-negligible horizontal movements of blocks along the RKB presumably continue even nowadays, although its structure is in shallow crustal levels significantly modified by the active transverse SBB rupture zone. The kinematics consistent with the fault system is gradually changed towards the north, where the current activity of the significant Elbe shear zone plays the dominant role. In several parts of the investigated area, e.g. near Tábor and Strakonice, the existent data are yet insufficiently interpretable and several geodynamic solutions are possible. In the future, more voluminous data should be incorporated into the analysis to increase reliability of the output expressing the regional kinematic conditions.

The knowledge presented in the model is in line with the results from earlier geodynamic studies in the Bohemian Massif: The kinematic conditions in southern and middle part of the Diendorf-Boskovice fault area involve blocks moving along the approximate SSW–NNE axis of that fault system (Roštínský et al. 2013; 2020), but in its northern part, WNW–ESE to NW–SE movements subparallel to the Elbe shear zone trend become similarly prevailing (Švábenský et al. 2014; Špaček et al. 2015; Pospíšil et al. 2017). The significant structures in the western Bohemian Massif surrounding the Mariánské Lázně fault (Vavryčuk et al. 2013; Štěpančíková et al. 2019) have the different NNW–SSE to N–S dominant geometric arrangement and represent another group of active tectonic phenomena within the Eastern Variscides, presumably combined there with a generation of young volcanic rocks (cf. Wendt and Dietrich 2003; Weinlich et al. 2006).

The RKB, as well as other significant subparallel fault systems in the southern Bohemian Massif (Vitis-Přibyslav, Diendorf-Boskovice), is located in a transition area between the two different recent stress domains in the northern Eastern Alps and northwestern Europe. Hence, faults of a wide strike spectrum could be reactivated in its region during alternating pushes from the south and the northwest: SW–NW, SSW–NNE, N–S, NNW–SSE or NW–SE. This tentative assumption is fairly consistent with the obtained results from the geodetic (RVM, GNSS) and geomorphological research along the RKB. Its data supported in this area mostly the strike-slip or normal regimes. Both longitudinal and transverse tectonic zones thus appear to be active simultaneously (Figs. 11, 18), as suggested earlier already by Popotnig et al. (2013) for the eastern BB. The increased number of facets and steep scarps in the southernmost Bohemian Massif (Fig. 10) is

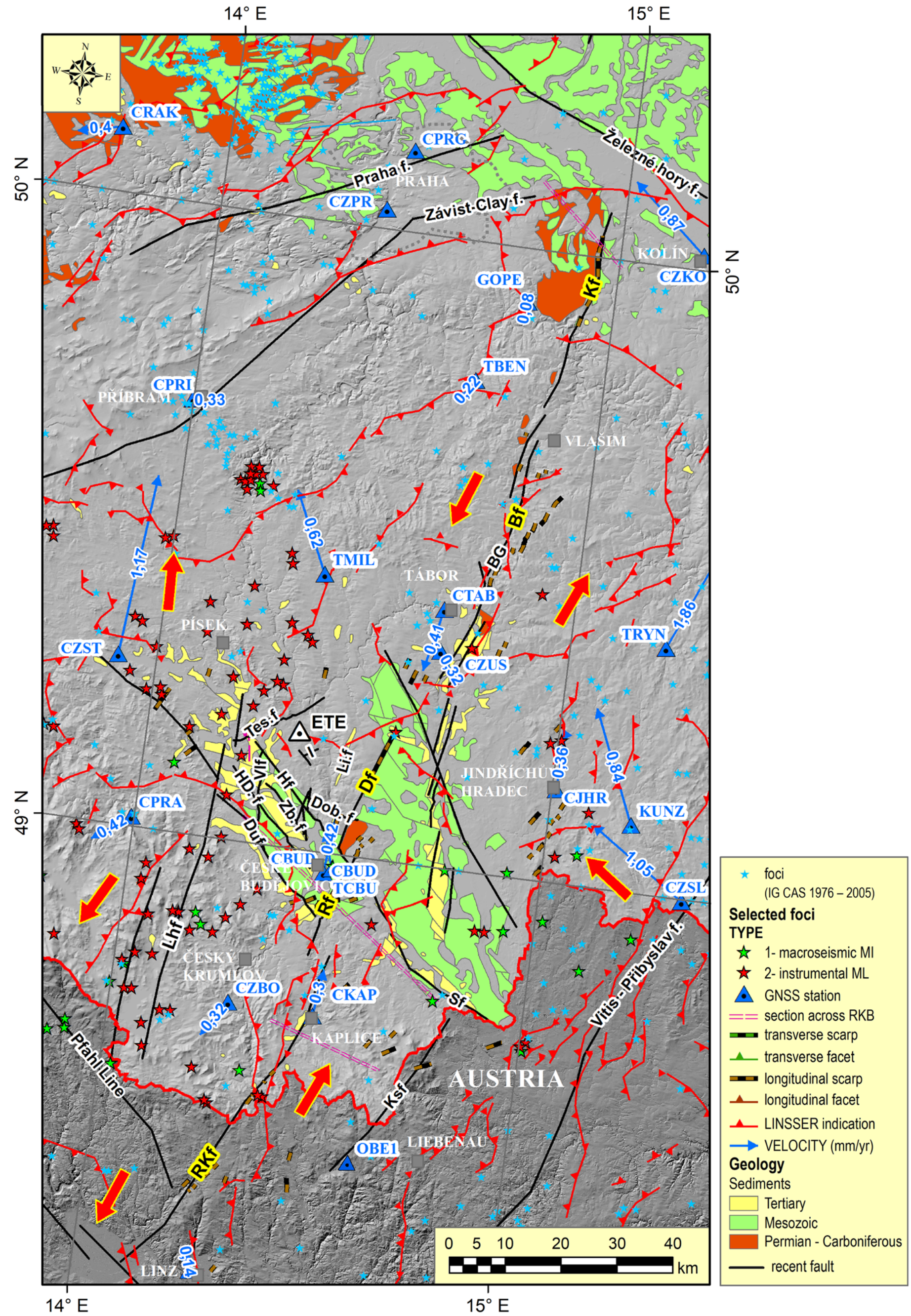

Fig. 18 Kinematic model of the RKB area, primarily based on GNSS-derived horizontal velocity vectors. Selected supporting geological, geophysical and geomorphological phenomena are added in the image, including the Linsser indications compiled for 4-km depth level. Earthquake foci after Špaček et al. 2011 and IG CAS: WEBNET 2022. Explanation of the fault abbreviations see in Figs. 1, 6; those of RKB sections are highlighted in yellow. The red arrows indicate interpreted movement directions of significant crustal blocks. ETE—Nuclear Power Plant Temelín

consistent with the ongoing extensive regional relief rejuvenation in front of the Eastern Alps (Wetzlinger et al. 2023). Additionally, the RKB ends near the Alpine front. Hence, it can be considered that the recent activity of the fault system is at least in its southern part geodynamically related more to the Alps Mountains than to the northern Bohemian Massif. Some of the repeating combined trends of linear features, commonly occurring in both RKB and SBB structures (Rodl-Kaplice fault: SW–NE, SSW–NNE and N–S; Blanice Graben: SSW–NNE and N–S; South Bohemian Basins: NW–SE and NNW–SSE; Fig. 10), can thus evolve also in the present time.

6 Conclusions

Based on the multidisciplinary information obtained, the large-scale Rodl-Kaplice-Blanice fault system as a structure of Variscan shear origin has been reactivated in the recent time: up to ~ 1 mm horizontally (sinistral movement; Fig. 18) and > 0.5 mm vertically (Fig. 11). Within the Bohemian Massif, the complex RKB can be subdivided into the three parts of different tectonic structure and kinematic character. The horizontal movements are highest there in its southern and middle sections (Rodl-Kaplice fault, Rudolfov fault, Drahotěšice fault), whereas noticeable vertical differentiation is going on mostly along the Blanice and Kouřim faults in its northern part. Towards the north, the dynamics of the RKB is gradually replaced with current movements in the transverse Elbe shear zone. The velocity vectors of GNSS stations in the area of South Bohemian Basins differ significantly from the subparallel trends along the RKB itself. It indicates continuing activity also within this important transverse tectonic structure largely dislocating the middle RKB in the shallow crust, including a formation of several NW–SE to NNW–SSE-oriented grabens in transtensional regime. Some of these disturbing elements represent the third type of structures currently composing the fault system.

Only rare earthquakes occur near the RKB, much more events have been recorded in the area towards the west. Besides faults of the SBB, these were presumably associated with the Lhenice fault. The latter RKB-subparallel rupture can have an analogous structural position as the main focused tectonic zone with regard to the assumed generation of both fault systems in lower part of the Variscan level (~ 10–12 km depth). Hence, the significant deep-seated faults in the RKB area seem to be linked to the floor of the Variscan crust similarly to other such tectonic phenomena in the Bohemian Massif.

The earlier installation of the large nuclear facility in a close RKB vicinity justifies the presented geodynamic analysis, although the investigated fault system is located in only slowly deformed part of the crust. The permanent safety-related monitoring of natural hazards near the nuclear power plant yet omitted evaluation of the GNSS data. At the present time, these data represent an important information about the regional horizontal movement activity and should be incorporated into the risk assessment of fundamental national infrastructure.

Acknowledgements The geomorphological analysis and compilation of the paper was performed with a support of long-term conceptual development of the research organisation: Institute of Geonics of the Czech Academy of Sciences, RVO: 68145535. A number of comments from anonymous reviewers helped to substantially improve the manuscript.

Author Contributions PR involved in original draft preparation, literature survey, methodology, geomorphological data processing, analysis and interpretation and visualisation (ArcGIS software); LP involved in draft idea, conceptualisation, original draft preparation, literature survey, methodology, geophysical data processing (Oasis Montaj software—GM-SYS extension), analysis and interpretation and visualisation (ArcGIS software); OŠ involved in original draft preparation, GNSS data processing (Bernese software) and analysis and interpretation; AM involved in geophysical data processing (Oasis Montaj software—GM-SYS extension); EN involved in remote sensing data processing and visualisation (ArcGIS software). All the authors involved in draft critical review and editing.

Funding Open access publishing supported by the National Technical Library in Prague. The authors PR and EN have declared their financial support in the acknowledgements section of the paper. The authors have no other relevant financial or non-financial interests to disclose.

Declarations

Conflict of interest All the authors declare no financial or competing interests relevant to the content of this article, representing a conflict of interest.

References

Aleksandrowski P, Kryza R, Mazur S, Żaba J (1997) Kinematic data on major Variscan fault and shear zones in the Polish Sudetes, NE Bohemian Massif. Geol Mag 134:727–739. https://doi.org/10.1017/S0016756897007590

Altamimi Z, Métivier L, Rebischung P, Rouby H, Collilieux X (2017) ITRF2014 plate motion model. Geophys J Int 209:1906–1912. https://doi.org/10.1093/gji/ggx136

Andreani L, Stanek KP, Gloaguen R, Krentz O, Domínguez-González L (2014) DEM-based analysis of interactions between tectonics and landscapes in the Ore Mountains and Eger Rift (East Germany and NW Czech Republic). Remote Sens 6:7971–8001. https://doi.org/10.3390/rs6097971

Aric K, Gutdeutch R, Heinz H, Meurers B, Seiberl W, Ádám A, Smythe D (1997) Geophysical investigations in the southern Bohemian Massif. Jb Geol BA 140:9–28

Arthaud F, Matte P (1977) Late Paleozoic strike-slip faulting in southern Europe and northern Africa: result of a right-lateral shear zone between the Appalachians and the Urals. Geol Soc Am Bull 88:1305–1320. https://doi.org/10.1130/0016-7606(1977)88%3c1305:LPSFIS%3e2.0.CO;2

Bábek O, Briestenský M, Přecechtělová G, Štěpančíková P, Hellstrom JC, Drystale RN (2015) Pleistocene speleothem fracturing in the foreland of the Western Carpathians: a case study from the seismically active eastern margin of the Bohemian Massif. Geol Quat 59:491–506. https://doi.org/10.7306/gq.1225

Babuška V, Růžek B, Dolejš D (2016) Origin of earthquake swarms in the western Bohemian Massif: Is the mantle CO_2 degassing, followed by the Cheb Basin subsidence, an essential driving force? Tectonophysics 668–669:42–51. https://doi.org/10.1016/j.tecto.2015.12.008

Badura J, Rauch M (2014) Tectonics of the Upper Nysa Kłodzka Graben, the Sudetes. Geol Sudet 42:137–148

Badura J, Zuchiewicz W, Štěpančíková P, Przybylski B, Kontny B, Cacoń S (2007) The Sudetic Marginal Fault: a young morphotectonic feature at the NE margin of the Bohemian Massif, Central Europe. Acta Geodyn Geomater 4(148):7–29

Balatka B, Sládek J (1962) River terraces in the Czech Lands. Publication House of the Czechoslovak Academy of Sciences, Prague (in Czech)

Balatka B, Kalvoda J, Steklá T, Štěpančíková P (2019) Morphostratigraphy of river terraces in the Eger valley (Czechia) focused on the Smrčiny Mountains, the Chebská pánev Basin and the Sokolovská pánev Basin. Acta Univ Carol Ser Geogr 54:240–259. https://doi.org/10.14712/23361980.2019.21

Bankwitz P, Schneider G, Kämpf H, Bankwitz E (2003) Structural characteristics of epicentral areas in Central Europe: study case Cheb Basin (Czech Republic). J Geodyn 35:5–32. https://doi.org/10.1016/S0264-3707(02)00051-0
Bárta O, Melichar R, Černý J (2021) How many extensional stages marked the Variscan gravitational collapse in the Bohemian Massif? Ann Soc Geol Polon 91:121–136. https://doi.org/10.14241/asgp.2021.08
Blížkovský M, Novotny A (1981) Stripped geological map of the Bohemian Massif based on revision of density data. Czech Geological Survey, Prague (in Czech)
Blížkovský M, Pokorný L, Weiss J (1975) Structural scheme of the Bohemian Massif based on geophysical data. Bull Geosci 50:1–9
Brandmayr M, Dallmeyer RD, Handler R, Wallbrecher E (1995) Conjugate shear zones in the Southern Bohemian Massif (Austria): implications for Variscan and Alpine tectonothermal activity. Tectonophysics 248:97–116. https://doi.org/10.1016/0040-1951(95)00003-6
Brandmayr M, Loizenbauer J, Wallbrecher E (1999) Contrasting p-T conditions during conjugate shear zone development in the Southern Bohemian Massif. Mitt Österr Geol Ges 90:11–29
Briestenský M, Stemberk J, Rowberry MD (2014) The use of damaged speleothems and in situ fault displacement monitoring to characterise active tectonic structures: an example from Západní Cave, Czech Republic. Acta Carsol 43:129–138
Buday T, Ďurica D, Opletal M, Šebesta J (1995) Importance of the Bělá and Klepáčov fault system and its continuation into the Carpathians. Uhlí-Rudy-Geol Průzk 2:275–282 (in Czech)
Burbank DW, Anderson RS (2011) Tectonic geomorphology, 2nd edn. Wiley-Black, Chichester
Büttner SH (2007) Late Variscan stress-field rotation initiating escape tectonics in the south-western Bohemian Massif: a far field response to late-orogenic extension. J Geosci 52:29–43. https://doi.org/10.3190/jgeosci.004
Čech V (1962) Explanatory notes to Overview geological map of the Czechoslovak Socialistic Republic, 1:200,000, Sheets M-33-XVII České Budějovice, M-33-XXXIII Vyšší Brod. Publication House of the Czechoslovak Academy of Sciences, Prague (in Czech)
Čech V (1989) Geological map of the Czechoslovak Socialistic Republic (Map of pre-Quaternary rocks), 1:200,000, Sheets M-33-XVII České Budějovice, M-33-XXXIII Vyšší Brod. Czech Geological Survey, Prague (in Czech)
CGS (2023) Geoscience maps 1:50,000. Czech Geological Survey, Prague (in Czech). https://mapy.geology.cz/geocr50/
Cháb J, Breiter K, Fatka O, Hladil J, Kalvoda J, Šimůnek Z, Štorch P, Vašíček Z, Zajíc J, Zapletal J (2010) Outline of the geology of the Bohemian Massif: the basement rocks and their Carboniferous and Permian cover. Czech Geological Survey, Prague
Chábera S, Huber KH (2000) Problems of the Vltava (Moldau) river drainage system development in the Tertiary. Jb Oö Mus-Ver 145:339–367 (in German)
Chlupáč I, Brzobohatý R, Kovanda J, Stráník Z (2002) Geological history of the Czech Republic. Publication House of the Czech Academy of Sciences, Prague (in Czech)
Cloetingh S, Cornu T, Ziegler PA, Beekman F, Environmental Tectonics Working Group (2006) Neotectonics and intraplate continental topography of the northern Alpine Foreland. Earth Sci Rev 74:127–196. https://doi.org/10.1016/j.earscirev.2005.06.001
Coubal M, Adamovič J (2000) Youngest tectonic activity on faults in the SW part of the Most Basin. Geolines 10:15–17
Coubal M, Málek J, Adamovič J, Štěpančíková P (2015) Late Cretaceous and Cenozoic dynamics of the Bohemian Massif inferred from the paleostress history of the Lusatian Fault Belt. J Geodyn 87:26–49. https://doi.org/10.1016/j.jog.2015.02.006
Coubal M, Zelenka P, Stemberk J Jr (2019) Record of Alpine tectonic activity of the Železné hory Fault expressed by brittle deformation within its southeastern segment. Geosci Res Rep 52:141–146. https://doi.org/10.3140/zpravy.geol.2019.10
CUZK (2022) ZABAGED® – Altimetry – DMR 5G. Digital Terrain Model of the Czech Republic of the 5th Generation. State Administration of Land Surveying and Cadastre. Available at: https://geoportal.cuzk.cz/(S(pg3ucxwcap0qdtv5cqqcrstk))/Default.aspx?mode=TextMeta&text=vyskopisZBG&side=vyskopis&menu=30. Accessed 7 January 2022
Czudek T (2005) Quaternary development of landscape relief in the Czech Republic. Moravian Museum, Brno (in Czech with English summary)
Dach R, Lutz S, Fridez P, Walser P (2015) Bernese GPS Software (Version 5.2). User manual. University of Bern, Bern.
Dallmeyer R, Franke W, Weber K (1995) Pre-Permian geology of Central and Eastern Europe. Springer Verlag, Berlin

Danišík M, Štěpančíková P, Evans NJ (2012) Constraining long-term denudation and faulting history in intraplate regions by multisystem thermochronology: An example of the Sudetic Marginal Fault (Bohemian Massif, central Europe). Tectonics 31:TC2003. https://doi.org/10.1029/2011TC003012
Decker K, Peresson H, Hinsch R (2005) Active tectonics and Quaternary basin formation along the Vienna Basin Transform fault. Quat Sci Rev 24:307–322. https://doi.org/10.1016/j.quascirev.2004.04.012
Decker K, Hintersberger E, Homolová D (2010a) Austrian Interfacing Project: Paleoseismology of Temelin's Near-Regional Faults. Interrim Report 2. Department of Geodynamics, University of Vienna, Vienna
Decker K, Hintersberger E, Homolová D (2010b) Austrian Interfacing Project: Paleoseismology of Temelin's Near-Regional Faults. Interrim Report 3. Department of Geodynamics, University of Vienna, Vienna
Devoti R, Pietrantonio G, Riguzzi F (2014) GNSS networks for geodynamics in Italy. Física De La Tierra 26:11–24. https://doi.org/10.5209/rev_FITE.2014.v26.46968
Dowgiałło J (2002) The Sudetic geothermal region of Poland. Geothermics 31:343–359
Dudek A, Frolíková I, Nekovařík Č (1991) The depth of intrusion of Hercynian granitoid plutons in the Bohemian Massif. Acta Univ Carol Ser Geol 3–4:249–256 (in Czech with English abstract)
Dvořák J (1985) Horizontal movements on deep faults in the Proterozoic basement of Moravia (Czechoslovakia). Jb Geol BA 127:551–556
Edel JB, Schulmann K, Rotstein Y (2007) The Variscan tectonic inheritance of the Upper Rhine Graben: evidence of reactivations in the Lias, Late Eocene-Oligocene up to the recent. Int J Earth Sci (Geol Rundsch) 96:305–325. https://doi.org/10.1007/s00531-006-0092-8
Egli D, Mosar J, Ibele T, Madritsch H (2017) The role of precursory structures on Tertiary deformation in the Black Forest – Hegau region. Int J Earth Sci (Geol Rundsch) 106:2297–2318. https://doi.org/10.1007/s00531-016-1427-8
Fairbridge RW (1968) The encyclopedia of geomorphology. Reinhold Book Corporation, New York, Amsterdam, London
Figdor H, Scheidegger AE (1977) Geophysical investigation of the Diendorf fault. Verh Geol BA 3:243–270 (in German with English abstract)
Finger F, René M, Gerdes A, Riegler G (2009) The Saxo-Danubian Granite Belt: magmatic response to postcollisional delamination of mantle lithosphere below the southwestern sector of the Bohemian Massif (Variscan orogen). Geol Carpath 60:205–212. https://doi.org/10.2478/v10096-009-0014-3
Fischer H (1965) Geomorphology of lower Mühlviertel in the Naarn drainage area. Geogr Jahresber Österr 30:49–130 (in German)
Fischer T, Horálek J, Hrubcová P, Vavryčuk V, Bräuer K, Kämpf H (2014) Intra-continental earthquake swarms in West-Bohemia and Vogtland: A review. Tectonophysics 611:1–27. https://doi.org/10.1016/j.tecto.2013.11.001
Flašar J, Štěpančíková P (2022a) Geomorphological evidence of tectonic activity of the Mariánské Lázně fault (Czech Republic) and its influence on stream network evolution. Acta Geodyn Geomater 19(205):5–25. https://doi.org/10.13168/AGG.2021.0039
Flašar J, Štěpančíková P (2022b) Plio-Pleistocene paleodrainage reconstruction using moldavite-bearing and morphostratigraphically related deposits (Southern Bohemia, Czech Republic). Palaeogeogr Palaeoclim Palaeoecol 586:110783. https://doi.org/10.1016/j.palaeo.2021.110783
Froitzheim N, Plašienka D, Schuster R (2008) Alpine tectonics of the Alps and Western Carpathians. In: McCann T (ed) The geology of Central Europe (Vol 2: Mesozoic and Cenozoic). The Geological Society of London, London, pp 1141–1232
Fuchs G (1991) Radical change of views on the Bohemian Massif. Jb Geol BA 134:701–710 (in German with English abstract)
Fuchs G, Matura A (1976) A review of geology of the Crystalline in the southern Bohemian Massif. Jb Geol BA 119:1–43 (in German with English abstract)
Fuchs G, Thiele O, Fuchs W, Scharbert S (1968) Overview map of the crystalline in the Western Mühlviertel and Sauwald, Upper Austria, 1:100,000, with explanatory notes. Geological Survey of Austria, Vienna (in German)
Führer FX (1978) Gravity anomalies at the southwestern margin of the Bayerischer Wald Mts. and their interpretations. Geol Rundsch 67:1078–1096. https://doi.org/10.1007/bf01983255 (in German with English abstract)
Geissler WH, Kämpf H, Kind R, Klinge K, Plenefisch T, Horálek J, Zedník J, Nehybka V (2005) Seismic structure and location of a CO_2 source in the upper mantle of the western Eger (Ohře) Rift, central Europe. Tectonics 24:TC5001. https://doi.org/10.1029/2004TC001672
Gerdes A, Friedl G, Parrish RR, Finger F (2003) High-resolution geochronology of Variscan granite emplacement – the South Bohemian Batholith. J Czech Geol Soc 48:53–54

Grenerczy G (2002) Tectonic processes in the Eurasian-African Plate boundary zone revealed by space geodesy. In: Stein S, Freymueller JT (eds) Plate boundary zones. AGU Monogr Geodyn Ser 30, pp 67–86. https://doi.org/10.1029/GD030p0067

Grenerczy G, Kenyeres A, Fejes I (2000) Present crustal movements and strain distribution in Central Europe inferred from GPS measurements. J Geophys Res Solid Earth 105(B9):21835–21846. https://doi.org/10.1029/2000JB900127

Griesmeier GEU, Iglseder C, Schuster R, Petrakakis K (2020) Polyphase deformation along the South Bohemian Batholith-Moldanubian nappes boundary – The Freyenstein Fault System (Bohemian Massif / Austria). Austr J Earth Sci 113:139–154. https://doi.org/10.17738/ajes.2020.0009

Grygar R, Jelínek J (2003) The Upper Morava and Nysa pull-apart grabens – the evidence of neotectonic dextral transtension on the Sudetic fault system. Acta Montana Ser A 24(131):51–59

Hanzlík J (1998) Mineral water springs and the seismic activity in the Western Bohemia area. Acta Montana Ser A 12(107):125–140

Havíř J (2000) Stress analyses in the epicentral area of Nový Kostel (Western Bohemia). Stud Geophys Geod 44:522–536. https://doi.org/10.1023/A:1021863617590

Havíř J (2002) Recent tectonic activity in the area northwards of Šternberk (Nízký Jeseník Mts) – present knowledge. Acta Montana Ser A 20(124):97–104

Havíř J (2004) Orientation of recent principal stress axes in the Jeseníky region. Acta Geodyn Geomater 1(135):49–57

Hearn EH, Johnson K, Thatcher W (2010) Space geodetic data improve seismic hazard assessment in California. In: Workshop on incorporating geodetic surface deformation data into UCERF3 Pomona, California, Eos Trans AGU 91(38):336. https://doi.org/10.1029/2010EO380007

Hefty J (2007) Geo-kinematics of Central and South-Eastern Europe resulting from combination of various regional GPS velocity fields. Acta Geodyn Geomater 4(148):173–189

Hintersberger E, Iglseder C, Schuster R, Huet B (2017) The new database "Tectonic Boundaries" at the Geological Survey of Austria. Jb Geol BA 157:195–207

Homolová D, Lomax J, Špaček P, Decker K (2012) Pleistocene terraces of the Vltava River in the Budějovice basin (Southern Bohemian Massif): new insights into sedimentary history constrained by luminescence data. Geomorphology 161–162:58–72. https://doi.org/10.1016/j.geomorph.2012.04.001

Hrubcová P, Środa P, CELEBRATION 2000 Working Group (2008) Crustal structure at the easternmost termination of the Variscan belt based on CELEBRATION 2000 and ALP 2002 data. Tectonophysics 460:55–75. https://doi.org/10.1016/j.tecto.2008.07.009

Hrubcová P, Środa P, Grad M, Geissler WH, Guterch A, Vozár J, Hegedűs E, SUDETES 2003 Working Group (2010) From the Variscan to the Alpine Orogeny: crustal structure of the Bohemian Massif and the Western Carpathians in the light of the SUDETES 2003 seismic data. Geophys J Int 183:611–633. https://doi.org/10.1111/j.1365-246X.2010.04766.x

Hrubcová P, Środa P, Špičák A, Guterch A, Grad M, Keller GR, Brückl E, Thybo H (2005) Crustal and uppermost mantle structure of the Bohemian Massif based on CELEBRATION 2000 data. J Geophys Res Solid Earth 110:B11305. https://doi.org/10.1029/2004JB003080

Iglseder C (2013) Report 2011–2012 on new geological knowledge from the Crystalline of the Bohemian Massif on the sheet 4319 Linz. Jb Geol BA 153:434–438 (in German)

Iglseder C (2014a) Report 2009 on geological works in the Crystalline of the Bohemian Massif on the sheet 4319 Linz (Haselgraben West). Jb Geol BA 154:361–363 (in German)

Iglseder C (2014b) Report 2010 on geological works in the Crystalline of the Bohemian Massif on the sheet 4319 Linz (Haselgraben West). Jb Geol B A 154:363–365 (in German)

International Atomic Energy Agency Safety Standards Series (2022) Seismic Hazards in Site Evaluation for Nuclear Installations, Specific Safety Guide No. SSG-9 (Rev 1). International Atomic Energy Agency, Vienna. https://www.iaea.org/publications/14665/seismic-hazards-in-site-evaluation-for-nuclear-installations

Jarosiński M, Bobek K, Głuszyński A, Durkowski K (2021) Present-day tectonic stress from borehole breakouts in the North-Sudetic Basin (northern Bohemian Massif, SW Poland) and its regional context. Int J Earth Sci 110:2247–2265. https://doi.org/10.1007/s00531-021-02073-1

Jelínek J (2008) Morphotectonic analysis of digital relief model – a suitable means of searching for zones of rock mass brittle failure. Geosci Eng 14(3):1–13

Kachlík V (1999) Relationship between Moldanubicum, the Kutná Hora Crystalline Unit and Bohemicum (Central Bohemia, Czech Republic): a result of the polyphase Variscan nappe tectonics. J Geosci 44:201–291

Kadlec J (2017) Blanice Graben. Nature of the Blaník Region Ser, pp 1–83. Czech Union for Nature Conservation in Vlašim, Vlašim (in Czech)
Kapłon J, Kontny B, Grzempowski P, Schenk V, Schenková Z, Balek J, Holešovský J (2014) GEOSUD/SUDETEN network GPS data reprocessing and horizontal site velocity estimation. Acta Geodyn Geomater 11(173):65–75. https://doi.org/10.13168/AGG.2013.0058
Kárník V, Procházková D, Schenk V, Schenková Z (1981) Seismicity of Czechoslovakia and Europe. In: Zátopek A, Beránek B (eds) Geophysical syntheses in Czechoslovakia. Publication House of the Slovak Academy of Sciences, Bratislava, pp 221–242
Keller EA, Pinter N (2002) Active tectonics: earthquakes, uplift and landscape. Prentice-Hall, Upper Saddle River
Kierulf HP (2017) Analysis strategies for combining continuous and episodic GNSS for studies of neotectonics in Northern-Norway. J Geodyn 109:32–40. https://doi.org/10.1016/j.jog.2017.07.002
Klomínský J, Jarchovský T, Rajpoot GS (2010) Atlas of plutonic rocks and orthogneisses in the Bohemian Massif. Czech Geological Survey, Prague
Kodym O (1963) Explanatory notes to Overview geological map of the Czechoslovak Socialistic Republic, 1:200,000, Sheet M-33-XXI Tábor. Publication House of the Czechoslovak Academy of Sciences, Prague (in Czech)
Kodym O (1989) Geological map of the Czechoslovak Socialistic Republic (Map of pre-Quaternary rocks), 1:200,000, Sheet 33-XXI Tábor. Czech Geological Survey, Prague (in Czech)
Kodym O, Fusán O, Matějka A (1967) Geological map of the Czechoslovakia, 1:500,000. Czech Geological Survey, Prague (in Czech)
Kontny B, Bosy J, Mąkolski K (2004): Local geodynamic network Karkonosze – the results of three years of measurements and first interpretations. Acta Geodyn Geomater 1(135):83–89
Krásný J (1980) Hydrogeology of the South Bohemia basins. J Geol Sci Ser Hydrogeol Eng Geol 14:7–81 (in Czech with English summary)
Krásný J, Císlerová M, Čurda S, Datel JV, Dvořák J, Grmela A, Hrkal Z, Kříž H, Marszalek H, Šantrůček J, Šilar J (2012) Underground waters of the Czech Republic (Regional hydrogeology of plain and mineral Waters). Czech Geological Survey, Prague (in Czech with English summary)
Krenmayr HG, Schnabel W, Reitner JM, van Husen D, Finger F, Linner M, Roetzel R, Rupp C, Bryda G, Mandl GW, Nowotny A, Pestal G, Schuster R (2006) Geological map of Upper Austria, 1:200,000. Geological Survey of Austria, Vienna (in German)
Kröll A, Motschka K, Meurers B, Slapansky P, Wagner L, Wessely G, Zych D (2006) Explanatory notes to maps of the Molasse basin in Salzburg – Upper Austria, 1:200,000. Geological Survey of Austria, Vienna (in German)
Krzyszkowski D, Przybylski B, Badura J (2000) The role of neotectonics and glaciation on terrace formation along the Nysa Kłodzka River in the Sudeten Mountains (southwestern Poland). Geomorphology 33:149–166. https://doi.org/10.1016/S0169-555X(99)00123-3
Land Oberösterreich (2021) Digitales Geländemodell 10m. Available at: https://www.data.gv.at/katalog/dataset/fa3568b0-ecb0-4b6d-866e-38c4fe98f839. Accessed 14 Ocober 2021
Lenhardt WA, Švancara J, Melichar R, Pazdírková J, Havíř J, Sýkorová Z (2007) Seismic activity of the Alpine-Carpathian-Bohemian Massif region with regard to geological and potential field data. Geol Carpath 58:397–412
Levi N, Habermueller M, Exner U, Piani E, Wiesmayr G, Decker K (2019) The stress field in the frontal part of the Eastern Alps (Austria) from borehole image log data. Tectonophysics 769:228175. https://doi.org/10.1016/j.tecto.2019.228175
Linsser H (1967) Investigation of tectonics by gravity detailing. Geophys Prospecting 3:480–515
Lyros E, Kostelecky J, Plicka V, Filler V, Sokos E, Nikolakopoulos K (2021) Detection of tectonic and crustal deformation using GNSS data processing: The case of PPGnet. Civil Eng J 7(1):14–23. https://doi.org/10.28991/cej-2021-03091633
Malecha A (1964) Tectonics and development of the Tertiary between the towns of Hluboká and Týn nad Vltavou. Čas Mineral Geol 9:167–176 (in Czech)
Malecha A, Pícha F (1963) Geological development of the southwestern part of the Třeboň Basin. Bull Geosci 38:297–310 (in Czech)
Malecha A, Špinar Z, Bořková-Gabrielová N, Mrázek A, Němejc F, Pacltová B, Řeháková Z, Slánská J (1962) New division and designation of stratigraphic units of the South Bohemian basins. Bull Geosci 37:161–170 (in Czech)
Malecha A, Suk M, Zikmund J (1964) Structure and basement of the South Bohemian basins. J Geol Sci Ser Geol 4:97–120 (in Czech)

Malkovský M (1975) Paleogeography of the Miocene of the Bohemian Massif. Bull Geosci 50:27–31
Malkovský M (1979) Tectogenesis of the platform cover of the Bohemian Massif. Knih Ústř Úst Geol 53:1–176 (in Czech)
Malkovský M (1980) Saxon tectogenesis of the Bohemian Massif. J Geol Sci Ser Geol 34:67–101
Malkovský M (1987) The Mesozoic and Tertiary basins of the Bohemian Massif and their evolution. Tectonophysics 137:31–42. https://doi.org/10.1016/0040-1951(87)90311-8
Mannová M, Matolín M (1995) Radiometric map of the Czech Republic 1:500,000 with explanatory notes. Czech Geological Survey, Prague
Matte P, Maluski H, Rajlich P, Franke W (1990) Terrane boundaries in the Bohemian Massif: result of large-scale Variscan shearing. Tectonophysics 177:150–170. https://doi.org/10.1016/0040-1951(90)90279-H
Melnyk A, Černý J, Pospíšil L, Adamovič J (2022) New geophysical and geological data on the Moldanubian plutonic complex and the Kaplice Fault, southern Bohemia. Int J Earth Sci 111:1315–1331. https://doi.org/10.1007/s00531-022-02182-5
Melnyk A (2017) Interpretation of gravity data in the area of granitic intrusions of the Moldanubian pluton near Kaplice. MSc thesis, Charles University. https://dspace.cuni.cz/handle/20.500.11956/83026?locale-attribute=en (in Czech)
Michon L, Van Balen RT, Merle O, Pagnier H (2003) The Cenozoic evolution of the Roer Valley Rift System integrated at a European scale. Tectonophysics 367:101–126. https://doi.org/10.1016/S0040-1951(03)00132-X
Mísař Z, Dudek A, Havlena V, Weiss J (1983) Geology of the Czechoslovak Socialistic Republic. Czech Publication House, Prague (in Czech), Bohemian Massif
Mlčoch B, Konopásek J (2010) Pre-Late Carboniferous geology along the contact of the Saxothuringian and Teplá-Barrandian zone in the area covered by younger sediments and volcanics (western Bohemian Massif, Czech Republic). J Geosci 55:81–94. https://doi.org/10.3190/jgeosci.068
Mrlina J, Kämpf H, Kroner C, Mingram J, Stebich M, Brauer A, Geissler WH, Kallmeyer J, Matthes H, Seidl M (2009) Discovery of the first Quaternary maar in the Bohemian Massif, Central Europe, based on combined geophysical and geological surveys. J Volcanol Geoth Res 182:97–112. https://doi.org/10.1016/j.jvolgeores.2009.01.027
NASA/USGS (2023) EarthExplorer. SRTM 1 Arc-Second Global Data Set, Landsat 7 ETM+ Data Set. https://earthexplorer.usgs.gov
Navrátilová V, Nol O (2018) Nuclear Power Plant Temelín – South, Evaluation of the exploratory territory for special interventions in the Earth's crust and proposal of next geological works. Technical report, Czech Radioactive Waste Repository Authority, Prague (in Czech)
Nehyba S, Roetzel R (2010) Fluvial deposits of the St. Marein-Freischling Formation – insights into initial depositional processes on the distal external margin of the Alpine-Carpathian Foredeep in Lower Austria. Austr J Earth Sci 103:50–80
Neunhöfer H, Hemmann A (2005) Earthquake swarms in the Vogtland/Western Bohemia region: Spatial distribution and magnitude–frequency distribution as an indication of the genesis of swarms? J Geodyn 39:361–385. https://doi.org/10.1016/j.jog.2005.01.004
Paoletti V, Hintersberger E, Schattauer I, Milano M, Deidda GP, Supper R (2022) Geophysical study of the Diendorf-Boskovice Fault System (Austria). Remote Sens 14:1807. https://doi.org/10.3390/rs14081807
Peresson H, Decker K (1997) Far-field effects of Late Miocene subduction in the Eastern Carpathians: E-W compression and inversion of structures in the Alpine–Carpathian–Pannonian region. Tectonics 16:38–56. https://doi.org/10.1029/96TC02730
Pešek J, Sivek M (2016) Coal-bearing basins and coal deposits of the Czech Republic. Czech Geological Survey, Prague
Peška P (1992) Stress indications in the Bohemian Massif: Reinterpretation of borehole televiewer data. Stud Geophys Geod 36:307–324. https://doi.org/10.1007/BF01625484
Peška P (1993) Overcoring measurements in the Příbram mine area and their relation to the regional stress field. Stud Geophys Geod 37:141–150. https://doi.org/10.1007/BF01613927
Peterek A, Reuther CD, Schunk R (2011) Neotectonic evolution of the Cheb Basin (Northwestern Bohemia, Czech Republic) and its implications for the late Pliocene to Recent crustal deformation in the western part of the Eger Rift. Z Geol Wiss 39:335–365
Pfleiderer S, Götzl G, Bottig M, Brüstle AK, Porpaczy C, Schreilechner M, Eichkitz C, Jud M, Sachsenhofer R, Zosseder K, Casper S, Goldbrunner J, Kriegl C, Kolmer C, Diepolder GW (2016) GeoMol – Geological 3D modelling of the Austrian Molasse Basin and applications in hydrogeology and geothermal energy within the border region of Upper Austria and Bavaria. Abh Geol BA 70:3–88 (in German with English abstract)

Pitra P, Burg JP, Guiraud M (1999) Late Variscan strike-slip tectonics between the Teplá-Barrandian and Moladnubian terranes (Czech Bohemian Massif): petrostructural evidence. J Geol Soc London 156:1003–1020

Popotnig A, Tschegg D, Decker K (2013) Morphometric analysis of a reactivated Variscan fault in the southern Bohemian Massif (Budějovice basin, Czech Republic). Geomorphology 197:108–122. https://doi.org/10.1016/j.geomorph.2013.04.042

Pospíšil L, Švábenský O, Roštínský P, Nováková E, Weigel J (2017) Geodynamic risk zone at northern part of the Boskovice Furrow. Acta Geodyn Geomater 14(185):113–129. https://doi.org/10.13168/AGG.2016.0033

Pospíšil L, Otava J, Hudečková E (2019) Utilization of archive geophysical data for geodynamical studies in the Sudetes: Example of Bělá fault zone (The Nízký Jeseník Mts). Acta Geodyn Geomater 16(195):281–291. https://doi.org/10.13168/AGG.2019.0024

Prachař I (2014) Nuclear Power Plant Temelín. Complex geological and seismological aspects requested for site with nuclear installatio. Research report, Prague / Horní Počernice (in Czech)

Přibyl V (1999) Vltava River Terrace System between Lipno and Rožmberk nad Vltavou. Acta Univ Carol Ser Geogr 2:157–171

Rajlich P (1990) Variscan shearing tectonics in the Bohemian Massif. Miner Slovak 22:33–40

Rajlich P, Synek J, Sarbach M, Schulmann K (1986) Hercynian-thrust related shear zones and deformation of the Varied Group on the contact of granulites (Southern Moldanubian, Bohemian Massif). Geol Rundsch 75:665–683. https://doi.org/10.1007/BF01820639

Reinecker J, Tingay M, Müller B, Heidbach O (2010) Present-day stress orientation in the Molasse Basin. Tectonophysics 482:129–138. https://doi.org/10.1016/j.tecto.2009.07.021

Roetzel R (1996) Report 1994/1995 on new geological knowledge from the Tertiary and Quaternary with notes to tectonics of the Diendorf fault on the sheet 22 Hollabrunn. Jb Geol BA 139:286–295 (in German)

Röhlich P, Šťovíčková N (1968) Deep fault tectonics and its development in the central part of the Bohemian Massif. Geologie 17:670–694 (in German with English abstract)

Rohrmüller J, Kämpf H, Geiss E, Grossmann J, Grun I, Mingram J, Mrlina J, Plessen B, Stebich M, Veress C, Wendt A, Nowaczyk N (2017) Reconnaissance study of an inferred Quaternary maar structure in the western part of the Bohemian Massif near Neualbenreuth, NE-Bavaria (Germany). Int J Earth Sci 107:1381–1405. https://doi.org/10.1007/s00531-017-1543-0

Roštínský P, Roetzel R (2005) Exhumed Cenozoic landforms on the SE flank of the Bohemian Massif in the Czech Republic and Austria. Z Geomorph 49:23–45

Roštínský P, Pospíšil L, Švábenský O (2013) Recent geodynamic and geomorphological analyses of the Diendorf-Čebín Tectonic Zone, Czech Republic. Tectonophysics 599:45–66. https://doi.org/10.1016/j.tecto.2013.04.008

Roštínský P, Pospíšil L, Švábenský O, Kašing M, Nováková E (2020) Risk faults in stable crust of the eastern Bohemian Massif identified by integrating GNSS, levelling, geological, geomorphological and geophysical data. Tectonophysics 785:228427. https://doi.org/10.1016/j.tecto.2020.228427

Šalanský K (1995) Magnetic map of the Czech Republic 1:500,000. Czech Geological Survey, Prague

Scheck M, Bayer U, Otto V, Lamarche J, Banka D, Pharaoh T (2002) The Elbe Fault System in North Central Europe – a basement controlled zone of crustal weakness. Tectonophysics 360:281–299. https://doi.org/10.1016/S0040-1951(02)00357-8

Schenk V, Schenková Z, Pospíšil L (1989) Fault system dynamics and seismic activity – examples from the Bohemian Massif and the Western Carpathians. Geophys Trans 35:101–116

Schenk V, Schenková Z, Jechumtálová Z (2009) Geodynamic pattern of the West Bohemian region based on permanent GPS measurements. Stud Geophys Geod 53:329–341. https://doi.org/10.1007/s11200-009-0021-y

Schenk V, Schenková Z, Jechumtálová Z, Pichl R (2012) Crustal deformations in the epicentral area of the West Bohemia 2008 earthquake swarm in central Europe. J Geophys Res Solid Earth 117:B07408. https://doi.org/10.1029/2011JB009053

Schenková Z, Schenk V, Mantlík F, Grácová M (2007) Regional geodynamic network HIGHLANDS, the Bohemian Massif. Acta Geodyn Geomater 4(148):207–215

Schenková Z, Kottnauer P, Schenk V, Cajthamlová-Grácová M, Mantlík F, Kujal R (2009) Investigation of the recent crustal movements of the eastern part of the Bohemian Massif using GPS technology. Acta Res Rep 18:17–25

Schermann O (1966) Wrench faulting at the eastern margin of the Bohemian Massif. Mitt Ges Geol Bergbaustud 16:89–103 (in German with English summary)

Schröder B (1987) Inversion tectonics along the western margin of the Bohemian Massif. Tectonophysics 137:93–100. https://doi.org/10.1016/0040-1951(87)90316-7

Schumacher ME (2002) Upper Rhine Graben: Role of preexisting structures during rift evolution. Tectonics 21:1006. https://doi.org/10.1029/2001TC900022
Šibrava V, Havlíček P (1980) Radiometric age of Plio-Pleistocene volcanic rocks in the Bohemian Massif. Bull Geosci 55:129–150
Skácelová Z, Rejchrt M, Mlčoch B (2008) The 3D model of the crystalline basement of the Cretaceous sediments (Dlouhá mez region). Geosci Res Rep 41:49–53 (in Czech with English abstract)
Špaček P (2011) Quaternary activity of the Hluboká fault. Research report, Institute of Physics of the Earth, Masaryk University, Brno
Špaček P, Sýkorová Z, Pazdírková J, Švancara J, Havíř J (2006) Present-day seismicity of the south-eastern Elbe Fault System (NE Bohemian Massif). Stud Geophys Geod 50:233–258. https://doi.org/10.1007/s11200-006-0014-z
Špaček P, Bábek O, Štěpančíková P, Švancara J, Pazdírková J, Sedláček J (2015) The Nysa-Morava Zone: an active tectonic domain with Late Cenozoic sedimentary grabens in the Western Carpathians foreland (NE Bohemian Massif). Int J Earth Sci (Geol Rundsch) 104:963–990. https://doi.org/10.1007/s00531-014-1121-7
Špaček P, Valenta J, Tábořík P, Ambrož V, Urban M, Štěpančíková P (2017) Fault slip versus slope deformations: experience from paleoseismic trenches in the region with low slip-rate faults and strong Pleistocene periglacial mass wasting (Bohemian Massif). Quat Int 451:56–73. https://doi.org/10.1016/j.quaint.2017.05.006
Špaček P, Štěpančíková P, Prachař I (2022) Faults of the Bohemian Massif (Source of analytical data on main faults and faulted areas with seismogenic potential). Masaryk University, Institute of Physics of the Earth. https://doi.org/10.48790/MWF4-SH44
Špičáková L, Uličný D, Koudelková G (2000) Tectonosedimentary evolution of the Cheb Basin (NW Bohemia, Czech Republic) between late Oligocene and Pliocene: a preliminary note. Stud Geophys Geod 44:556–580. https://doi.org/10.1023/A:1021819802569
Stackebrand W, Franzke HJ (1989) Alpidic reactivation of the Variscan consolidated lithosphere – the activity of some fracture zones in Central Europe. Z Geol Wiss 17:699–712
Stemberk J Jr, Coubal M, Stemberk J, Štěpančíková P (2019) Stress analysis of fault slips data recorded within the Dědičná štola gallery in the Rychlebské hory Mts (NE part of the Bohemian Massif). Acta Geodyn Geomater 16(195):315–330. https://doi.org/10.13168/AGG.2019.0027
Štěpančíková P, Hók J, Nývlt D, Dohnal J, Sýkorová I, Stemberk J (2010) Active tectonics research using trenching technique on the south-eastern section of the Sudetic Marginal Fault (NE Bohemian Massif, central Europe). Tectonophysics 485:269–282. https://doi.org/10.1016/j.tecto.2010.01.004
Štěpančíková P, Fischer T, Stemberk J Jr, Nováková L, Hartvich F, Figueiredo PM (2019) Active tectonics in the Cheb basin: Youngest documented Holocene surface faulting in Central Europe? Geomorphology 327:472–488. https://doi.org/10.1016/j.geomorph.2018.11.007
Štěpančíková P, Rockwell TK, Stemberk J Jr, Rhodes EJ, Hartvich F, Luttrell K, Myers M, Tábořík P, Rood DH, Wechsler N, Nývlt D, Ortuño M, Hók J (2022) Acceleration of Late Pleistocene activity of a Central European fault driven by ice loading. Earth Planet Sci Lett 591:117596. https://doi.org/10.1016/j.epsl.2022.117596
Šťovíčková N (1973) Deep fault tectonics and its relation to endogenous geological processes. Publication House of the Czechoslovak Academy of Sciences, Prague (in Czech with English summary)
Švábenský O, Weigel J, Pospíšil L (2012) Geodynamic network SNĚŽNÍK: reprocessing and analyses of satellite data in the Czech part over the period 1997–2011. Acta Geodyn Geomater 9(167):339–347
Švábenský O, Pospíšil L, Weigel J, Roštínský P, Witiska M (2014) Results of repeated measurements at the Železné hory-Tišnov Fault System surroundings. Acta Geodyn Geomater 11(175):211–223. https://doi.org/10.13168/AGG.2014.0009
Švancara J, Gnojek I, Hubatka F, Dědáček K (2000) Geophysical field pattern in the West Bohemia geodynamic active area. Stud Geophys Geod 44:307–326. https://doi.org/10.1023/A:1022175228804
Sýkorová Z, Pazdírková J, Zacherle P, Vlach R, Špaček P (2019) Catalog of natural earthquakes located in the NE Czech Republic IPE-MONET. https://doi.org/10.48790/2D3W-4X62. Accessed 23 February 2020
Szczygieł J, Sobczyk A, Hercman H, Mendecki MJ, Gąsiorowski M (2021) Damaged speleothems and collapsed karst chambers indicate paleoseismicity of the NE Bohemian Massif (Niedźwiedzia Cave, Poland). Tectonics 40:e2020TC006459. https://doi.org/10.1029/2020TC006459
Tamay J, Galindo-Zaldivar J, Soto J, Gil AJ (2021) GNSS constraints to active tectonic deformations of the South American continental margin in Ecuador. Sensors 21:4003. https://doi.org/10.3390/s21124003
Thiele O (1984) Nappe structure and axial plan of the Moldanubicum in the Bohemian Massif (Austria). Jb Geol BA 126:513–523 (in German with English summary)
Thiele O (1961) Age of the Donau fault. Verh Geol BA, pp 131–133 (in German).

Tong X, Sandwell DT, Smith-Konter B (2013) High-resolution interseismic velocity data along the San Andreas Fault from GPS and InSAR. J Geophys Res Solid Earth 118:369–389. https://doi.org/10.1029/2012JB009442

Tyráček J, Havlíček P (2009) The fluvial record in the Czech Republic: a review in the context of IGCP 518. Global Planet Change 68:311–325. https://doi.org/10.1016/j.gloplacha.2009.03.007

Uličný D, Čech S, Grygar R (2003) Tectonics and depositional systems of a shallow-marine, intra-continental strike-slip basin: exposures of the Český Ráj Region, Bohemian Cretaceous Basin (field trip – Day 2). Geolines 16:133–148

Uličný D, Špičáková L, Grygar R, Svobodová M, Čech S, Laurin J (2009) Palaeodrainage systems at the basal unconformity of the Bohemian Cretaceous Basin: roles of inherited fault systems and basement lithology during the onset of basin filling. Bull Geosci 84:577–610. https://doi.org/10.3140/bull.geosci.1128

Ulrych J, Ackerman L, Balogh K, Hegner E, Jelínek E, Pécskay Z, Přichystal A, Upton BGJ, Zimák J, Foltýnová R (2013) Plio-Pleistocene basanitic and melilititic series of the Bohemian Massif: K-Ar ages, major/trace element and Sr–Nd isotopic data. Geochemistry 73:429–450. https://doi.org/10.1016/j.chemer.2013.02.001

Valenta J, Stejskal V, Štěpančíková P (2008) Tectonic pattern of the Hronov-Poříčí trough as seen from pole-dipole geoelectric measurements. Acta Geodyn Geomater 5(150):185–195

Vauchez A, Tommasi A, Mainprice D (2012) Faults (shear zones) in the Earth's mantle. Tectonophysics 558–559:1–27. https://doi.org/10.1016/j.tecto.2012.06.006

Vavryčuk V, Bouchaala F, Fischer T (2013) High-resolution fault image from accurate locations and focal mechanisms of 2008 swarm earthquakes in West Bohemia, Czech Republic. Tectonophysics 590:189–195. https://doi.org/10.1016/j.tecto.2013.01.025

Verner K, Buriánek D, Vrána S, Vondrovic L, Pertoldová J, Hanžl P, Nahodilová R (2009) Tectonometamorphic features of geological units along the northern periphery of the Moldanubian Zone (Bohemian Massif). J Geosci 54:87–100. https://doi.org/10.3190/jgeosci.046

Veselá M (1976) The Jihlava Furrow in the geological structure development of the Jihlava environs. J Geol Sci Ser Geol 28:189–205 (in Czech with English summary)

Vrána S, Bártek J (2005) Retrograde metamorphism in a regional shear zone and related chemical changes: The Kaplice Unit of muscovite-biotite gneisses in the Moldanubian Zone of southern Bohemia, Czech Republic. J Czech Geol Soc 50:43–57

Vrána S, Janoušek V (2006) Late-orogenic Variscan magmatism: the case of quartz monzodiorite dykes from the Blanice Graben, southern Bohemia. J Czech Geol Soc 51:231–248

Vrána S, Slabý J, Bendl J (2005) The Kaplice dyke swarm of biotite granodiorite porphyry and its relationship to the Freistadt granodiorite, Moldanubian Batholith. J Czech Geol Soc 50:9–17

Vrána S, Štědrá V (1997) Geological model of western Bohemia related to the KTB Borehole in Germany. J Geol Sci Ser Geol, pp 1–240

Vyskočil P (1996) Recent crustal movements, their properties and results of studies in the territory of Czech Republic. In: Kopecký A, Loyda L, Vyskočil P (eds) Seismicity, neotectonics and recent dynamics with special regard to the territory of the Czech Republic. Research Institute of Geodesy, Topography and Cartography, Zdiby, pp 77–120

Wagner LR (1998) Tectono-stratigraphy and hydrocarbons in the Molasse Foredeep of Salzburg, Upper and Lower Austria. In: Mascle A, Puigdefàbregas C, Luterbacher HP, Fernàndez M (eds) Cenozoic foreland basins of Western Europe. Geol Soc London Spec Publ 134, pp 339–369

Wagner GA, Gögen K, Jonckhere R, Wagner I, Woda C (2002) Dating of Quaternary volcanoes Komorní hůrka (Kammerbühl) and Železná hůrka (Eisenbühl), Czech Republic, by TL, ESR, alpha-recoil and fission track chronometry. Z Geol Wiss 30:191–200

Wallbrecher E, Brandmayr M, Handler R, Loizenbauer J, Maderbacher F, Platzer R (1993) Conjugated shear zones in the southern Bohemian Massif: Variscan and Alpine developments. Mitt Österr Miner Ges 138:238–252 (in German with English abstract)

WEBNET (2022) West Bohemia Local Seismic Network (Data set since 1991). Inst Geophys, Acad Sci Czech Republic. https://doi.org/10.7914/SN/WB

Weinlich FH, Faber E, Boušková A, Horálek J, Teschner M, Poggenburg J (2006) Seismically induced variations in Mariánské Lázně fault gas composition in the NW Bohemian swarm quake region, Czech Republic – A continuous gas monitoring. Tectonophysics 421:89–110. https://doi.org/10.1016/j.tecto.2006.04.012

Wendt J, Dietrich R (2003) Determination of recent crustal deformations based on precise GPS measurements in the Vogtland earthquake area. J Geodyn 35:235–246. https://doi.org/10.1016/S0264-3707(02)00065-0

Wessely G, Draxler I, Gangl G, Gottschling P, Heinrich M, Hofmann T, Lenhardt W, Matura A, Pavuza R, Peresson H, Sauer R (2006) Geology of the Austrian Federal States (Lower Austria). Geological Survey of Austria, Vienna (in German)
Wetzlinger K, Robl J, Liebl M, Dremel F, Stüwe K, von Hagke C (2023) Old orogen – young topography: evidence for relief rejuvenation in the Bohemian Massif. Austr J Earth Sci 116:17–38. https://doi.org/10.17738/ajes.2023.0002
Zachariáš J, Hübst Z (2012) Structural evolution of the Roudný gold deposit, Bohemian Massif: a combination of paleostress analysis and review of historical documents. J Geosci 57:87–103. https://doi.org/10.3190/jgeosci.117
Žák J, Verner K, Janoušek V, Holub F, Kachlík V, Finger F, Hajná J, Tomek F, Vondrovic L, Trubač J (2014) A plate-kinematic model for the assembly of the Bohemian Massif constrained by structural relationships around granitoid plutons. In: Schulmann K, Martínez Catalán JR, Lardeaux JM, Janoušek V, Oggiano G (eds) The Variscan orogeny: extent, timescale and the formation of the European crust. Spec Publ, Geol Soc London, pp 169–196
Zeman J (1978) Deep-seated faults in the Bohemian Massif. J Geol Sci Ser Geol 31:155–185
Ziegler PA (1990) Geological atlas of Western and Central Europe, 2nd edn. Shell International Petroleum Mij. B.V. and Geological Society, London
Ziegler PA, Dèzes P (2007) Cenozoic uplift of Variscan Massifs in the Alpine foreland: Timing and controlling mechanisms. Global Planet Change 58:237–269. https://doi.org/10.1016/j.gloplacha.2006.12.004
Zulauf G, Bues C, Dörr W, Vejnar Z (2002) 10 km Minimum throw along the West Bohemian shear zone: Evidence for dramatic crustal thickening and high topography in the Bohemian Massif (European Variscides). Int J Earth Sci (Geol Rundsch) 91:850–864. https://doi.org/10.1007/s00531-001-0250-y

Authors and Affiliations

Pavel Roštínský[1] · Lubomil Pospíšil[2,3] · Otakar Švábensky[3] · Anastasiia Melnyk[4] · Eva Nováková[1]

✉ Pavel Roštínský
pavel.rostinsky@ugn.cas.cz

Lubomil Pospíšil
geo-pospisil@volny.cz

Otakar Švábenský
svabensky.o@fce.vutbr.cz

Anastasiia Melnyk
anastasiam335@gmail.com

Eva Nováková
eva.novakova@ugn.cas.cz

1 Institute of Geonics, Department of Environmental Geography, The Czech Academy of Sciences, Drobného 28, Brno, Czech Republic

2 Faculty of Mining and Geology, Department of Geodesy and Mine Surveying, VSB – Technical University of Ostrava, 17. Listopadu 15, Ostrava, Czech Republic

3 Faculty of Civil Engineering, Institute of Geodesy, Brno University of Technology, Veveří 94, Brno, Czech Republic

4 Faculty of Mining and Geology, Department of Geological Engineering, VSB – Technical University of Ostrava, 17. Listopadu 15, Ostrava, Czech Republic